February 2021

Ph.D. Dissertation

Antimicrobial and anti-endotoxic activities and mechanisms of action of short amphipathic peptides derived from avian host defense peptides

Graduate School of Chosun University

Department of Biomedical Sciences

Dinesh Kumar

Antimicrobial and anti-endotoxic activities and mechanisms of action of short amphipathic peptides derived from avian host defense peptides

조류생체방어펩타이드로부터 유래된 짧은
양친매성펩타이드의 항균 및 항내독소활성과
작용기작

2021년 2월 25일

Graduate School of Chosun University

Department of Biomedical Sciences

Antimicrobial and anti-endotoxic activities and mechanisms of action of short amphipathic peptides derived from avian host defense peptides

Advisor: Prof. Song Yub Shin

This dissertation is submitted to the Graduate School of Chosun University in partial fulfillment of the requirements for the degree of Doctor of Philosophy in Science

October 2020

Graduate School of Chosun University

Department of Biomedical Sciences

Dinesh Kumar

Ph. D. Dissertation of

Dinesh Kumar is certified by

Chairman (Chosun Univ.) : Prof. Seung Joo Cho .....

Committee Members:

Chosun Univ. : Prof. Sung Tae Yang .....

Chonnam Univ. : Prof. Chul Won Lee .....

Korea Basic Science Institute: Ph.D. (P.I.) Jeong Kyu Bang .....

Chosun Univ. : Prof. Song Yub Shin .....

December 2020

Graduate School of Chosun University

CONTENTS

LIST OF TABLES

PART I

PART II

LIST OF FIGURES

PART I

PART II

초 록

조류생체방어펩타이드로부터 유래된 짧은 양친매성펩타이드의 항균 및 항내독소활성과 작용기작

디네쉬 쿠마
지도교수: 신송엽, Ph.D.
의과학과
조선대학교 대학원

PART I

항균 펩티드 (AMP)는 항생제 내성 병원체와 싸우기 위해 점점 더 많은 관심을 받고 있다. dCATH (duck cathelicidin)는 강력한 살균 활성을 가진 20 잔류 조류 cathelicidin이다. 그러나, 그것의 치료적 적용은 높은 포유류 세포 독성 때문에 제한적이다. 향상된 항균 및 세포 선택 특성을 가진 치료적으로 유용한 AMP를 개발하기 위해 dCATH를 기반으로 한 일련의 12개 아미노산으로 구성된 짧은 양친매성 펩타이드를 설계하였다. 이 중 Trp 및 Lys가 풍부한 dCATH 12-4 및 dCATH 12-5는 적혈구 및 대식세포에서 보다 박테리아 세포에 대해 더 높은 선택성을 나타냈다. 또한 이들 펩타이드는 LPS로 자극된 대식세포에서 NO 및 TNF-α 분비를 현저하게 감소시켜 항 염증 특성을 나타내었다. 다양한 형광단 기반 연구 및 공 초점 현미경 관찰은 dCATH 12-4 및 dCATH 12-5가 막 견고성을 방해하지 않고 박테리아 세포막을 관통하여 세포질에 축적될 수 있음을 보여주었다. 현미경 검사와 겔 지연 DNA 결합 분석의 결과는 설계된 두 펩타이드가 모두 박테리아 DNA와 결합하여 DNA 합성을 중지시켜 세포 사멸을 초래할

수 있음을 시사하였다. 형광 분광법 및 유세포 분석 분석은 설계된 펩타이드가 LPS 올리고머에 대한 강한 결합을 유도하여 LPS 응집체를 해리시켜 LPS가 캐리어 단백질 리포 다당류 결합 단백질 (LBP) 또는 대식세포의 CD14 수용체에 결합하는 것을 방지하는 것으로 나타났다. 또한, dCATH 12-4 및 dCATH 12-5는 항생제 내성 병원체에 대한 다양한 기존 항생제와 시너지 효과를 보여 병용 요법에 대한 유망한 보조제로서의 능력을 나타내었다. 요약하면, 이러한 결과는 박테리아 감염 및 패혈증을 퇴치하기 위한 살균 및 면역 조절 특성을 가진 짧은 AMP의 설계에 기여할것이다.

PART II

닭의 창자(chicken intestine)에서 발현되는 카텔리시딘(cathelicidin)인 파울리시딘-1 (Fowl-1)은 항균 및 항염 작용이있는 것으로 알려져 있다. 그러나, 그것의 높은 숙주 세포 독성으로 인해 제약 개발이 궁극적으로 제한되었다. 본 연구에서 일련의 N- 및 C- 말단이 잘린 19-meric Fowl-1 펩타이드을 합성하였다. 이러한 잘린 펩타이드 중 Fowl-1(8-26)은 항 염증 활성을 감소시키면서 인간 적혈구 세포 독성없이 광범위한 항균 활성을 나타냈다. 또한 Fowl-1(8-26)-WRK는 더 많은 양친매성을 나타내기 위해 Fowl-1(8-26)에서 Thr5→Trp, Ile7→Arg 및 Asn11→Lys 치환을 통해 설계되었다. 그 결과 항균성과 항 염증성을 모두 나타냈다. 본 연구는 또한 LPS로 유도된 염증에 대한 Fowl-1(8-26)-WRK의 억제 활성이 주로 LPS가 펩타이드에 결합하기 때문임을 입증되었다. 흥미롭게도, 인간

cathelicidin LL-37 및 melittin에 비해 Fowl-1(8-26)-WRK는 약물 내성 박테리아에 대해 더 강력한 활성을 나타내었다. 또한 생리적 염분과 인간 혈청에 내성이 있고 클로람페니콜, 시프로플록사신, 옥사실린과 같은 기존 항생제와 함께 시너지 효과를 발휘하여 기존 항생제와 결합하여 유망한 보조제임을 시사하였다. 또한 막 탈분극, SYTOX Green 흡수 및 유세포 분석은 막 무결성을 손상시켜 박테리아를 죽이는 것으로 나타났다. 따라서 본 연구는 Fowl-1(8-26)-WRK가 항생제 내성 감염 치료를 위한 항균 및 항염증제로서 향후 개발 가능성이 높다는 것을 시사하였다.

ABSTRACT

Antimicrobial and anti-endotoxic activities and mechanisms of action of short amphipathic peptides derived from avian host defense peptides

Dinesh Kumar
Advisor: Prof. Song Yub Shin
Department of Biomedical sciences
Graduate School of Chosun University

PART I

Antimicrobial peptides (AMPs) have gained increasing attention to combat antibiotic-resistant pathogens. dCATH (duck cathelicidin) is a 20-residue avian cathelicidin with potent bactericidal activity. However, its therapeutic application is limited due to high mammalian cell cytotoxicity. To develop therapeutically useful AMPs with enhanced antimicrobial and cell-selective property, we designed a series of 12-meric (dodeca) short amphiphilic peptides based on dCATH. Among these, Trp and Lys-rich dCATH 12-4 and dCATH 12-5 exhibited higher selectivity towards bacterial cells than erythrocytes and macrophages. Additionally, these AMPs significantly reduced NO and TNF-α secretion in LPS-stimulated macrophage cells, suggesting their anti-inflammatory properties. Various fluorophore-based studies and confocal microscopic observations demonstrated that dCATH 12-4 and dCATH 12-5 could penetrate the bacterial cell membrane and accumulate in the cytoplasm, without disrupting membrane integrity. Results from the microscopic examination and gel-retardation DNA binding assay suggested that both the

designed AMPs could bind with bacterial DNA, subsequently leading to cell death via arrest of DNA synthesis. Fluorescence spectroscopy and flow cytometry analysis revealed that the designed AMPs induced strong binding to LPS oligomers which resulted in dissociation of LPS aggregates, thereby preventing LPS from binding to the carrier protein lipopolysaccharide-binding protein (LBP) or alternatively to CD14 receptors of macrophage cells. Additionally, both dCATH 12-4 and dCATH 12-5 demonstrated synergistic actions with various conventional antibiotics against antibiotic resistant pathogens, thus indicating their ability as promising adjuncts to combination therapy. In summary, these findings contribute to the design of short AMPs with bactericidal and immunomodulatory properties for combating bacterial infection and sepsis.

PART II

Fowlicidin-1 (Fowl-1), a cathelicidin expressed in chicken intestine, is known to have both antimicrobial and anti-inflammatory properties. However, its pharmaceutical development has been ultimately compromised by its high host cytotoxicity. In this study, a series of N- and C-terminal-truncated 19-meric Fowl-1 peptides were synthesized. Among these truncated peptides, Fowl-1(8-26) exhibited broad-spectrum antimicrobial activity without human erythrocyte cytotoxicity while reducing anti-inflammatory activity. Further, Fowl-1(8-26)-WRK was designed via $Thr^{5}\rightarrow$Trp, $Ile^{7}\rightarrow$Arg, and $Asn^{11}\rightarrow$Lys substitutions in Fowl-1(8-26) to exhibit more amphipathicity. The results revealed that it exhibited both antimicrobial and anti-inflammatory properties. This study also demonstrated that the inhibitory activity of Fowl-1(8-26)-WRK against LPS-induced inflammation was mainly due to the binding of LPS to the peptide.

Interestingly, compared with human cathelicidin LL-37 and melittin, Fowl-1(8-26)-WRK showed more potent activity against drug-resistant bacteria. It was also resistant to physiological salts and human serum and acted synergistically in combination with conventional antibiotics, such as chloramphenicol, ciprofloxacin, and oxacillin, suggesting that combined with conventional antibiotics, it is a promising adjuvant. Furthermore, membrane depolarization, SYTOX Green uptake, and flow cytometry revealed that it kills bacteria by damaging their membrane integrity. Therefore, this study suggests that Fowl-1(8-26)-WRK has considerable potential for future development as an antimicrobial and anti-inflammatory agent for treating antibiotic-resistant infections.

PART I

Antimicrobial and anti-inflammatory activities of short dodecapeptides derived from duck cathelicidin: Plausible mechanism of bactericidal action and endotoxin neutralization

1. Introduction

Since their discovery in 1929, antibiotics have ruled the healthcare industry for almost nearly a century. However, in the past two decades, alarming data about increasing bacterial resistance to conventional antibiotics have been reported worldwide. The World Health Organization (WHO) has classified antimicrobial resistance as one of the major global health challenges of the 21st century. In 2017, WHO listed 12 families of antibiotic-resistant bacteria as "superbugs" and reported that these bacteria may soon become untreatable by any currently available antimicrobial drug [1]. Moreover, treatment of bacterial infections with conventional antibiotics often leads to release of lipopolysaccharide (LPS) in blood stream, which in turn leads to localized inflammation [2]. Thus, there is a pressing demand for identification and development of alternative class of antimicrobial agents that can effectively combat antimicrobial-resistant bacteria and possess anti-inflammatory properties as well.

Recently, antimicrobial peptides (AMPs) or host defense peptides have received increasing attention as a novel class of antibiotics due to their broad-spectrum antimicrobial activity against a wide range of microbial pathogens, such as gram-positive and gram-negative bacteria, multi-drug resistant (MDR) bacteria, fungi, parasites, and even enveloped viruses [3]. AMPs have an advantage over conventional antibiotics with regard to their bacterial-killing mechanism. While most of the antibiotics target specific biosynthetic pathways crucial for cell wall or protein synthesis, AMPs kill bacteria primarily by physically targeting the plasma membrane and destabilizing its integrity, which results in leakage of cytoplasmic contents, thus making it impossible for bacteria to develop resistance [4]. Interestingly, some special classes of AMPs can also penetrate the cell membrane and target the intracellular organelles, and thereby lead to cell death [5]. Most of the AMPs adopt four types of secondary conformations in microbial membrane environment namely, α-helices, β-sheets, linear, and loop structures. Among them, α-helical peptides have been extensively studied for their enhanced antimicrobial action. Although AMPs are diverse in their sizes, structures, and activities, they are

mostly amphipathic, that is, they retain both polar (positively charged) and nonpolar (hydrophobic) amino acid residues in spatially distinct regions [6]. This amphiphilic nature of AMPs facilitates their interactions with negatively charged microbial plasma membranes, followed by insertion into the microbial lipid membrane, thus altering membrane permeability and impairing internal homeostasis [7]. Peptides, comprising perfect facial amphipathic structures, have demonstrated superior membrane targeting ability, enhanced cell penetration ability, and improved cell selectivity [8, 9]. Therefore, maintaining a balanced amphipathicity is often considered to be a vital strategy in designing α-helical AMPs. Considering this, several natural peptides have been used as templates and have been empirically modified by replacing, truncating (deleting), adding, or scrambling one or more amino acid sequences in order to optimize the facial amphiphilicity of synthetic peptides [10].

Among an ever-increasing number of AMPs that have been reported till date, two major families, namely cathelicidins and defensins, exist in vertebrate species. Previous reports suggest that human cathelicidin LL-37, CATH 1 and avian cathelicidin, fowlicidin-1 were highly active against bacteria, fungi, and viruses [11]. In addition, LL-37 was found to inhibit LPS-induced inflammatory activity in macrophage cells by binding to them and thus neutralizing the inflammatory potential of LPS [12]. Despite their potent antimicrobial function, therapeutic application of natural cathelicidin is limited due to its high toxicity towards mammalian cells and expensive cost of production, owing to its large size. Hence, recent investigations are focused towards rational design approach for development of short α-helical peptides from cathelicidin. In our earlier work, we discovered that short peptides, derived from LL-37 and fowlicidin-1, demonstrated improved antimicrobial and anti-inflammatory activities by selectively binding and disrupting the bacterial cell membrane [13, 14].

In this study, we designed a 12-meric short α-helical AMP (dCATH 12) by truncating N-terminal amino acid residues of dCATH (duck cathelicidin) peptide [15]. Further, dCATH 12 was empirically modified into five analog peptides in

order to achieve uninterrupted facial amphipathicity with the hydrophobic and cationic amino acids clustered into spatially distinct regions. All the engineered peptides were initially characterized for their secondary structure conformations in a membrane-like environment by circular dichroism (CD). The antimicrobial efficiency was then tested against a panel of gram-positive, gram-negative, multi-drug resistant (MDR) bacteria, and yeast strains. Hemolytic activity and cytocompatibility studies were performed to evaluate the cell selectivity of designed peptides. The anti-inflammatory activities of dCATH 12 and its mutated analogs were evaluated by examining their ability to inhibit the release of pro-inflammatory cytokines from LPS-stimulated RAW264.7 macrophage cells. The analog AMPs that displayed high cell selectivity and enhanced anti-inflammatory activity, were selected and further evaluated for stability in salts and human serum. The bactericidal efficiency of selected analogs was assessed with time-kill kinetic assay. Additionally, their synergistic effects in combination with three conventional antibiotics (chloramphenicol, oxacillin and ciprofloxacin), were also investigated. In order to understand the mechanisms underlying antimicrobial activities of selected dodeca AMPs, we studied the effects of peptides on bacterial membrane permeability and integrity using several fluorochrome-based assays and confocal microscopy. In addition, we identified a possible mechanism of action responsible for the anti-inflammatory activity of designed AMPs by studying their ability to selectively bind and neutralize the *E. coli* LPS.

2. Materials and Methods

2.1 Materials

Rink amide-4-methylbenzhydrylamine (MBHA) resin, 9-fluorenyl-methoxycarbonyl (Fmoc) protected amino acids, and other chemicals and solvents used for peptide synthesis were bought from Novabiochem (La Jolla, CA, USA). Dulbecco's modified Eagle's medium (DMEM) and fetal bovine serum (FBS) were obtained from SeouLin Bioscience (Seoul, South Korea). The TNF-α ELISA kit was procured from R&D Systems (Minneapolis, MN, USA). All buffers were prepared using Milli-Q ultrapure water (Merck Millipore, USA). Invitrogen SYTOX green and *E. coli* bacterial plasmid pBR322 were purchased from Thermo Fisher Scientific, South Korea. All other reagents including 3-(4,5-dimethylthiazol-2-yl)-2,5-diphenyl-2H-tetrazolium bromide (MTT), LPS purified from *Escherichia coli* O111:B4, calcein, 3, 3′-dipropylthiadicarbocyanine iodide (diSC_3-5), 1-N-phenylnaphthylamine (NPN), *o*-nitrophenyl-β-galactosidase (ONPG), Propidium iodide and FITC-labelled LPS (*E. coli* O111:B4), were supplied from Sigma-Aldrich (St. Louis, MO, USA). All reagents were of analytical grade.

2.2 Peptide synthesis

All peptides were synthesized using Fmoc solid-phase method on Rink amide MBHA resin (0.56 mmol/g). Dicyclohexylcarbodiimide (DCC) and 1-hydroxybenzotriazole (HOBt) were used as coupling reagents, and a 10-fold excess of Fmoc-amino acids was added during every coupling cycle. After cleavage and deprotection with a mixture of TFA/H_2O/thioanisole/phenol/ethanedithiol/triisopropylsilane (81.5:5:5:5:2.5:1, v/v/v/v/v/v) for 2 h at room temperature, the crude peptide was repeatedly extracted with diethyl ether. The purity of peptides was determined by RP-HPLC on an analytical Vydac C_{18} column (250 × 20 mm, 15 μm, 300 Å) using an appropriate 0–90% water/acetonitrile gradient in the presence of 0.05% TFA. The molecular

mass of peptides was determined using triple-quadrupole equipped electrospray ionization (ESI)-LC-MS (API2000, AB SCIEX). FITC-labeled peptides of dCATH 12-4 and dCATH 12-5 synthesized by coupling FITC to amine group of linker 6-aminocaproic acid (ACA) were supplied from ANYGEN CO., LTD (Gwangju, Korea).

2.3 Peptide sequence analysis

The primary sequence analysis and physicochemical parameters of the peptides were calculated by bioinformatics programs including ProtParam (ExPASy Proteomics Server: http://www.expasy.org/tools/protparam.html) and the antimicrobial peptide database ((http://aps.unmc.edu/AP/main.php). The secondary structures of the peptides were predicted online using the de novo peptide structure prediction server "PEP-FOLD 3.5" in the RPBS portal (http://mobyle.rpbs.univ-paris-diderot.fr/cgi-bin/portal.py#forms::PEP-FOLD3) [16] and three- dimensional structure projections were visualized using UCSF Chimera software v1.13 (University of California, San Francisco) [17]. The helical wheel projection was performed online using the NetWheels (http://lbqp.unb.br/NetWheels) [18].

2.4 Circular dichroism (CD) spectroscopy

CD spectra of the peptides at a concentration of 100 μg/mL were detected on a J-715 CD spectrophotometer (Jasco, Japan) equipped with a 1 mm path length quartz cell at 25 °C. Spectra were collected at a wavelength ranging from 190 to 250 nm in 10 mM PBS, 30 mM sodium dodecyl sulfate (SDS), 50% (v/v) 2,2,2-trifluoroethanol (TFE), and 0.1% *E. coli* LPS. The spectra were averaged from three runs per peptide and acquired data were converted to mean residue ellipticity (θ) in degrees.cm^2/dmol. The percentage of α-helical content of the peptides was then determined using DICHROWEB (http://dichroweb.cryst.bbk.ac.uk/) [19].

2.5 Bacterial strains and mammalian cells

Three strains of gram-positive bacteria (*Bacillus subtilis* [KCTC 3068], *Staphylococcus epidermidis* [KCTC 1917], and *Staphylococcus aureus* [KCTC 1621]) and three strains of gram-negative bacteria (*Escherichia coli* [KCTC 1682], *Pseudomonas aeruginosa* [KCTC 1637], and *Salmonella typhimurium* [KCTC 1926]) were procured from the Korean Collection for Type Cultures (KCTC) of the Korea Research Institute of Bioscience and Biotechnology (KRIBB). Methicillin-resistant *Staphylococcus aureus* strains (MRSA; CCARM 3089, CCARM 3090, and CCARM 3095) and multidrug-resistant *Pseudomonas aeruginosa* strains (MDRPA; CCARM 2095, and CCARM 2109) were obtained from the Culture Collection of Antibiotic-Resistant Microbes (CCARM) of Seoul Women's University in Korea. Vancomycin-resistant *Enterococcus faecium* (VREF; ATCC 51559) was supplied from the American Type Culture Collection (Manassas, VA, USA). RAW264.7 (mouse macrophage), NIH-3T3 (mouse embryonic fibroblast) and SH-SY5Y (human bone marrow) cells were purchased from the American Type Culture Collection (Manassas, VA).

2.6 Antimicrobial assay

Antimicrobial susceptibility of the designed peptides against standard bacteria, drug- resistant bacteria and yeast was studied according to guidelines of clinical and laboratory standards institute (CLSI) [20, 21]. Prior to assays, all strains were cultured overnight to stationary phase at 37 °C (for bacteria) and 28 °C (for yeast) in their respective medium. The overnight cultures were 10-fold diluted in fresh Muller-Hinton (MH) broth (Difco, USA) and grown for additional few hours at 37 °C and 28 °C to achieve mid-log phase growth. This mid-log phase cultures were diluted with MHB and added to sterile 96-well plates containing two-fold serially diluted peptides (from 2 to 128 μM) in 1:1 ratio to give final cell concentration of 2×10^6 CFU/wells. Melittin treated cells were used as positive control for both bacteria and yeast while untreated cells

were used as a negative control. The minimal inhibitory concentration (MIC) was defined as the lowest peptide concentration that causes 100% inhibition of microbial growth after incubation at 37 °C (for bacteria) and 28 °C (for yeast) for 24 h. In addition, the MICs of the peptides were also determined in the presence of different salts and human serum. 2×10^6 CFU/mL of *E. coli* (KCTC 1682), and *S. aureus* (KCTC 1621) were treated with peptides in MHB supplemented with different salts at their physiological concentrations (150mM NaCl or 4.5 mM KCl or 6 μM NH_4Cl or 1 mM $MgCl_2$ or 2.5 mM $CaCl_2$) or 20% human serum. Each test was reproduced at least three times using six replicates.

2.7 Hemolytic activity

The hemolytic activity of peptides was evaluated by measuring the amount of free hemoglobin by the lysis of erythrocytes using sheep red blood cells (sRBCs). Fresh sRBCs were washed three time with PBS (pH 7.2), centrifuged at 1000 × g for 5 min at 4 °C and re-suspended in PBS to attain a dilution of approximately 4% (v/v) of erythrocytes. A 50 µl portion of the erythrocyte suspension were incubated with 50 µl of serially diluted peptides (2-512 µM) dissolved in PBS for 1 h at 37 °C. After centrifugation (1,000 × g, 5 min, 4 °C), the supernatant was transferred to a new 96-well plate. Absorbance of supernatant (hemoglobin) was recorded using a microplate ELISA reader (Bio-Tek Instruments EL800, USA) at 540 nm. As a positive control, 100% hemolysis was induced by treating sRBCs with 0.1% Triton X-100. Melittin was used as a reference peptide. The value for "zero hemolysis" was determined using PBS. The percentage of hemolysis was calculated as follows:

$$hemolysis\ \% = \frac{Asample - APBS}{ATriton\ - APBS} \times 100$$

2.8 Cytotoxicity assay

To examine the cytotoxicity of the peptides RAW 264.7, NIH-3T3 and SH-SY5Y cells were cultured in Dulbecco's modified Eagle's medium (DMEM) supplemented with antibiotics (100 U/ml penicillin and 100 µg/ml streptomycin) and 10% fetal calf serum at 37°C in a humidified chamber under a 5% CO_2 atmosphere. Growth inhibition was evaluated using 3-(4,5-dimethylthizol-2-yl)-2,5-diphenyltetrazolium bromide (MTT) assays to measure cell viability. Briefly, the cells were seeded in 96-well plates (2×10^4 cells/well) and cultured for 24 h at 37 °C. Increasing concentrations of the peptides were added and allowed to react with the cells for 48 h, followed by the addition of 20 µl MTT (5 mg/ml in PBS) for another 4 h at 37 °C. Formazan crystals were dissolved by adding 40 µl of 20% (w/v) SDS containing 0.01 M HCl and incubating for 2 h. Absorbance at 550 nm was measured using a microplate ELISA reader (Molecular Devices, Sunnyvale, CA, USA). Cell survival was calculated using the following formula:

$$survival\ \% = \frac{A550\ of\ peptide - treated\ cells}{A550\ of\ untreated\ cells} \times 100$$

2.9 Quantification of nitrite and inflammatory cytokine production in LPS-stimulated macrophage cells

Peptide-induced inhibition of nitric oxide (NO) and pro-inflammatory cytokines production in LPS-stimulated macrophage cells were measured as previously described [22]. In brief, RAW 264.7 murine macrophage cells (2×10^6 cell/mL) were plated and adhered to a 96 well plates (100 μL/well) and stimulated with LPS from *E. coli* O111:B4 (20 ng/mL) in the presence or absence of peptides for 24 h. After 24 h incubation, the culture supernatant was collected and mixed with equal volume of Griess reagent (1% sulfanilamide, 0.1% naphthylethylenediamine dihydrochloride and 2% phosphoric acid) and incubated at room temperature for 10 min. Nitrite production was quantified by measuring absorbance at 540 nm, and concentrations were determined using a

standard curve generated with $NaNO_2$. Similarly, the release of pro-inflammatory cytokines were detected using DuoSet ELISA mouse TNF-α (R&D Systems, Minneapolis, USA) according to the manufacturer's protocol.

2.10 Reverse-transcription polymerase chain reaction (RT-PCR)

RAW264.7 cells were seeded into 6-well plates at 2×10^6 cells/well and stimulated with *E. coli* O111:B4 LPS (20 ng/mL) in the presence or absence of peptides. After incubation of 3 h (for TNF-α) and 6 h (for inducible nitric oxide synthase (iNOS)), total RNA was extracted using TRIzol® reagent (Invitrogen) and RNA concentration quantified using Nanodrop spectrophotometer (BioDrop, UK). cDNA was synthesized from 2 μg of total RNA using Oligo-$d(T)_{15}$ primers and PrimeScript Reverse Transcriptase kit (Takara, Japan) according to the manufacturer's protocol. The cDNA products were amplified using following primers: iNOS (forward 5´-CTGCAGCACTTGGATCAGGAACCTG-3´, reverse 5´-GGGAGTAGCCTGTGTGCACCTGGAA-3´); TNF-α (forward 5´-CCTGTAGCCCACGTCGTAGC-3´, reverse 5´-TTGACCTCAGCGCTGAGTTG-3´) and GAPDH (forward 5´-GAGTCAACGGATTTGGTCGT-3´, reverse 5´-GACAAGCTTCCCGTTCTCAG-3´) [23, 25]. The PCR amplification was carried out for initial denaturation at 94 °C for 5 min, followed by forty cycles of denaturation at 94 °C for 1 min, annealing at 55 °C for 120 sec and extension at 72 °C for 1 min, with a final extension at 72 °C for 5min. The PCR products were separated by electrophoresis and visualized under UV illumination.

2.11 Chequerboard assay

MRSA (CCARM 3095) and MDRPA (CCARM 2095) were used to investigate a possible synergistic effect of the peptides with chloramphenicol, oxacillin and ciprofloxacin. Initially, 2-fold serial dilutions of antibiotics and peptide solution were prepared and added in 1:1 ratio to 96-well plate. An equal

volume of bacterial solution (100 μL) at ~10^6 CFU/mL was added to each well. The plates were then incubated in a shaking incubator at 37 °C for 24 hours. Bacterial growth was assessed spectrophotometrically at A_{600nm} using microplate ELISA reader (EL800, Bio-Tek instrument). The fractional inhibitory concentration (FIC) index (FICI) was calculated as follows:

FICI = [(MIC of peptide in combination) / (MIC of peptide alone)] + [(MIC of antibiotic in combination) / (MIC of antibiotic alone)].

Where, FICI ≤ 0.5 is considered to indicate synergy; 0.5 < FICI ≤ 1.0 is considered additive; 1.0 < FICI ≤ 4.0 is considered indifferent; and FICI > 4.0 is considered antagonism.

2.12 Killing kinetics assay

Time-killing assays were performed by the broth macrodilution method, according to Clinical and Laboratory Standards Institute guidelines [24] Briefly, mid-log phase *E. coli* (KCTC 1682) was adjusted to 1×10^6 CFU/mL in MHB media and treated with peptides and antibiotics at 0.5× MIC and 1× MIC for 0 to 24h at 37 °C. At each time of exposure, 50 μL aliquots of mixture was diluted with fresh MHB media for tenfold (up to 1000 times), then 100 μL of diluted bacterial suspension was plated onto MH agar plates to obtain viability counts. Colonies were counted after incubation for 24 h at 37 °C. Killing curves were constructed by plotting log10 CFU/mL versus time over 24h. Bactericidal activity was defined as reduction of 99.9% (≥2.5 log10) of the total number of CFU/mL in original inoculum. Bacteriostatic activity was defined as maintenance of the original inoculum concentration or reduction of less than 99.9% (<2.5 log10) pf the total number of CFU/mL in original inoculum [25].

2.13 Morphological examination of bacterial cells

Mid-log phase of *E. coli* (KCTC 1682) was diluted to an OD_{600} of 0.05 and incubated with 1 × MIC of dCATH 12 analogs and antibiotics (Nalidixic acid and chloramphenicol) at 37 °C. OD measurements were taken at fixed interval for 4 hours. Bacterial smears prepared from 2 h control and peptide treated cells were Gram-stained and imaged under light microscope.

2.14 Calcein dye leakage assay

To determine the ability of peptides to permeabilize the bacterial membrane models, large unilamellar vesicles (LUVs) composed of egg yolk phosphatidylethanolamine (EYPE)/egg yolk phosphatidylglycerol (EYPG) (7:3, w/w) entrapped with calcein dye were prepared prepared by vortexing the dried lipid in a dye buffer solution (70 mM calcein, 10 mM Tris, 150 mM NaCl, 0.1 mM EDTA, pH 7.4) [26]. The suspension was subjected to 10 freezethaw cycles in liquid nitrogen and extruded 21 times through polycarbonate filters (2 stacked 100-nm pore size filters) with a LiposoFast extruder (Avestin, Inc. Canada). Untrapped calcein was removed by gel filtration on a Sephadex G-50 column. Peptide-induced membrane permeability was measured (excitation λ = 490 nm, emission λ = 520nm) by increase in fluorescence intensity of calcein released from LUVs upon addition of 2× MIC of peptides. Membrane-active peptides will instantly perturb the LUVs and cause a rapid release of the dye. Complete calcein release was obtained by using 0.1% Triton X-100.

2.15 Bacterial membrane depolarization assay

The ability of peptides to depolarize the intact *S. aureus* cytoplasmic membrane was determined using the membrane potential-sensitive cationic probe $DiSC_3$-5 as previously described [27]. Briefly, mid-log phase *S. aureus* (KCTC 1621) cells were harvested and washed three times with 5 mM HEPES buffer (pH 7.4, containing 20 mM glucose and 100 mM KCl) and the cells were resuspended to an A_{600nm} of 0.05 in same buffer and incubated with 20 nM $DiSC_3$-5 (Sigma, USA) until a stable reduction of the fluorescence was observed,

implying the complete intake of dye into cytoplasm. The peptides (2× MIC) were then added to bacterial suspension, and changes in fluorescence intensity were recorded (excitation λ = 622 nm, emission λ = 670 nm) using a RF-5301 PC spectrofluorophotometer (Shimadzu, Japan). 0.1 % Triton X-100 was added to completely dissipate the membrane potential. When added to the bacteria, $diSC_3$-5 is entered into the cytoplasmic membrane and its fluorescence is self-quenched under the influence of membrane potential. Upon disruption of the cytoplasmic membrane, $diSC_3$-5 is released into the buffer, resulting in an increase in fluorescence.

2.16 SYTOX green uptake assay

To assess the effects of the AMPs on bacterial membrane integrity, SYTOX green uptake assay was performed as previously described [14]. In brief, mid-log phase of *S. aureus* (KCTC 1621) was washed and resuspended to an A_{600nm} of 0.08 in 5 mM HEPES buffer (pH 7.4, containing 20 mM glucose and 100 mM KCl). To this bacterial suspension, 1 mM of SYTOX green dye (Thermo Fisher Scientific, USA) was added and incubated in dark for 10 to 15 min. Thereafter, the peptides (2× MIC) were added and release of SYTOX green was detected (excitation λ = 485 nm, emission λ =520nm) by increase in fluorescence. SYTOX green is a DNA-binding dye, which emits fluorescence when bound to nucleic acids. The dye permeates only the cells with a compromised plasma membrane. Thus, its accumulation inside cytoplasm indicates membrane permeabilization.

2.17 Membrane permeability assay

The hydrophobic fluorescent probe NPN (1-N-phenylnaphthylamine) was used to determine outer membrane permeability of gram-negative bacteria. Briefly, mid-log phase of *E. coli* (KCTC 1682) cells were washed thrice in 5 mM HEPES buffer (pH 7.4, containing 20 mM glucose and 5 mM KCN) and diluted to an A_{600nm} of 0.05 in same buffer. 1mM stock solution of NPN was

prepared by dissolving in acetone. From the stock solution, 30 μL was added to bacterial suspension to reach final concentration of 10 μM and the background fluorescence was recorded (excitation λ = 350 nm, emission λ = 420 nm) until the stable fluorescence was achieved. The peptides are added while increasing the concentration and the fluorescence was recorded with respect to time until there was no further increase in fluorescence. Similarly, the inner membrane permeability of peptides was assessed by measuring the release of β-galactosidase from *E. coli* ML-35 using ONPG (*o*-nitrophenyl-β-galactosidase) a nonchromogenic substrate for cytoplasmic β-galactosidase enzyme. Briefly, mid-log phase of *E. coli* ML-35 were suspended to an A_{600nm} of 0.5 in sample buffer (10 mM sodium phosphate, 100 mM NaCl, pH 7.4) containing 1.5 mM ONPG. The permeabilization of the inner membrane after addition peptides was assessed spectrophotometrically at 405 nm. Increase in fluorescence indicates the hydrolysis of ONPG to *o*-nitrophenol. The inner membrane permeability was determined by the influx of ONPG, that was subsequently cleaved into the yellow product *o*-nitrophenol by β-galactosidase in the cytoplasm.

2.18 Flow cytometry

The bacterial membrane integrity was assessed by flow cytometry as previously described [14]. Briefly, mid-log phase of *E. coli* (KCTC 1682) were washed thrice and diluted to 1 × 10^5 CFU/mL in 1× PBS. The peptides (2 × MIC) were added to the bacterial cell suspension at the fixed propidium iodide (PI) concentration (10 μg/mL) and incubated for 1h at 37 °C with agitation. The unbound dyes are washed with PBS and flow cytometry data were recorded using fluorescence-activated cell sorter (FACS Calibur, Beckman Coulter Inc., USA) at an excitation wavelength of 488 nm.

2.19 Zeta Potential Measurements

In order to investigate the ability of peptides to neutralize the the negative charge on cell membrane surface, zeta potential was measured by Zetasizer Nano ZS Instrument (Malvern, UK) at 25 °C as previously described [28]. The peptides were serially diluted to 1 to 64 μM using 0.5 mM potassium phosphate buffer (pH 7.4) to minimize any influence of pH. 100 μL of each peptide stock solution was added to 900 μL of *E. coli* cells at OD_{600} = 0.5. Filtered buffer without peptide is used as positive control. The bacterial suspensions were dispensed into disposable zeta cells s and allowed to equilibrate at 25 °C for 2 min.

2.20 Confocal laser-scanning microscopy

E. coli (KCTC 1682) (~10^6 CFU/mL) cells were incubated with FITC-labeled peptides (2× MIC) at 37 °C for 30 min, and bacterial cells were washed three times with 1× PBS. The cells were smeared into glass slide and intake of FITC-labelled peptides into bacterial cytoplasm was observed using a Zeiss Axioplan 2 optical microscope (Japan) with a 488 nm band-pass filter for excitation of FITC.

2.21 DNA-binding assay

Gel retardation experiments was performed to evaluate the ability of peptides to bind with intra-cellular DNA. In brief, 100 ng of bacterial plasmid pBR322 (Thermo Fisher Scientific, USA) were mixed with different concentrations of peptides in binding buffer (pH 8.0, 10 mM Tris buffer containing 5% glycerol, 50 μg/mL BSA, 1 mM EDTA, and 20 mM KCl). The mixture of DNA and peptide was incubated at room temperature for 1 h and then analyzed by 1% agarose gel electrophoresis in 0.5% TAE buffer. The plasmid bands were detected by UV illuminator (Bio-Rad, USA).

2.22 PI uptake assay

Alterations in membrane permeability was studied by measuring the change in fluorescence of PI in MRSA (CCARM 3090) as described earlier [29],

with slight modifications. Briefly, the cell suspension was prepared in a similar manner as in OD_{600} experiment with the only difference in the incubation time (24 h). Thereafter, cells were centrifuged; pellets were washed and re-suspended in PBS. Cells were treated with PI at 10 μM and aliquots of 3 ml were transferred and incubated in dark at room temperature for 15 min. With excitation wavelength of 535 nm and emission wavelength of 625 nm, PI fluorescence was monitored for 30 min using a RF-5301 PC Spectrofluorophotometer (Shimadzu, Japan).

2.23 Drug resistance assay

To explore the acquired resistance tendency of *S. aureus* (KCTC 1621) *to* TZP4 and ciprofloxacin, the drug resistance assay was assessed by sequential passages as previously described [30, 31]. MIC testing was firstly conducted for the peptides using the above methods. Then, the 0.5 × MIC well from the previous MIC assay plate was re-suspended and the bacteria was cultured in fresh MHB medium. The inoculum was subjected to the next passage MIC testing, and the process was repeated for 12 passages.

2.24 LPS binding assay

The ability of peptides to bind with LPS was determined using a fluorescent probe BODIPY-TR cadaverine (BC) (Sigma, USA) displacement assay as previously described [32]. Briefly, LPS from *E. coli* 0111:B4 (25 μg/mL) was incubated with BC (2.5 μg/mL) in a quartz cuvette containing 50 mM Tris buffer (pH 7.4). Peptides were added over 100 sec time interval and the fluorescence was recorded at an excitation wavelength of 580 nm and an emission wavelength of 620 nm with a RF-5301 PC Spectrofluorophotometer (Shimadzu, Japan). The values were converted to %ΔF (AU) using the following equation:

$$\%\,\Delta F\,(A.U.) = [(F_{obs} - F_0) / (F_{100} - F_0)] \times 100$$

where F_{obs} is the observed fluorescence at a given peptide concentration, F_0 is the initial fluorescence of BC with LPS in the absence of peptides, and F_{100} is the BC fluorescence with LPS cells upon the addition of 10 mg/mL polymyxin B (a prototype LPS binder) which is used as positive control.

2.25 Dissociation of LPS-FITC aggregates

The ability of peptides to disaggregate FITC-LPS oligomers was performed as described previously [33]. Briefly, FITC-LPS (1 μg/mL) was added in a quartz cuvette containing 1× PBS and background fluorescence was measured at emission of 515 nm using 5301 PC spectrofluorophotometer. After addition of different concentration of peptides, the variations in emission of FITC was recorded (excitation λ = 488 nm, emission λ = 512 nm). The emissions of both PBS and peptides alone were taken as positive control. Dissociation of the aggregates of FITC-LPS results in an increase in the fluorescence of FITC because of dequenching [34]. The changes in emissions were tracked until the system reached equilibrium.

2.26 Effect of peptides on LPS binding to macrophages

Ability of the peptides to bind to FITC-conjugated LPS (Sigma, USA) was performed as previously described [35]. Briefly, FITC-LPS (1 μg/mL) was incubated with peptides (10 μM final concentration) for 1 h at 4 °C, thereafter, 5×10^5 cells/mL of RAW264.7 macrophage cells are treated with FITC-LPS/peptide mixture and incubated at 37 °C for 30 min. The cells were then washed with ice cold PBS (pH 7.4) extensively to remove the unbound LPS. The binding of FITC-LPS to RAW264.7 cells was analyzed by measuring median fluorescence intensity using flow cytometry (FACS Calibur, Beckman Coulter Inc., USA). A prototype LPS binding inhibitor PMB (Polymyxin B) and LL-37 were used as positive control. Background fluorescence was assessed by using RAW 264.7 cells incubated without FITC-LPS or peptides. Data are from one of five separate experiments.

2.27 Effect of peptides on receptor bound LPS

RAW264.7 macrophage cells (5×10^5 cells/mL) were incubated for 1h with FITC-LPS (1 μg/mL) in absence of peptides. The pre-incubated cells were washed three times with 1× PBS to remove unbound LPS. The peptides were then added to the cells and incubated for additional 1h and then washed again. The binding of FITC-LPS to RAW264.7 cells after treatment of peptides was analyzed by flow cytometry.

2.28 Statistical analysis

All statistical analysis in this study was performed with SPSS 16.0 software using one-way analysis of variance (ANOVA). The data are expressed as the means ± standard deviation (SD) from at least three independent experiments. Differences with a P-value of less than 0.05 were considered statistically significant.

3. Results

3.1 Peptide design and synthesis

To develop short α-helical AMPs exhibiting potent antimicrobial and anti-inflammatory activities, we designed 12-meric analogs from N-terminal truncation and C- terminal amidation of dCATH AMP, as listed in Table 1. The parent peptide, dCATH is a 20-residue AMP made up of 10 hydrophobic residues and 7 positively charged residues. Initially, four analog peptides were designed by truncating two, four, six, and eight amino acids at the N-terminal ends of dCATH peptide. dCATH and its truncated analogs could not adopt the amphipathic α-helical structure since the hydrophobic and charged residues were dispersed all around the molecule. However, the 12-meric analog dCATH 12 has an amphipathic structure as a whole, except one hydrophobic residue, Ile (I3), and one cationic residue, Arg (R12), that are located in polar and non-polar faces, respectively (Fig. 1A). This dodecamer variant represents an optimal length for inducing antimicrobial properties, while still allowing peptides to retain amphipathic secondary structures. Previous studies have reported that dodeca AMPs derived from long cathelicidin AMP, such as LL-37, showed potent antimicrobial and anti-inflammatory activities [9, 36]. Therefore, we fixed dCATH 12 as an ideal template and further modified it into five analog peptides in order to retain uninterrupted facial amphipathicity. The analog peptides were designed based on the α-helical-wheel diagram and three-dimensional projections of dCATH 12 (Fig. 1). First, dCATH 12-1 was designed by replacing Ile (I3), present in the polar face of dCATH 12, with Lys (K3) to increase the net positive charge. Selection of Lys over Arg, as a polar residue, was due to its high helical propensity and lower cytotoxicity [37]. In addition, the introduction of cationic side chains, Lys, has been reported to promote interactions with negatively charged bacterial membranes [38]. dCATH 12-2 was obtained from dCATH 12-1 by substituting Arg (R12) with Trp (W12) at the boundary of the hydrophobic face to increase hydrophobicity and improve membrane insertion. It has been reported that addition of Trp residues to AMPs displayed more potent antimicrobial activity than other

hydrophobic residues such as Leu, Ile, Phe, and Tyr [39]. Furthermore, to achieve a perfect amphipathic helix, dCATH 12-3 and dCATH 12-4 were designed by substituting Lys (K8) and Ile (I2) in place of Ala (A8 and A2). Several previous studies have suggested that AMPs, containing more Trp side chains in the hydrophobic phase, may induce efficient interaction with microbial membrane surfaces, allowing them to partition well into the bilayer interface. This is due to presence of indole ring in Trp interacting with the interfacial region of membrane [39]. For this reason, dCATH 12-5 was designed by replacing Ile (I2) with Trp (W2), which resulted in desired amphipathic structure with three Trp side chains. All the analog peptides were amidated at the C-terminus to increase their antimicrobial activity and helix stability [40].

3.2 Characterization of peptides

The purity (95% <) and molecular weight of the designed AMPs were verified by RP-HPLC and ESI-MS, respectively. As shown in Table 1, the measured molecular weights of each peptides concurred with the theoretically calculated values, indicating successful peptide synthesis. All synthetic peptides were found to be cationic in nature. The hydrophobicity of designed AMPs was reliably reflected by different HPLC retention times (R_t). For all the dodeca analog AMPs, the values of the hydrophobic moment (μH), which determines the degree of amphipathicity of α-helical peptides, were consecutively enhanced from 0.505 to 0.971. This observation suggested an improved equilibrium between the hydrophobicity and hydrophilicity when compared with the native peptide, dCATH.

3.3 Secondary structure of peptides

The secondary structures of the designed dodeca AMPs in membrane-mimetic environments were investigated using CD spectroscopy (Fig. 2) and the α-helical content (%) of each AMPs in 50% TFE (hydrophobic environment of microbial membrane), 30 mM SDS (negatively charged microbial membrane), and

0.1% LPS micelles (outer surface of microbial membrane) are shown in Table 2. dCATH 12 and its mutant analogs adopted a clear random coil conformation in aqueous buffer, having a negative minimum between 190 and 220 nm. In contrast, all peptides took α-helical conformation in membrane-mimetic environments exhibiting considerable negative minima at 208 and 222 nm. Among the 12-meric analog AMPs, Trp rich dCATH 12-4 and dCATH 12-5 displayed high helicity in all membrane-mimetic environment with highest α-helical conformation observed (42.8% and 40.4% respectively) in 0.1% LPS. The above results were consistent with the predicted secondary structure (Fig. 1B). These results suggest that secondary structure formation in the membrane-mimetic environment demonstrates the ability of the peptides to interact with the bacterial membrane.

3.4 Biocompatibility assays

The cytotoxicity of the engineered peptides against mammalian cells was tested by measuring their ability to cause lysis of sheep red blood cells (sRBCs) and by determining the survival rate of mammalian cells. The toxicities of dCATH peptide and its analogs against sRBCs are shown in Fig. 3A and 3B. All tested peptides exhibited negligible or no hemolytic activity at higher concentration (256 μM), while the parent peptide, dCATH and its counterpart analog, dCATH 18 induced 40% and 100% hemolysis at 64 μM, respectively. Subsequently, we evaluated the viability of RAW 264.7 macrophage cells (Fig.32C & D) and NIH-3T3 fibroblast cells (Fig. 3E & F) in response to peptide treatment. Similar to the hemolysis results, dCATH and dCATH 18 eliminated approximately 40-50% of both RAW 264.7 and NIH-3T3 cells, even at 10 μM concentration. Meanwhile, all the designed analog peptides showed <10% cytotoxicity at 20 μM, except for dCATH 16 which resulted in 35% and 50% cytotoxicity, respectively. Melittin, on the contrary, displayed toxicity against all cells, including sRBCs (erythrocytes), even at very low concentration. Cytotoxicity exhibited by dCATH and its analogs tended to increase with their respective hydrophobicity (R_t). As presented in Table 1, dCATH and dCATH 18 exhibited higher hydrophobicity (R_t = 26.8 and 29 min,

respectively) and lower amphipathic moment (μH=0.431 and 0.426, respectively) and thus induced higher toxicity compared to other analogs. These findings confirmed that the length of the peptide and hydrophobicity were highly correlated with its cytotoxicity.

3.5 Antimicrobial activity and cell selectivity

The antimicrobial activities of dCATH AMP and its derived analogs against clinically relevant gram-negative and gram-positive bacteria, fungi, and several antibiotic-resistant bacteria were tested in terms of bacteriostatic inhibitory concentrations, indicated by minimum inhibitory concentration (MIC) (Table 3). The geometric means (GM) of MICs was calculated to evaluate the average antimicrobial effect of each peptide against all the tested pathogens (Table 4). The native AMP dCATH and its truncated analogs effectively inhibited microbial growth over a range of concentrations close to that of melittin (GM_{all} = 16.4 μM). Among the 12-meric analogs, the Trp rich AMPs dCATH 12-3, dCATH 12-4, and dCATH 12-5, with perfect amphipathic structure, demonstrated two to three-fold increased antimicrobial potency against both bacterial and fungal species compared to the parent peptide, dCATH 12. These data suggested that the folding of peptide into amphipathic helix and inclusion of multiple Trp residues significantly enhanced the antimicrobial activity of the peptides. Additionally, MICs of LL-37, buforin-2 and other conventional antibiotics against selective strains was presented in Table 5.

Based on the antimicrobial and hemolytic activities, the cell selectivity of AMPs towards the negatively charged microbial cell membranes and the zwitterionic mammalian cell membranes was evaluated by calculating the therapeutic index (TI) (Table 4). The TI is defined as the ratio of the HC_{10} to the geometric mean of the MIC (GM), where HC_{10} is the peptide concentration required to induce 10% hemolysis. A larger TI value indicates higher cell selectivity. Of all the designed AMPs, dCATH 12-4 and dCATH 12-5 displayed the highest TIs against all strains of bacteria and fungi (TI_{all} = 80.0 and TI_{all} = 89.8, respectively) which was ≈200-

225 times greater than the TI of the native peptide, dCATH (TI_{all} = 0.4). These results indicate that dCATH 12 and its counterpart analog peptides are potent antibiotics with high antimicrobial activity and low toxicity. Although dCATH and melittin showed relatively similar MICs, the higher hemolytic activity displayed by both peptides made them less desirable candidates for therapeutic applications. Therefore, the dodeca AMP, dCATH 12 and its analogs were selected and further examined for their anti-inflammatory properties at peptide concentrations less than or equal to 10 μM.

3.6 Inhibition of NO and inflammatory cytokine production in LPS-stimulated macrophages

NO and TNF-α are two important inflammatory products that are mainly associated with promotion of the inflammatory response. To assess anti-inflammatory activity of dCATH 12 and its analogs, we measured their abilities to inhibit nitric oxide (NO) production and pro-inflammatory cytokine (TNF-α) production in LPS-stimulated RAW 264.7 cells. As illustrated in Fig. 4A, at the concentration of 5 μM, dCATH 12-4 and dCATH 12-5 efficiently inhibited nitrite production by 51.4% and 91.6% (data not shown) respectively, while dCATH 12 and its other mutated analogs displayed less than 10% reduction in nitrite release. Similarly, the effects of peptides on the production of representative pro-inflammatory cytokine, TNF-α were determined by sandwich ELISA (Fig. 4B). At a concentration of 10 μM, dCATH 12-4 and dCATH 12-5 displayed 47.3% and 65% inhibition of TNF-α production, respectively. However, dCATH 12 and other analog peptides showed less than 10% of inhibition of TNF-α.

To further evaluate the effect of dCATH 12-4 and dCATH 12-5 on LPS-induced activation of iNOS and TNF-α mRNA expression, a semi-quantitative RT-PCR was performed. Expression of iNOS and TNF-α mRNA increased significantly after RAW 264.7 was exposed to LPS (20 ng/mL). However, after treatment with these peptides, mRNA expression of LPS-induced iNOS and TNF-α was found to be significantly decreased (Fig. 4C & 4D). Compared to LL-37, a well-studied

endotoxin neutralizer, dCATH 12-5 showed efficient inhibition in mRNA expression of both iNOS and TNF-*α*. In contrast, dCATH 12-4 exhibited comparatively less inhibition in gene expression than dCATH 12-5. These data are in agreement with the observed inhibition of NO and TNF-*α* production by peptides. Considering their antimicrobial and anti-endotoxin properties, dCATH 12-4 and dCATH 12-5 were chosen for further evaluation by functional characterization.

3.7 Salt and serum sensitivity assays

The antimicrobial activities of most AMPs were reported to be different in the presence or absence of physiological salts [41]. Hence, we investigated the influence of salts on antimicrobial activity of selected analogs against *E. coli* and *S. aureus*. As shown in Table 6, the addition of monovalent (Na^+, K^+, and NH_4^+), divalent (Mg^{2+} and Ca^{2+}), and trivalent (Fe^{3+}) cations had partial or no effect on the antimicrobial activity of the AMPs. Serum stability of the selected AMPs was also analyzed to make sure whether the peptides could be degraded by proteases in serum or interact with the serum components. After incubating with 20% fresh human serum, activities of both dCATH 12-4 and dCATH 12-5 remained unchanged or slightly decreased. Such extraordinary stability in mammalian serum and the strong salt-tolerant property indicate the potential of these peptides for systemic therapeutic applications.

3.8 Synergy with conventional antibiotics

The synergistic effects of dCATH 12-4 and dCATH 12-5 AMPs with three conventional antibiotics, chloramphenicol, ciprofloxacin, and oxacillin, were investigated against multi-drug-resistant *Pseudomonas aeruginosa* (MDRPA) and methicillin-resistant *Staphylococcus aureus* (MRSA), using a checkerboard assay. The FICI data for peptide-antibiotic combinations are summarized in Table 7. Overall, dCATH 12-4 and dCATH 12-5 showed effective synergistic effect (FICI range: 0.313 ~ 0.5) with all three antibiotics against MRSA and MDRPA. However,

the control peptide, LL-37 did not work synergistically with any antibiotic (FICI range: 0.75 ~ 1.25). Overall, the results revealed that, dCATH 12-4 and dCATH 12-5 could serve as potential feed additives for reducing the dose of antibiotics.

3.9 Time-killing kinetic assay

To evaluate whether the peptides have a bacteriostatic or bactericidal effect, a time-killing kinetics of *E. coli* exposed to selected peptides and antibiotics at their MIC and 0.5 × MIC was performed. Bactericidal antibiotic nalidixic acid and bacteriostatic drug chloramphenicol were used as a control. As depicted in Fig. 5A, incubation of *E. coli* cells with dCATH 12-4 and dCATH 12-5 at concentration of 0.5 × MIC resulted in bacteriostatic effect with reduction in bacterial cell counts less than 3 $\log_{10}$ CFU/mL, whereas nalidixic acid and chloramphenicol failed to decrease the bacterial cell count at 0.5 × MIC. In contrast, dCATH 12-4 and dCATH 12-5 exhibited good bactericidal activity than nalidixic acid at their MIC concentrations as can be seen by reduction in bacterial cell counts to less than 2 $\log_{10}$ CFU/mL after three hours of peptide treatment. Meanwhile, the bacteriostatic antibiotic chloramphenicol maintained its bacterial count even after 12 hours of incubation, further confirming its bacteriostatic activity. Collectively, these observations revealed that dCATH 12-4 and dCATH 12-5 mediate bacterial killing through bactericidal mechanism of action at their MIC and bacteriostatic mechanism at 0.5 × MIC.

3.10 Bacteriolysis and morphological examination of E. coli cells.

Ability of peptides to lyse *E. coli* cells was monitored by measuring the optical density (OD_{550}) of the culture incubated with 1 × MIC of peptides (Fig. 6A). The OD_{550} of bacterial culture treated with Nalidixic acid, dCATH 12-4 and dCATH 12-5 was found to be increasing with time and after 3 h incubation, the turbidity was reduced to 90%. However, the bacteriostatic drug chloramphenicol did not showed any reduction when treated at MIC concentration. Treatment with membrane disrupting peptide melittin showed no increase in OD and culture

turbidity was drastically reduced over time. Microscopic images of *E. coli* cells treated with Nalidixic acid and dCATH 12 analogs resulted in filamentation of cells after 2 hours of treatment (Fig. 6B). Thus, the increase in OD_{550} in peptides treated cells can be attributed to formation of filaments.

3.11 Drug resistance assay

We next investigated whether a reference strain of *S. aureus* (KCTC 1621) would evolve drug resistance after multiple exposures to dCATH 12-4 and dCATH 12-5 at 0.5 × MIC (Fig. 7). After 12 passages, while the MICs of ciprofloxacin increased by 64-fold for *S. aureus* (KCTC 1621), while the MICs of dCATH 12 analogs increased by 4-fold. This result indicated selected peptides can hardly develop drug resistance unlike ciprofloxacin.

3.12 Mechanism of antimicrobial action

3.12.1 Membrane permeability and integrity assays

Most of the cationic AMPs primarily targets bacterial membrane and induce cell death via membrane disruption. In order to investigate the mechanism of antimicrobial action of selected dodeca AMPs, we first evaluated the peptide-membrane interaction by measuring the release of the fluorescent marker, calcein from large unilamellar vesicles (LUVs) that mimic the membranes of the gram-negative bacteria (EYPE:EYPG=7:3, w/w). In addition to this, we also studied the effects of AMPs on membrane permeability and integrity of *S. aureus* and *E. coli* using several fluorophore-based studies including cytoplasmic membrane depolarization using $diSC_3$-5, cytoplasmic membrane uptake of SYTOX green dye, outer membrane permeability using NPN inner membrane permeability using ONPG. Highly membrane-active peptides will instantly perturb the bacterial membrane and cause a rapid release of the dyes, which results in increase of the fluorescence intensity. As shown in Fig. 8, at their 2 × MIC, the pore-forming or membrane disrupting peptides, such as melittin and LL-37, induced a rapid and complete dissipation of bacterial membrane. On the contrary, dCATH 12-4,

dCATH 12-5, and buforin-2 (potent intracellular targeting peptide) were found to be ineffective in disrupting the membrane even at higher concentrations (16 μM). Collectively, these results indicate dCATH 12-4 and dCATH 12-5 do not interact with either outer or inner membranes of gram-negative bacteria.

3.12.2 Surface disruption and internalization of dCATH 12 analogs

Flow cytometry analysis was employed to further characterize the membrane integrity of bacterial cell after peptide treatment. Propidium iodide (PI) fluorescently stains the nucleic acids of cells, following cytoplasmic membrane disruption. In the absence of peptide, the *E. coli* cells exhibited only 9.8% PI fluorescent signaling, thus indicating viable cell membranes (Fig. 9). Treatment with membrane-targeting AMPs, such as melittin and LL-37 resulted in 71.88% and 70.07% of PI uptake, respectively. In contrast, at 2 × MIC, dCATH 12-4 and dCATH 12-5 exhibited very low PI fluorescent signals of 9.53% and 6.31%, respectively. This observation can be correlated with intracellular-targeting AMP, buforin-2 which exhibited 4.17% of PI fluorescence. These results suggest that the dCATH 12-4 and dCATH 12-5 do not target cytoplasmic membrane or cause disruption in membrane integrity.

3.12.3 Surface charge neutralization

Zeta potential measurement was performed in order to study the effect of the peptides on *E. coli* membrane surface charges. As shown in **Fig. 10**, the *E. coli* cells showed a zeta potential of -31.3 ± 0.50 mV in the absence of the peptides. Upon addition of increasing concentration of membrane disrupting peptide melittin, the *E. coli* zeta potential values increased and rapidly neutralized at concentration of 8μM for ~ 4.2 mV. In contrary, both dCATH 12-4 and dCATH 12-5 did not tend to neutralize the surface charge even at 64 μM. Similar result was observed with intracellular targeting peptide buforin-2. These findings indicate that despite having high charge, dCATH 12-4 and dCATH 12-5 does not have any effect in neutralizing the negative charge in bacterial surface.

3.12.4 Confocal Laser-Scanning Microscopy

In order to determine the ability of peptides to translocate across bacterial membrane without disrupting them, *E. coli* cells were incubated with fluorescein isothiocyanate (FITC)-labelled dCATH 12-4, dCATH 12-5, and buforin-2 and their localization was observed using confocal laser-scanning microscopy (Fig. 11A). Similar to buforin-2, dCATH 12-4 and dCATH 12-5 penetrated the membrane of *E. coli*, and accumulated in the cytoplasm of the bacterial cells. This was confirmed by detection of green fluorescence inside the bacterial cells, indicating the internalization of FITC-labeled peptide into the cytoplasm of the bacteria.

3.12.5 DNA-binding assay

From the previous results, it is evident that dCATH 12-4 and dCATH 12-5 AMPs inhibit bacterial growth by translocating into cell membrane, without causing membrane disruption. This suggests that selected dodeca analogs could possibly target intra-cellular components, such as DNA. In order to assess this speculation, binding of peptides to *E. coli* DNA (pBR322) was detected using gel retardation electrophoresis assay. DNA binding was determined as a shift in the plasmid DNA bands. As depicted in Fig. 11B, complete retardation of the *E. coli* DNA was observed at 8 μM for both dCATH 12-4 and dCATH 12-5, and 16 μM for buforin-2, a well-known DNA binding peptide.

3.12.6 Effects of combinations of dCATH 12-5 with antibiotics on propidium iodide uptake of MRSA (CCARM 3090)

Since PI shows enhanced fluorescence only when it binds to DNA, therefore, we have evaluated the effect of peptide–antibiotic combination of membrane integrity using PI uptake assay. Cells treated with combination of dCATH 12-5 (1/8 MIC) and antibiotic (1/4 MIC) showed a significant increase in the PI fluorescence after 24 h whereas negligible PI fluorescence was observed in cells treated with either dCATH 12-5 alone (1/4 MIC) or antibiotic alone (1/4 MIC)

and untreated cells (**Fig. 12**). These results suggested that the combination of dCATH 12-5 and antibiotic caused loss of membrane integrity of MRSA after 24 h incubation and membrane became more permeable. Hence, cellular material such a DNA exposed to PI when added after 24 h of incubation and showed enhanced fluorescence.

3.13 Mechanism of anti-inflammatory activity

3.13.1 LPS binding assay

To assess whether the inhibition of NO and TNF-α production and their gene expression in LPS-stimulated RAW 264.7 cells was due to direct neutralization of LPS by designed AMPs, we investigated the LPS binding affinity of dCATH 12-4 and dCATH 12-5, using the BODIPY-TR-cadaverine (BC) displacement assay (Fig. 13). Initially, the BC fluorescence is quenched when it accumulates on cell-free LPS, but the introduction of the active peptides (LPS-binding peptides) molecularly displaces BC and its quenching is alleviated, indicating successful binding of peptides with LPS. As illustrated in Fig. 13, dCATH 12-5 produced a stronger dose-dependent enhancement in fluorescent intensity than its parent peptide, dCATH 12, and LL-37 (potent LPS-neutralizing agent). At 10 μM, dCATH 12-5 displayed ~75% binding to LPS while LL-37 showed 68% binding. On the contrary, dCATH 12-4 was found to be less effective in binding with LPS than dCATH 12-5. However, it displayed 68% binding at 20 μM.

3.13.2 Dissociation of FITC-LPS aggregates

LPS forms aggregates in aqueous suspension which are subsequently monomerized by LBP and transferred to CD14 receptors of macrophage cells. All LPS-neutralizing compounds are known to dissociate the LPS aggregates [42]. We investigated the ability of dCATH 12 and its analogs to dissociate the *E. coli* 0111:B4 FITC-LPS aggregates. The fluorescence of FITC-LPS aggregates is self-quenched but should increase when the aggregates dissociate. The dose-dependent

effect of the peptides on LPS-FITC fluorescence is shown in Fig. 14. The data revealed that dCATH 12-4, dCATH 12-5, and LL-37 showed strong effects in dissociating FITC-LPS aggregates at increasing concentrations. On the contrary, the parent peptide, dCATH 12 induced slight increase in the dissociation effect (~ 2 μM) which diminished as the concentration increased. These observations are in agreement with the results from LPS-peptide binding test. In contrast, a well-studied LPS binder, Polymyxin B (PMB) failed to disaggregate LPS even at higher concentrations.

3.13.3 Effect of peptides on FITC-LPS binding to RAW264.7 cells

When FITC-conjugated LPS is incubated with macrophage cells in the presence of serum, it binds to the cells via the action of LBP present in serum. To examine the effects of dCATH 12 and selected analogs on the binding of *E. coli* 0111:B4 FITC-LPS to RAW 264.7 cells, detailed flow cytometric studies were performed. As shown in Fig. 15A, pre-incubation of FITC-LPS with dCATH 12-4 and dCATH 12-5 markedly suppressed the binding of LPS to RAW 264.7 cells, implying successful peptide-LPS binding. Similar results were observed with LL-37 and PMB. In contrast, the parent peptide, dCATH 12 did not significantly inhibit the binding of LPS to the cells.

3.13.4 The ability of peptides to remove LPS bound to CD14

In order to investigate the ability of peptides in neutralizing the receptor-bound LPS, RAW264.7 macrophages were pre-incubated with FITC-LPS for 1 h. The cells were then washed and treated with peptides. As shown in Fig. 15B, all the peptides except for dCATH 12 and PMB significantly displaced the receptor bound-LPS. These findings indicate that dCATH 12-4 and dCATH 12-5 neutralize LPS by directly binding to LPS as well as by competing with it on their respective receptors (CD14 or TLR4). Similar results were observed with LL-37. However, the parent peptide, dCATH 12 and prototype LPS, inhibitor PMB were not able to disintegrate the LPS after its binding to receptor. These observations are consistent

with the previous studies suggesting that LL-37 neutralizes LPS by direct binding and by inhibiting their action on CD14 receptor [35, 43], whereas PMB which has higher affinity towards gram-negative bacterial membrane, can neutralize only the free LPS and not the receptor bound LPS [22, 44].

4. Discussion

Over the past decades, a rapid increase in antimicrobial resistance has become an overwhelming hurdle in the development of new antibiotics. Recently, antimicrobial peptides (AMPs) or host defense peptides (HDPs) have received widespread attention as a novel class of antibiotics due to their broad-spectrum activity against a wide range of microbial pathogens, such as gram-negative and gram-positive bacteria, MDR bacteria, fungi, parasites, and even, enveloped viruses. The net positive charge and amphipathicity of AMPs are important prerequisites for antimicrobial action, which allow the peptides to insert into the lipid bilayer of negatively charged bacterial membranes [45]. Many reports indicate that natural or synthetic AMPs, with longer amino acid chains, are mostly associated with increased cytotoxicity [46]. Hence, short peptides are commonly preferred for therapeutic applications, not only due to their less expensive synthesis but also due to their lower toxicity. In particular, 12-meric analogs derived from natural peptides, have proven to be more effective against microbial pathogens than without inducing toxicity towards mammalian cells [47].

Considering these features, we attempted to develop short dodeca α-helical AMPs from 20-residue duck cathelicidin, dCATH peptide, with enhanced cell selectivity without loss of antimicrobial potency. As explained earlier in the results, N-terminal amino acid residues of dCATH were truncated in order to achieve 12-meric short AMP, named dCATH 12. Several studies revealed that peptides with perfectly segregated hydrophobic and cationic faces increase antimicrobial potency with high cell selectivity [9]. Therefore, we aimed at optimizing the α-helix structure of dCATH 12 to achieve uninterrupted facial amphipathicity. Accordingly, a series of short peptide variants were designed by modifying dCATH 12 on the basis of α-helical wheel diagram (Fig. 1). We adopted rational design strategies, gathered from previous studies, which included the following: (1) maintaining the short sequence length of 12 amino acid residues with charge above +5; (2) replacing the hydrophobic amino acids in polar face with Lys and charged amino acids in non-polar face with Trp or Ile, in order to increase charge and

hydrophobicity [48]; (3) maximizing of hydrophobic moment with three fixed Lys residues and Trp residues to enhance the propensity of α-helix formation [49]; (4) incorporation of amino acids possessing helix-forming tendencies rather than helix-breaking tendencies [37]. Lys residues were speculated to intensify peptide interactions with negatively charged bacterial membranes, while bulky hydrophobic side chains, comprising multiple Trp residues were hypothesized to provide lipophilic anchors that could facilitate membrane insertion.

CD spectra data (Fig. 2) revealed that among the designed 12-meric analog AMPs, Trp rich dCATH 12-4 and dCATH 12-5 adopted high α-helical conformation in all membrane-mimicking environments (Table 2) suggesting its strong interaction with the membrane. When interacting with biological membrane, the indole ring present in Trp side chains tends to partition near the membrane-water interface. Previous studies have suggested that antimicrobial activity of AMPs was correlated with its propensity to form the α-helix structure [50]. Justifying this hypothesis, dCATH 12 and its counterpart analogs displayed excellent antimicrobial activity compared to melittin (Tables 3 & 4). With respect to geometric mean (GM_{all}) values, the dodeca analogs with idealized facial amphipathicity, including dCATH 12-3, dCATH 12-4, and dCATH 12-5, showed 2 to 3-folds stronger antimicrobial activity than that of the parent, dCATH 12. While dCATH 12-1, whose amphipathicity is disrupted by the presence of Arg (R12) in hydrophobic face, displayed comparatively less antimicrobial activity. These data suggested that the disruption of amphipathicity can decrease the antimicrobial activity of AMPs to a slight extent. In addition to this, the reduction in hydrophobicity of dCATH 12-1 (R_t = 14.4) also may be the reason for the reduced antimicrobial activity. Overall, this study revealed that amphipathicity and hydrophobicity are the key regulators of antimicrobial function. However, the antimicrobial activity of AMPs could not be used as the only criterion to be a strong candidate for treatment. Hemolysis and cytotoxicity of peptides to host cells were considered to be a major limitation to the application of AMPs in human therapeutics. As hypothesized on the basis of their short length of amino acids,

dCATH 12 and its mutated analogs exhibited minimal or no toxicity towards erythrocytes or other mammalian cells. Whereas, the native peptide dCATH and melittin, displayed high hemolysis and cytotoxicity (Fig. 3). The cell selective properties of designed AMPs towards the negatively charged bacterial membrane over zwitterionic mammalian cell membranes was evaluated by calculating TI. Among all the designed analogs of AMPs, dCATH 12-5 showed high cell selectivity, with a TI value of 89.8, which was ≈3 fold higher than the parent fragment, dCATH 12 and ≈225 fold higher than the 20-residue parent peptide, dCATH. The reduced cell selectivity of dCATH and melittin could be attributed to their length of sequence and increased hydrophobicity.

Even though, the dCATH 12-4 and dCATH 12-5 analogs were found to be therapeutically effective in combating antibiotic-resistance bacteria, most of the antimicrobial agents face a major bottleneck when it comes to therapeutic application since they are known to induce inflammatory response in mammalian cells [51]. The outer membrane of the gram-negative bacteria is comprised of LPS, an anionic glucosamine-based phospholipid. Killing of gram-negative bacteria by any antimicrobial agents results in the release of LPS into the blood stream. LPS aggregates into oligomers induce the monocytes and macrophages to secrete large amounts of pro-inflammatory cytokines, including TNF-α, IL-6, and IL-1β, which in turn contribute to the pathophysiology of septic shock and other immune diseases. For this reason, much attention has been focused on development of novel cationic AMPs that possess both antimicrobial and LPS-neutralizing abilities. Recent studies have found that human cathelicidin, LL-37 and its counterpart analog peptides show potent antimicrobial and anti-inflammatory activities [13]. In this study, we investigated the effects of dCATH 12 peptide and its analogs on LPS-induced macrophage inflammation. The results herein showed that dCATH 12-4 and dCATH 12-5, which are rich in Ile and Trp, significantly inhibited NO and pro-inflammatory mediator, TNF-α secretion and their mRNA expression induced by *E. coli* LPS in RAW 264.7 macrophage cells (Fig. 4). In contrast, the parental peptide, dCATH 12, failed to attenuate the LPS-induced cytokine response.

Interestingly, dCATH 12-3 which had difference of only one amino acid (Ala [A2]) from dCATH 12-4 and dCATH 12-5, also failed to inhibit NO and TNF-α release. This indicates the importance of substituting Ile (I2) and Trp (W2) in dCATH 12-4 and dCATH 12-5, respectively. Given its potent antimicrobial, anti-inflammatory, and cell selective properties, we chose these two dodeca AMPs for further studies to evaluate their therapeutic potential in detail.

A major limitation for the use of cationic AMPs for clinical applications is their possible inactivation in the presence of physiological salts and human serum [52]. It is evident that the charge of any cationic compound will be affected in a higher ionic strength environment. Likewise, it is also reported that cationic AMPs, whose function is highly dependent on the electrostatic interaction with negatively charged bacterial membrane, may also be disturbed in presence of physiological concentration of salts. However, in this study, both dCATH 12-4 and dCATH 12-5 analogs maintained its antimicrobial activity in presence of physiological salts and 20% human serum (Table 6). Interestingly, we also observed that both peptides exerted improved antimicrobial activity against *E. coli* in the presence of monovalent cations (Na^+, K^+ and NH_4^+). This salt-resistance displayed by the designed peptides can be explained by the high net positive charge of the AMPs, which evades the counter effects of cations and facilitate peptide-membrane interactions [53]. Another possibility is that, the incorporation of Trp residues in hydrophobic face of peptides could enhance the affinity of AMPs for the bacterial membrane [54]. These observations suggest that the resistance of dCATH 12-4 and dCATH 12-5 to salts and serum indicate their promising roles for future therapeutic use to treat bacterial infections.

The increase in antibiotic-resistant bacterial infections has serious implications on the future of healthcare. As discussed earlier, both dCATH 12-4 and dCATH 12-5 exerted significant antimicrobial activity against all tested resistant bacterial strains (Table 3). In order to evaluate application of designed AMPs in combination with conventional antibiotics, we investigated their synergistic effects in combination with three conventional antibiotics with different

mechanism of antimicrobial actions. Chloramphenicol is a bacteriostatic broad-spectrum antibiotic that inhibits bacterial protein synthesis through binding with the bacterial 50S ribosomal subunit. Ciprofloxacin is a broad-spectrum fluoroquinolone that acts by inhibiting DNA gyrase and topoisomerase types II and IV, and oxacillin is a narrow-spectrum β-lactam antibiotic that inhibits bacterial cell wall synthesis. The checkerboard assay data demonstrated that both dCATH 12-4 and dCATH 12-5 showed greater synergistic effect with all three antibiotics against MDRPA and MRSA. However, the control peptide LL-37 did not reach the cutoff value to be considered as synergistic with any of the tested antibiotics (Table 7). The reduction of MIC of antibiotics could be due to the increased membrane permeability of MRSA or MDRPA in the presence of the peptide. To prove this hypothesis, the PI uptake assay for antibiotic-dCATH 12-5 combination and dCATH 12-5 or antibiotic alone was performed. The fluorescence intensity of PI in each antibiotic-dCATH 12-5 combination (chloramphenicol–dCATH 12-5, ciprofloxacin–dCATH 12-5 and oxacillin–dCATH 12-5 combinations) provided increased fluorescence as compared to either dCATH 12-5 or antibiotic alone (Fig. 12). Therefore, we demonstrated that dCATH 12-4 and dCATH 12-5 as adjuvant, significantly improved the sensitivity of antibiotics to overcome the antimicrobial resistance and has a strong potential to be used with variety of antibiotics for the treatment of MRSA and MDRPA infections.

Mechanism of antimicrobial action. The predominant mechanism of positively charged AMPs, like melittin and LL-37, lies in selective binding of peptides to the negatively charged hydroxylated phospholipids and LPS of the bacterial membranes, followed by rapid perturbation and dissipation of lipid matrix of bacterial membranes, which leads to cell death via leakage of cytoplasmic contents [55]. However, there is an increasing speculation that these effects are not the only mechanisms of microbial killing. A growing number of AMPs have been documented to translocate across bacterial membrane and accumulate intracellularly, where they target various intracellular organelles and mediate cell

killing [56]. Notably, α-helical peptides such as buforin-2 and indolicidin, and conventional antibiotics such as nalidixic acid and ciprofloxacin were reported to across cytoplasmic membrane without membrane destruction, and bind to nucleic acids, eventually inhibiting DNA, RNA and protein synthesis [57, 58].

As both the designed analogs exhibited better antimicrobial properties than melittin, LL-37 and other conventional antibiotics (Table 6), we intended to investigate the time-dependent bactericidal kinetics of the peptides against gram-negative (*E. coli*) bacteria. As depicted in Fig. 4B, at their MICs both dCATH 12 analogs exerted good bactericidal activity than nalidixic acid (bactericidal drug) after 3h of treatment and complete killing of bacterial colony was achieved after 12 h of incubation. Interestingly, these analogs also found to demonstrate bacteriostatic action at 0.5 × MIC where the stable bacterial count was observed even after 24 h incubation. In other hand, a potent bacteriostatic antibiotic chloramphenicol failed to control bacterial growth at 0.5 × MIC. To further confirm the bactericidal action of peptides, ability of peptides to lyse *E. coli* cells was monitored by measuring the turbidity of the culture incubated with bactericidal concentrations of peptides (Fig. 6A). The optical density (OD_{550}) of bacterial culture treated with nalidixic acid, dCATH 12-4 and dCATH 12-5 was found to be increasing with time and after 3 h incubation, the turbidity was reduced to 90%. However, the bacteriostatic drug chloramphenicol did not showed any decrease when treated at MIC concentration. Treatment with membrane disrupting peptide melittin showed no increase in OD and culture turbidity was drastically reduced over time. In order to study the mechanism behind the increase in the OD of the cells, we examined the morphological changes in the *E. coli* cells as a result of treatment with dCATH 12 analogs and antibiotics at their bactericidal concentration at 2 hours. As shown in Fig. 6B, *E. coli* cells treated with nalidixic acid and dCATH 12 analogs resulted in elongation of cells and formation of aseptate filaments after 2 hours of treatment. Thus, the increase in OD_{550} in peptides treated cells can be due to the formation of filaments. Based on many previous studies it has been evident that filamentation of bacteria occurs as a result of

inhibition of DNA synthesis which blocks cell division [57, 59]. Nalidixic acid and ciprofloxacin were proven to bind with bacterial DNA and interfere with the replication of DNA by inhibiting DNA gyrase enzyme [60, 61]. Thus, we have speculated that bactericidal action of dCATH 12-4 and dCATH 12-5 peptides could be mediated by intracellular mechanism rather than membrane disruption.

To further prove the intracellular mechanism of dCATH 12-4 and dCATH 12-5, we studied their effects on membrane permeability and integrity using various fluorochrome-based studies including, dye leakage assay, membrane depolarization assay, SYTOX Green uptake assay, flow cytometry, NPN, and ONPG assay. The membrane lysing peptides, such as melittin and LL-37 and membrane penetrating peptide, buforin-2 were used as control. The results revealed that similar to buforin-2 peptide, both dCATH 12-4 and dCATH 12-5 analogs did not induce membrane permeabilization in *S. aureus* and *E. coli* bacteria (Fig. 8 and 9). These results were also reflected in zeta potential analysis (Fig. 10) where melittin was observed to neutralize surface charge of *E. coli* rapidly at lower concentration (8 μM) while both dCATH 12 analogs failed to neutralize the negative charge of *E. coli* even at 64 μM. Collectively, these results suggested that cytoplasmic membrane of the bacterial cell is not the ultimate target of the designed analog AMPs. Proving this speculation, determination of site of action of AMPs by confocal microscopic observations revealed that both FITC-labelled dCATH 12-4 and dCATH 12-5 accumulate inside cytoplasm, without disrupting the membrane (Fig. 11A). This finding indicates that the major site of action of dCATH 12-4 and dCATH 12-5 is the cytoplasm of bacteria. Considered together, these results suggested that the primary targets of the selected dodeca AMPs could be the intracellular components rather than bacterial membrane. Furthermore, DNA binding studies revealed that similar to buforin-2, both analogs directly bind with *E. coli* DNA at 8 μM, further confirming their intracellular targeting properties (Fig. 11B). Based on these results, it can be reasonably assumed that similar to buforin-2 or nalidixic acid, both dCATH 12-4 and dCATH 12-5 analogs mediate bactericidal action by binding with DNA and inhibiting DNA synthesis (Fig. 16A).

Considering the fact that both dCATH 12-4 and dCATH 12-5 possess relatively high hydrophobicity (R_t=16.2 and R_t=17.3) and net charge (+6), it is possible that these peptides displayed high affinity towards negatively charged bacterial membrane. However, to penetrate the plasma membrane, some AMPs such as Trojan peptides must possess strong hydrophobic amino acids to facilitate rapid translocation of AMPs into the cell membrane [62]. Indolicidin, a well-studied intracellular-targeting AMP, contains three Trp side chains in non-polar region. This Trp-rich helps indolicidin to adopt transmembrane orientations (boat-type conformation) to cross both outer and inner membrane to bind with DNA [63]. Considering this speculation, dCATH 12-4 containing two Trp and two Ile residues and dCATH 12-5, containing three Trp residues, in non-polar region of α-helix were believed to act similar to that of indolicidin. The superior potency of Trp-containing amphipathic AMPs could be attributed to the strong affinity of Trp for membrane interfaces which facilitates the penetration of peptides into lipid bilayer membrane [64].

Mechanism of anti-inflammatory action. The mechanism by which dCATH 12 analogs neutralizes LPS-induced pro-inflammatory response is a matter of debate. However, based on many previous studies, it has been deduced that a majority of AMPs can induce anti-inflammatory action through two possible mechanisms (1) direct binding of cationic AMPs and neutralization of the anionic amphiphilic lipid A domains of LPS via electrostatic interactions, thereby resulting in the LPS aggregates (oligomers) to dissociate via hydrophobic interactions between the alkyl chains of LPS and non-polar side chains of AMPs. Inhibition of the binding of LPS to LPB [65] (2) AMPs can bind to CD14 receptor on macrophages and competitively inhibit the binding of LPS-LPB complex to CD14, thus making it unavailable for TLR-4 receptor [39]. In order to elucidate the exact mechanism behind the enhanced anti-inflammatory action of selected dodeca analogs, we first studied their ability to interact with LPS. The net charge value of dCATH 12-4 and dCATH 12-5 is +6, which allows them to interact with negatively charged bacterial

membranes and LPS. Based on the results of the CD spectra analysis, it was evident that both dCATH 12-4 and dCATH 12-5 showed unordered conformation in buffer but exhibited predominantly α-helical structure in LPS micelles (Fig. 2), indicating the possible interaction of peptides with LPS [66]. This hypothesis was further confirmed by LPS binding assay using a fluorescent probe BODIPY TR cadaverine (BC). BC binds strongly to lipid A moiety of native LPSs. When AMPs binds to LPS, BC probe is displaced, and its fluorescence is increased. Both dCATH 12-4 and dCATH 12-5 analogs caused strong dose-dependent increases in fluorescent intensity similar to that of LL-37 (Fig. 12). At lower concentration (5 to 10 μM), dCATH 12-5 was found to be most effective in alleviating BC fluorescence than LL-37. In contrast, the parent peptide dCATH 12 failed to increase fluorescence even at high concentration (40 μM). These observations clearly indicated successful binding of peptides to lipid-A domains of LPS which resulted in displacement of pre-bound BC [67].

It is well known that only aggregated form of LPS can induce inflammatory response [68]. Most of the LPS binding peptides have tendency to disaggregate LPS oligomers into monomers and thereby, block them from binding to LBP [31]. Therefore, it is necessary to investigate the ability of AMPs to dissociate LPS aggregates. As revealed in Fig. 9, dCATH 12-4, dCATH 12-5, and LL-37 effectively induced disaggregation of FITC-LPS in a concentration-dependent manner, which consequently correlated with LPS binding assay data (Fig. 8). Interestingly, both LL-37 and dCATH 12-5 peptides showed increasing linear dose-dependent curve, while dCATH 12-4 showed stable activity after 20 μM, indicating its threshold concentration for neutralizing LPS.

The results obtained so far indicated that dCATH 12-4 and dCATH 12-5 analogs have ability to bind with LPS. However, strong binding of peptides to LPS alone is not sufficient to block the biological activity of LPS. Magainin-2 was found to be inefficient in detoxifying LPS action, despite its ability to bind with LPS [31]. To prevent activation of macrophages, AMPs needs to inhibit the interaction of LPS to the CD14 receptor of macrophages. To investigate this mechanism, we

treated the RAW 264.7 macrophage cells with pre-incubated FITC-LPS/peptide mixture and analyzed the fluorescence of cells bound to FITC-LPS, using flow cytometer. As presented in Fig. 15A, all peptides, except dCATH 12 significantly blocked FITC-LPS from binding to macrophages further indicating successful binding of peptides with LPS. The pre-incubation of AMPs with FITC-LPS, prior to treatment to the cells, could possibly neutralize the action LPS. The results from the flow cytometric study revealed that LPS binding activity of dCATH 12-4 and dCATH 12-5 was similar to that of PMB and LL-37 and confirmed their ability to directly interact with LPS.

Though these findings are sufficient to conclude the possible mechanism behind the endotoxin neutralization activity of the designed peptides, previous studies reported that in addition to direct binding with LPS, human cathelicidin peptides, like LL-37 and CAP18, are known to neutralize LPS by competitively binding with it on the CD14 receptor [31, 69]. On the contrary, magainin and PMB do not possess this ability. They are known to detoxify LPS only by directly binding with lipid moieties of LPS [70]. To analyze whether dCATH 12 and its analogs has this characteristic, we pretreated macrophage cells with FITC-LPS for 1 h, allowing them to strongly bind to CD14 receptor. The unbound LPS was washed, followed by treatment of AMPs, and the fluorescence of cells bound with FITC-LPS was analyzed flow-cytometrically. It has been observed that both dCATH 12-4 and dCATH 12-5 analogues and LL-37 can efficiently replace FITC-LPS already bound to the CD14 receptor. On the contrary, the parent peptide, dCATH 12 and PMB had less or no effect in removing pre-bound FITC-LPS (Fig. 15B). An interesting finding was that despite its high affinity for free LPS, PMB failed to bind with LPS that was pre-bound to CD14 receptor. This could be attributed to the inability of PMB to interact with mammalian cell surface receptor [22]. Collectively, these results indicate that, similar to LL-37, dCATH 12-4 and dCATH 12-5 analogs possess dual ability to bind with exogenous LPS and competitively inhibit LPS bound to cell surface receptor (Fig. 16B).

5. Conclusion

In summary, a series of short 12-meric amphipathic α-helical AMPs were designed, based on 20 residue dCATH, and screened for their antimicrobial and anti-inflammatory activities. Though, all dodeca analogs displayed high antimicrobial activity with minimal cytotoxicity, only Trp and Lys rich AMPs, dCATH 12-4 and dCATH 12-5 showed ability to induce anti-endotoxin properties. These dual properties could be attributed to the perfect equilibrium between cationicity and hydrophobicity and well-engineered facially amphipathic structures, indicating the importance of perfect amphipathic design and incorporation of Trp side chains in non-polar regions. Several fluorochrome-based assays and microscopic studies revealed that the selected AMPs translocated into bacterial cytoplasm and killed the cells through DNA binding. Additionally, dCATH 12-4 and dCATH 12-5 efficiently bound with *E. coli* LPS and exhibited strong endotoxin-neutralizing activity in macrophage cells. In conclusion, the combined effects of bactericidal and immunomodulatory activities, makes dCATH 12-4 and dCATH 12-5 attractive candidates for treatment of sepsis. In addition to this, both AMPs also found to function synergistically in combination with different conventional antibiotics against MDR pathogens, making them as a promising adjuvant in combination therapy. Overall, our findings in this study demonstrate a potential design strategy for optimizing AMPs, which would promote the development of peptide-based antimicrobial biomaterials with broad-ranging clinical and therapeutic applications.

Table 1. Amino Acid Sequences and Physicochemical Properties of dCATH and its Analogs

Peptides	Amino acid sequences [a]	Molecular mass (Da)		Net charge	R_t[b]	μH[c]
		Calculated	Observed			
dCATH	KRFWQLVPLAIKIYRAWKRR	2629.24	2628.88	+7	26.8	0.431
dCATH 18	FWQLVPLAIKIYRAWKRR-NH_2	2343.88	2344.41	+5	29.0	0.426
dCATH 16	QLVPLAIKIYRAWKRR-NH_2	2010.49	2011.21	+5	24.1	0.456
dCATH 14	VPLAIKIYRAWKRR-NH_2	1769.20	1770.60	+5	21.7	0.405
dCATH 12	LAIKIYRAWKRR-NH_2	1572.95	1573.44	+5	16.4	0.505
dCATH 12-1	LA**K**KIYRAWKRR-NH_2	1587.97	1588.61	+6	14.1	0.656
dCATH 12-2	LA**K**KIYRAWKR**W**-NH_2	1617.99	1618.00	+5	17.1	0.879
dCATH 12-3	LA**K**KIYR**K**WKR**W**-NH_2	1675.09	1675.40	+6	15.1	0.847
dCATH 12-4	L**IK**KIYR**K**WKR**W**-NH_2	1717.17	1718.00	+6	16.2	0.941
dCATH 12-5	L**WK**KIYR**K**WKR**W**-NH_2	1790.22	1790.24	+6	17.3	0.971

[a] Bold and underlined characters are the amino acid residues that were substituted in this study.

[b] Retention time of (R_t) was measured by analytical RP-HPLC with C_{18} column (5 mm; 4.6 mm × 250 mm; Vydac).

[c] Mean hydrophobic moment (μH) calculated from http://heliquest.ipmc.cnrs.fr/cgi-bin/ComputParams.py.

Table 2. Percentage of α-helical contents of dCATH 12 and its analogs in different membrane mimicking environment.

Peptides	% α-helix			
	Buffer	50% TFE	30 mM SDS	0.1% LPS
dCATH 12	RC	26.56	7.93	26.91
dCATH 12-1	RC	6.24	7.52	8.73
dCATH 12-2	RC	22.78	8.04	29.50
dCATH 12-3	RC	27.42	23.60	23.51
dCATH 12-4	RC	41.28	36.63	42.87
dCATH 12-5	RC	38.39	29.75	40.40

RC: Random coil

Table 3. Antimicrobial Activities of dCATH and its Analogs against Different Microorganisms

Microorganism	Minimal inhibitory concentration (MIC)[a] (μM)										
	dCATH	dCATH 18	dCATH 16	dCATH 14	dCATH 12	dCATH 12-1	dCATH 12-2	dCATH 12-3	dCATH 12-4	dCATH 12-5	Melittin
Gram-positive organisms											
S. aureus (KCTC 1621)	8	8	8	8	8	4	4	4	4	2	4
S. epidermidis (KCTC 1917)	8	16	16	16	4	8	8	4	4	4	8
B. subtilis (KCTC 3068)	8	8	16	4	8	8	4	4	2	2	4
Resistant Gram-positive organisms											
MRSA[b] (CCARM 3089)	16	32	32	32	32	32	32	16	16	16	32
MRSA (CCARM 3090)	16	16	16	32	32	16	16	16	8	8	16
MRSA (CCARM 3095)	8	32	32	32	32	16	16	16	8	8	32
VREF[c] (ATCC 51559)	16	32	32	16	32	16	16	8	8	8	16
Gram-negative organisms											
E. coli (KCTC 1682)	8	16	32	16	16	8	16	8	8	4	16
P. aeruginosa (KCTC 1637)	16	16	16	8	4	4	4	4	2	2	4
S. typhimurium (KCTC 1926)	4	8	16	8	8	4	2	2	2	2	2
Resistant Gram-negative organisms											
MDRPA[d] (CCARM 2095)	16	32	32	32	32	32	16	16	8	8	32
MDRPA (CCARM 2109)	16	32	32	32	16	32	32	8	8	4	32
Yeast											
C. albicans (KCTC 7965)	8	16	8	16	8	8	8	8	8	8	16
C. albicans (KCTC 7121)	16	16	16	16	16	8	8	8	4	4	16

[a] MIC was determined as the lowest concentration of peptide that caused 100 % inhibition of microbial growth.

[b] MRSA: methicillin-resistant Staphylococcus aureus.

[c] VREF: vancomycin-resistant Enterococcus faecium.

[d] MDRPA: multidrug-resistant Pseudomonas aeruginosa.

Table 4. Hemolytic Activities and Therapeutic Indexes (TIs) of the Peptides

Peptide	HC_{10} (□ M)[a]	GM (□ M)[b]				TI[c] (HC_{10}/GM)			
		Gram-positive bacteria	Gram-negative bacteria	Yeast	All	Gram-positive bacteria	Gram-negative bacteria	Yeast	All
dCATH	5.1	11.4	12	12	11.7	0.4	0.4	0.4	0.4
dCATH 18	1.3	20.5	20.8	16	20	0.1	0.1	0.1	0.1
dCATH 16	180	21.7	25.6	12	21.7	8.3	7	15	8.3
dCATH 14	>256	20	19.2	16	19.1	25.6	26.7	32	26.7
dCATH 12	>256	21.1	15.2	12	17.7	24.3	33.7	42.7	28.9
dCATH 12-1	>256	14.2	16	8	14	36.1	32	64	36.6
dCATH 12-2	>256	13.7	14	8	13	37.4	36.6	64	39.4
dCATH 12-3	>256	9.7	7.6	8	8.7	52.8	67.4	64	58.9
dCATH 12-4	>256	7.1	5.6	6	6.4	71.1	91.4	85.3	80
dCATH 12-5	>256	6.8	4	6	5.7	75.3	128	85.3	89.8
Melittin	1	16	17.2	16	16.4	0.1	0.1	0.1	0.1

[a] HC_{10} is the peptide concentration that caused 10% hemolysis of sheep red blood cells (sRBCs).

[b] GM denotes the geometric mean of MIC values from selected bacterial and fungal strains.

[c] Therapeutic index (TI) is the ratio of the HC_{10} value (□ M) over GM (□ M).

When no detectable hemolytic activity was observed at 256 μM, a value of 512 μM was used to calculate the TI.

Table 5. Antimicrobial activities of control AMPs and conventional antibiotics.

Peptide	MIC (μM)			
	S. aureus (KCTC 1621)	*E. coli* (KCTC 1682)	MDRPA (CCARM 2095)	MRSA (CCARM 3090)
LL-37	16	16	32	32
Buforin-2	32	32	64	64
Chloramphenicol	64	64	1024	128
Ciprofloxacin	64	128	512	512
Oxacillin	128	128	512	512
Nalidixic acid	32	64	128	64

Table 6. Minimum Inhibitory Concentration (MIC) Values of dCATH 12-4, dCATH 12-5 and LL-37 in the Presence of Salts and Human Serum (20%) against *E. coli* and *S. aureus*

Peptides	Control	150 mM NaCl	4.5 mM KCl	6 μM NH_4Cl	1 mM $MgCl_2$	2.5 mM $CaCl_2$	4 μM $FeCl_3$	20% Human serum
				MIC (μM) against *E. coli* (KCTC 1682)				
dCATH 12-4	8	4	2	2	8	8	8	8
dCATH 12-5	8	4	4	2	4	4	8	8
LL-37	8	16	8	8	16	16	16	8
				MIC (μM) against *S. aureus* (KCTC1621)				
dCATH 12-4	2	8	4	8	4	4	8	4
dCATH 12-5	2	2	4	2	4	4	8	4
LL-37	8	16	8	8	8	16	16	8

Table 7. Synergy between the peptides and conventional antibiotics against MRSA and MDRPA.

Strains	Antibiotics	Peptides	MIC_A	[A]	FIC_A	MIC_P	[P]	FIC_P	FICI [a]	Interpretation
MRSA	CHL	dCATH 12-4	128	32	0.25	8	2	0.25	0.5	synergy
(CCARM	CHL	dCATH 12-5	128	32	0.25	8	2	0.25	0.5	synergy
3090)	CHL	LL-37	128	64	0.5	32	8	0.25	0.75	additive
	CIP	dCATH 12-4	512	128	0.25	8	2	0.25	0.5	synergy
	CIP	dCATH 12-5	512	64	0.125	8	2	0.25	0.375	synergy
	CIP	LL-37	512	256	0.5	32	16	0.5	1.0	additive
	OXA	dCATH 12-4	512	64	0.125	8	2	0.25	0.375	synergy
	OXA	dCATH 12-5	512	64	0.125	8	2	0.25	0.375	synergy
	OXA	LL-37	512	128	0.25	32	16	0.5	0.75	additive
MDRPA	CHL	dCATH 12-4	1024	64	0.0625	8	2	0.25	0.313	synergy
(CCARM	CHL	dCATH 12-5	1024	128	0.125	8	2	0.25	0.375	synergy
2095)	CHL	LL-37	1024	512	0.5	16	8	0.5	1.0	additive
	CIP	dCATH 12-4	512	64	0.125	8	2	0.25	0.375	synergy
	CIP	dCATH 12-5	512	64	0.125	8	2	0.25	0.375	synergy
	CIP	LL-37	512	128	0.25	16	16	1.0	1.25	indifferent
	OXA	dCATH 12-4	512	64	0.125	8	2	0.25	0.375	synergy
	OXA	dCATH 12-5	512	64	0.125	8	2	0.25	0.375	synergy
	OXA	LL-37	512	128	0.25	16	8	0.5	0.75	additive

CHL: Chloramphenicol, CIP: Ciprofloxacin, OXA: Oxacillin

MIC_A: MIC of antibiotic alone, [A]; MIC of antibiotic in combination, MIC_P: MIC of peptide alone, [P]: MIC of peptide in combination.

FIC_A: fractional inhibitory concentration of antibiotic, FIC_P: fractional inhibitory concentration of peptide

FICI: fractional inhibitory concentration index, [a] FICI = [A] / MIC_A + [P] / MIC_P

FICI of ≤ 0.5 was interpreted as synergy, $0.5 < FICI \leq 1.0$ as additive, $1.0 < FICI \leq 4.0$ as indifferent, and an FICI > 4.0 as antagonism.

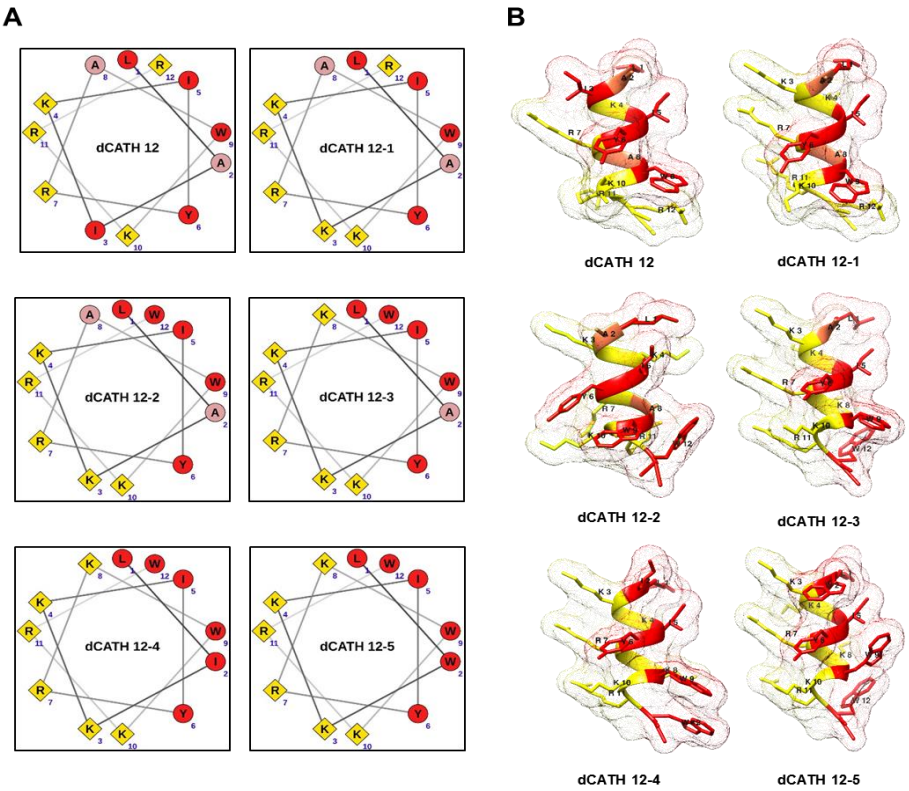

Fig. 1. (A) Helical wheel projection diagrams of dodeca dCATH 12 and its analogs. Positively charged (polar) residues are indicated by yellow diamonds, and hydrophobic (non-polar) residues are indicated by red circles (B) Three-dimensional structure projections of dCATH 12 and its analogs. Yellow sticks represent polar residues and red sticks represents nonpolar residues.

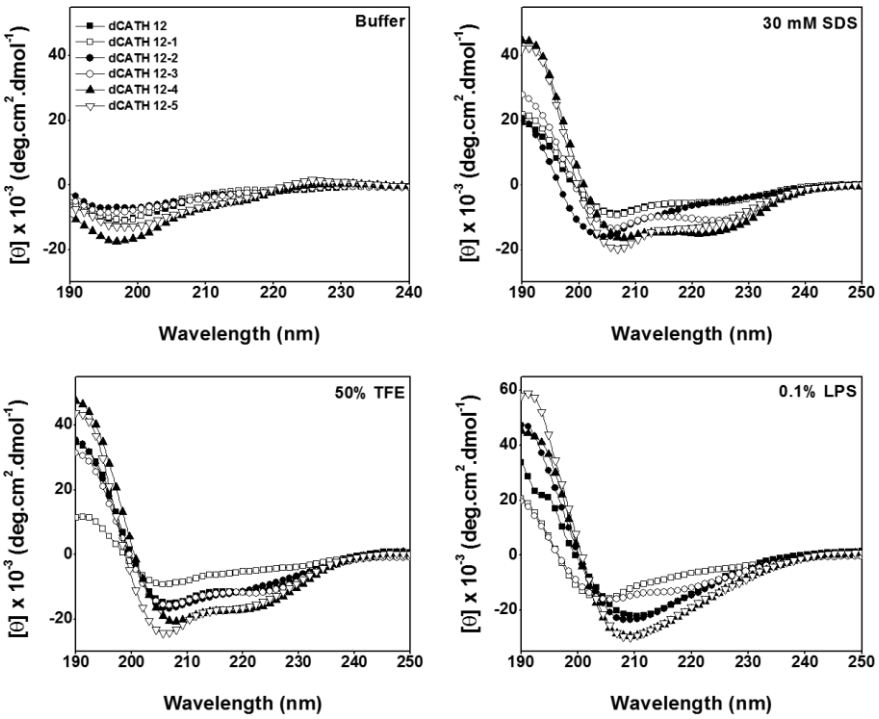

Fig. 2. The CD spectra of dCATH 12 and its analog AMPs in 10 mM PBS (pH 7.4), and 30 mM SDS, 50% TFE, 0.1% LPS. The peptide concentration was fixed at 40 μM. The values from three scans were averaged per sample.

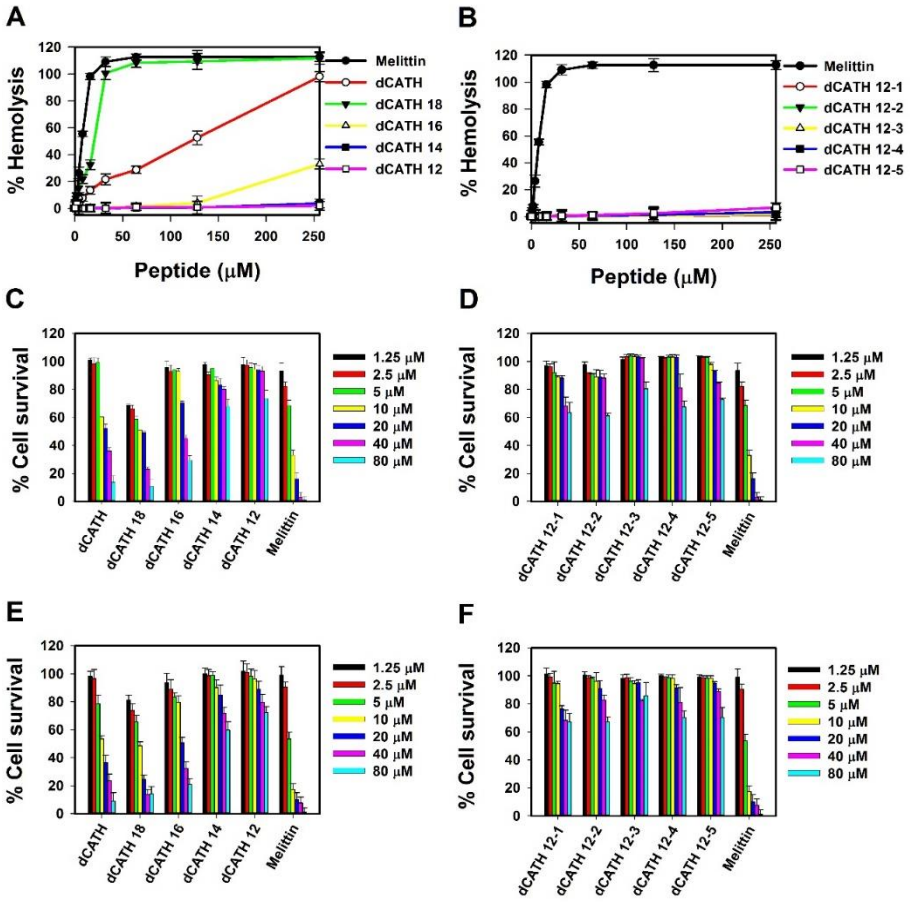

Fig. 3. Toxicities of dCATH and its analogs, measured as hemolysis in sheep red blood cells (A and B) and cytotoxicity against mouse macrophage RAW 264.7 cells (C and D), and mouse embryonic fibroblast NIH-3T3 cells (E and F). All measurements were obtained in triplicate. Error bars represent mean ± standard error of the mean (SEM).

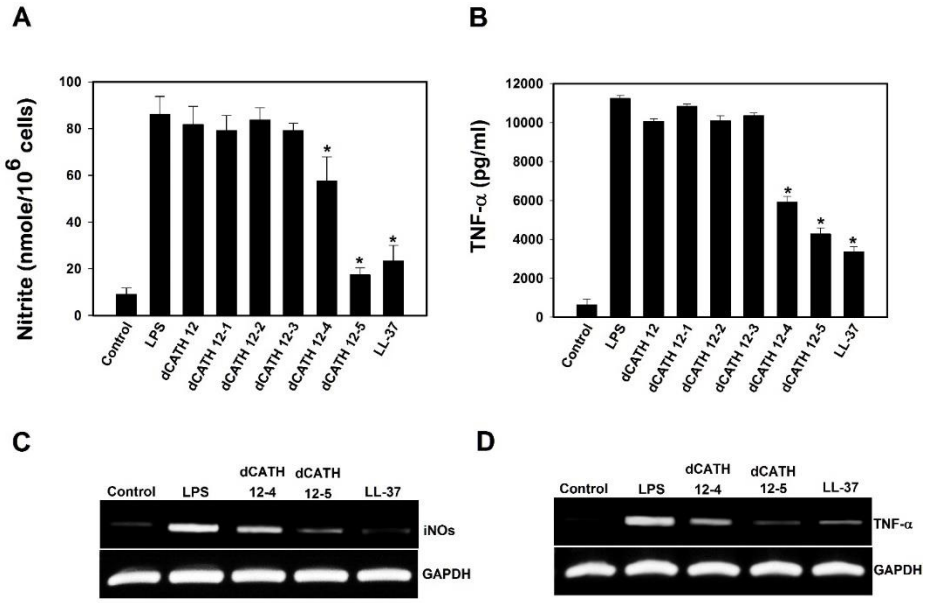

Fig. 4. Effects of dCATH 12 and its analogs on production of (A) NO and (B) TNF-α from LPS-stimulated RAW264.7 macrophage cells. Secreted NO and TNF-α were measured from the supernatants after 24 h of LPS-stimulation by ELISA. Effects of dCATH 12-4 and dCATH 12-5 analogs on the mRNA levels of (C) iNOS and (D) TNF-α in LPS-stimulated RAW264.7 cells. Total RNA was isolated after 3 h (for TNF-α) and 6 h (for iNOS) and analyzed for determining the levels of iNOS and TNF-α mRNAs by RT-PCR. RAW264.7 cells (5×10^5 cells/well) were stimulated with LPS (20 ng/mL) in the presence and absence (control) of peptides (For NO: 5 μM and TNF-α: 10 μM). All data represent at least three independent experiments and are expressed as mean ± standard error of the mean (SEM). Data were analyzed by one-way ANOVA with Bonferroni's post-test. Asterisks indicate statistically significant differences ($^*p < 0.001$) for each agonist.

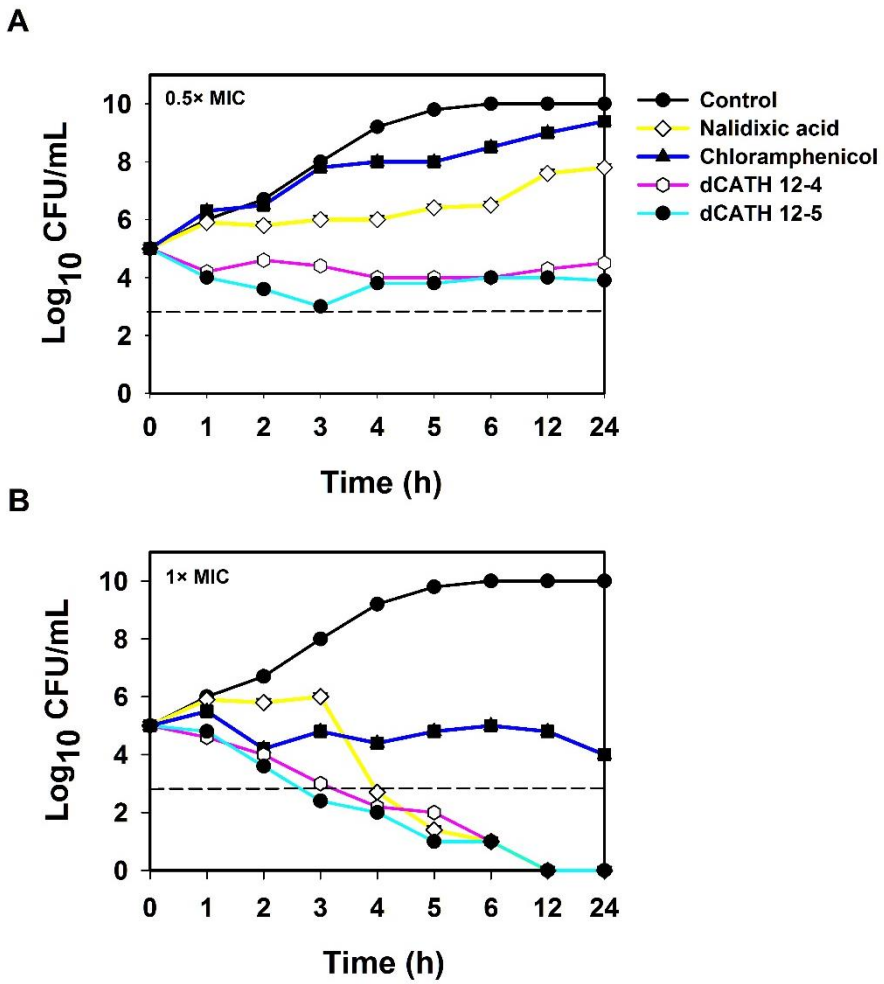

Fig. 5. Time-kill curves of dCATH 12-4, dCATH 12-5 and conventional antibiotics against *E. coli* (KCTC 1682) at (A) 0.5 × MIC and (B) 1× MIC. The dotted line indicates 50% reduction from initial OD.

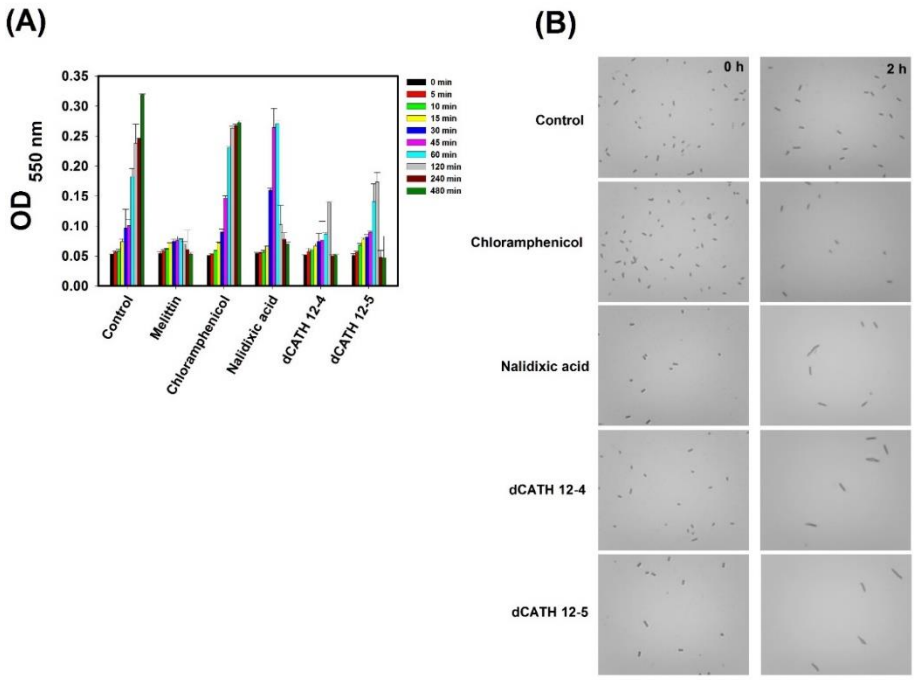

Fig. 6 (A) Time-dependent bacteriolysis assay. *E. coli* (KCTC 1682) exposed to 1 × MIC of dCATH 12 analogs, nalidixic acid (bactericidal) and chloramphenicol (bacteriostatic) were observed by measuring OD_{550} values at various time interval for 4h. (B) Morphological changes induced in cells of *E. coli* by dCATH 12 analogs and antibiotics. Smears were prepared from 2 h cultures, gram-stained and imaged under optical microscope.

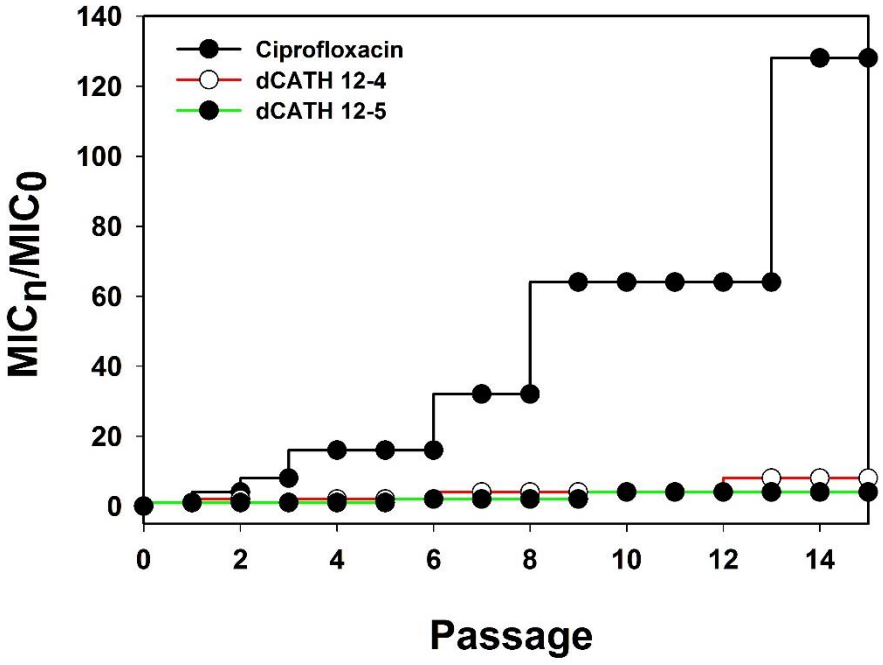

Fig 7. Drug resistance development of *S. aureus* (KCTC 1621) in the presence of sub-MIC concentration of dCATH 12-4, dCATH 12-5 and ciprofloxacin.

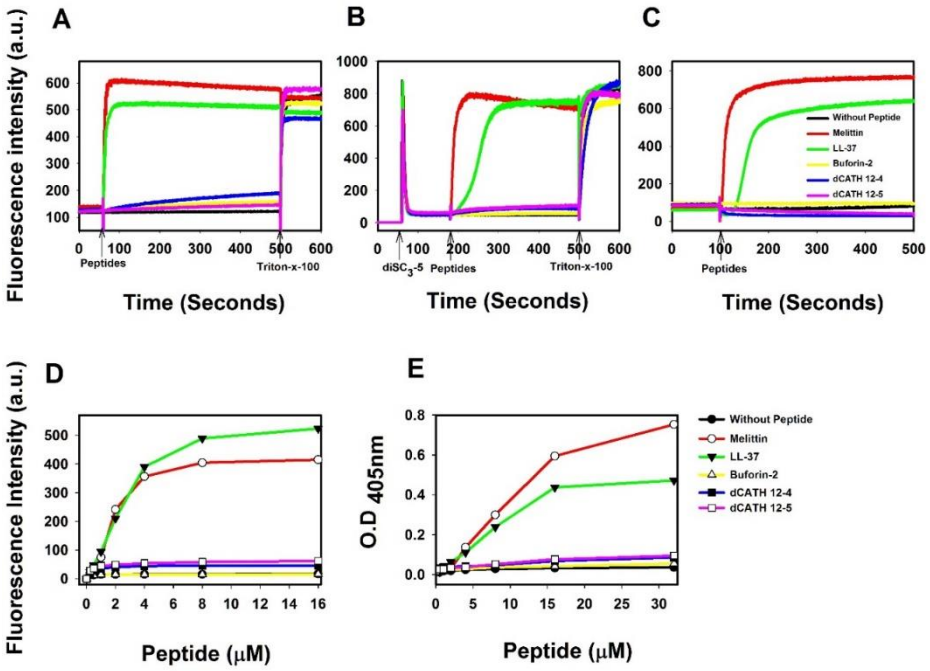

Fig. 8. (A) Calcein leakage induced by the peptides against large unilamellar vesicles (LUVs) composed of EYPE/EYPG (7:3, v/v). (B) Cytoplasmic membrane depolarization of *S. aureus* (KCTC 1621) treated with the peptides (2 × MIC), as assessed by the release of the membrane potential-sensitive dye $DiSC_3$-5. (C) SYTOX green uptake of *S. aureus* (KCTC 1621) treated with the peptides (2 × MIC). (D) The outer membrane permeability of the peptides. Membrane uptake of NPN of *E. coli* (KCTC 1682) in the presence of different concentrations of the peptides. (E) Inner membrane permeability of the peptides. Hydrolysis of ONPG due to release of cytoplasmic β-galactosidase of *E. coli* ML-35 cells treated with peptides at different concentration was measured spectroscopically at the absorbance of 405 nm as a function of time.

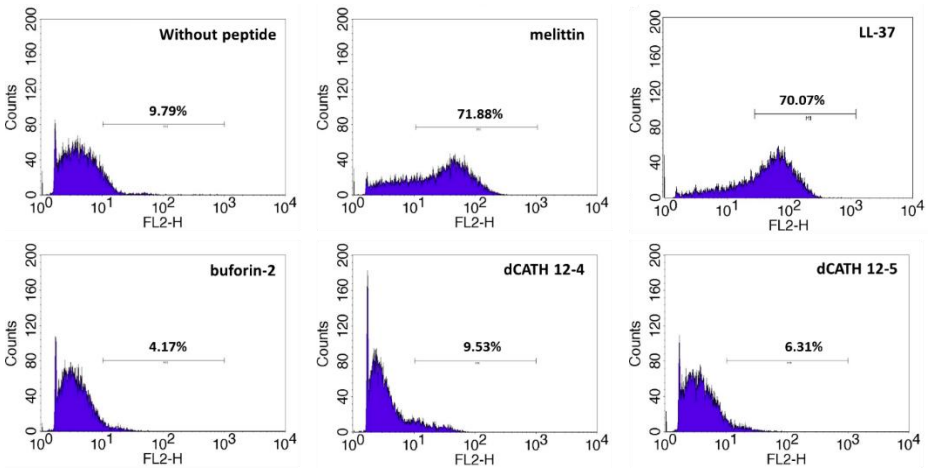

Fig. 9. Flow cytometric analysis. Exponential-phase *E. coli* KCTC 1682 cells were treated with peptides (2 × MIC), and membrane integrity disruption was measured by increase in Propidium iodide (PI, 10 μg/mL) fluorescence intensity at 37 °C for 1 h. Increments of the log fluorescence signal indicates PI uptake resulting from peptide treatment.

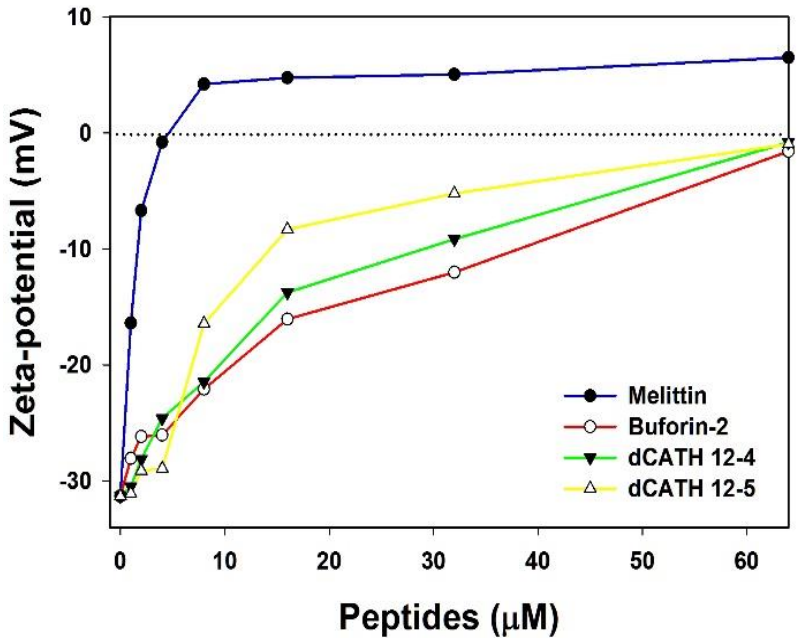

Fig. 10. The effect of dCATH 12-4 and dCATH 12-5 on the surface charge of *E. coli* cells. The dotted line indicates a neutral surface net charge, to highlight the peptide concentration range at which *E. coli* surface neutrality and possible overcompensation are achieved.

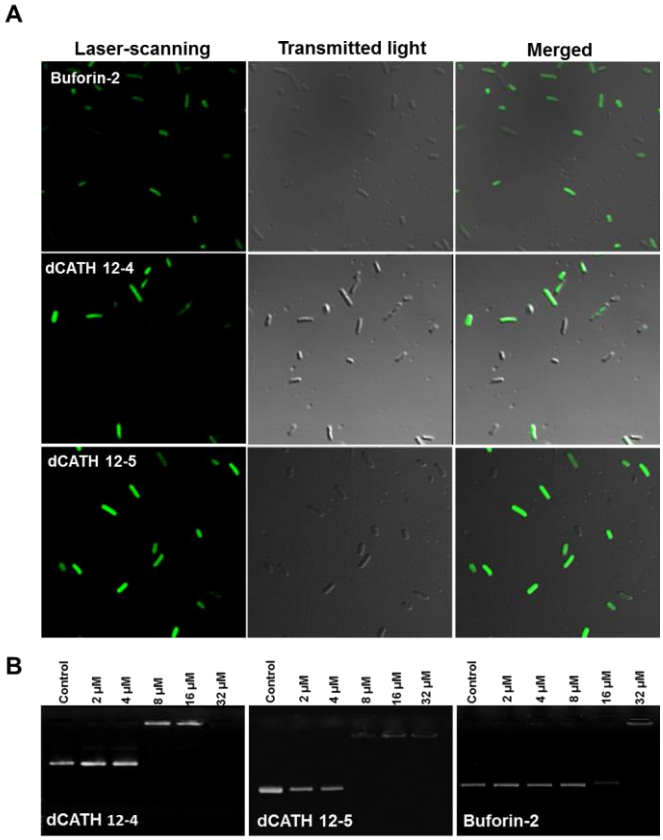

Fig. 11 (A). Confocal laser-scanning microscopy of *E. coli* (KCTC 1682) treated with FITC-labeled peptides. Approximately 1 × 10^6 CFU/mL of cells were incubated with FITC-labeled peptides (2 × MIC) for 30 min. Panels on the left, middle, and right represent laser-scanning images, transmitted light scanning image (normal image), and merged image of *E. coli*, respectively. (B). Interaction of AMPs (dCATH 12-4, dCATH 12-5 and buforin-2) with plasmid DNA (100 ng; pBR322). The peptide was incubated for 1 h with plasmid DNA at the indicated peptide concentration. The mobility of the DNA was determined using gel retardation assays. Peptide concentration is shown at the top.

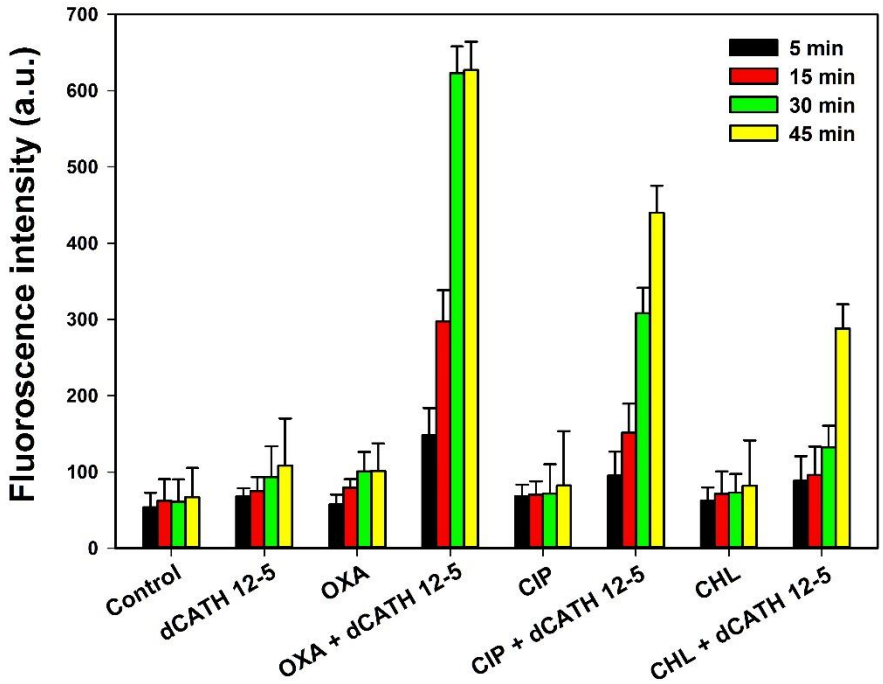

Fig. 12. Effects of combinations of dCATH 12-5 with antibiotics on propidium iodide uptake of MRSA (CCARM 3090). 0.25 × MIC of dCATH 12-5 and antibiotics were used when alone, and 0.125 × MIC of dCATH 12-5 + 0.25 × MIC of antibiotic when in combination. Error bars indicate the standard deviation of the means of three independent experiments. Control: bacteria alone. OXA: Oxacillin, CIP: Ciprofloxacin, CHL: Chloramphenicol.

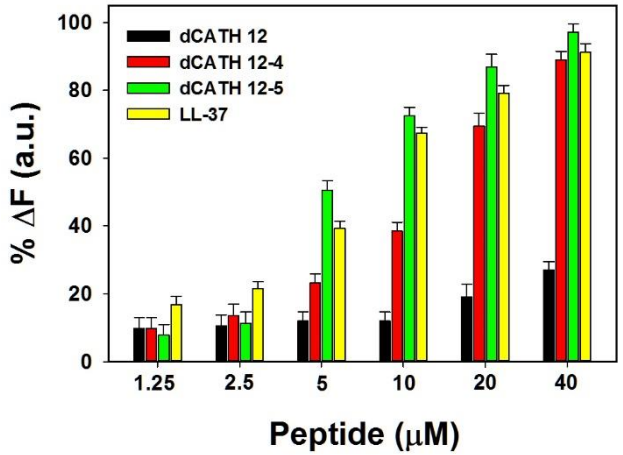

Fig. 13. Peptide binding affinity to LPS from *E. coli* 0111: B4. The fluorescence intensity was monitored at an excitation wavelength of 580 nm and an emission wavelength of 620 nm. The percentage fluorescence was calculated using formula: $\%\Delta F\ (AU) = [(F_{obs}-F_0) / (F_{100}-F_0)] \times 100$, where F_{obs} is the observed fluorescence at a given peptide concentration, F_0 is the initial fluorescence of BC with LPS in the absence of peptides, and F_{100} is the BC fluorescence with LPS cells upon the addition of 10 μg/mL Polymyxin B.

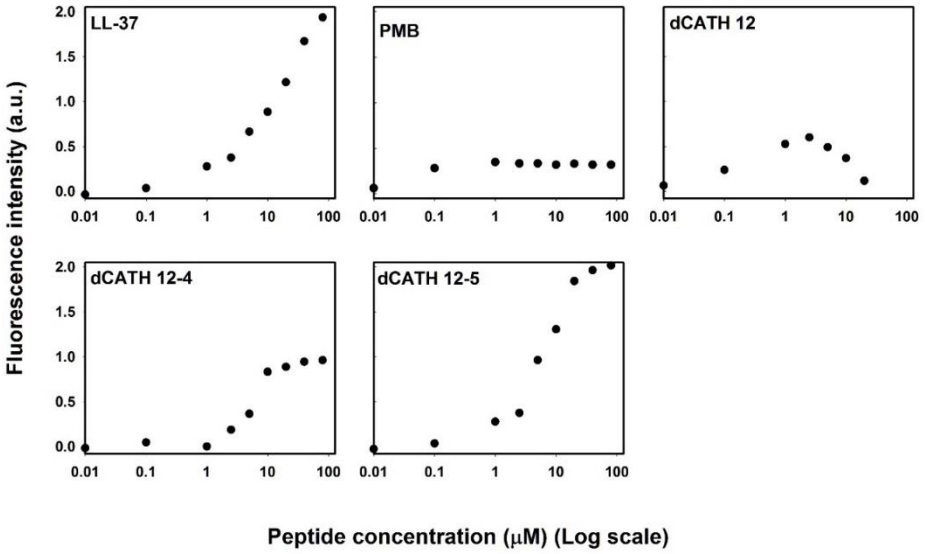

Fig. 14. Dissociation of *E. coli* 0111:B4 FITC-LPS aggregates in the presence of increasing concentrations of peptides. Increase in fluorescence of FITC-LPS was plotted with respect to the peptide concentration in micro molar. The change in FITC emission after each treatment was monitored until emission reached equilibrium. FITC increased its emission when the distance between its monomers increased because of a reduced self-quenching.

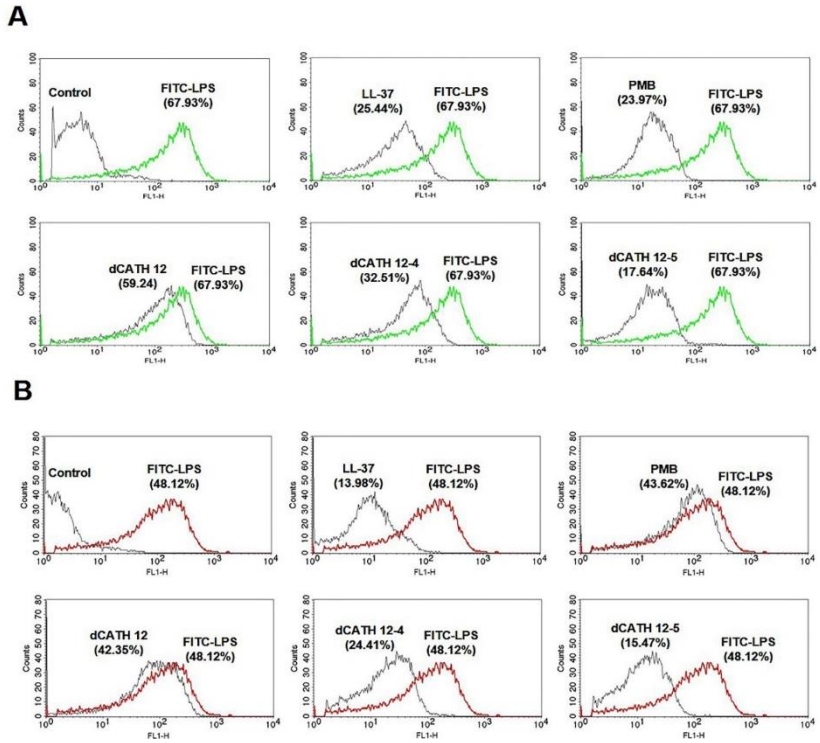

Fig. 15. Flow cytometry analysis of RAW264.7 macrophages treated with FITC-LPS (1 μg/mL) from *E. coli* 0111:B4 (green and red lines). (A) FITC-LPS was pre-incubated with individual peptides (10 μM) for 1h and then RAW264.7 cells (5×10^5 cells/mL) were treated with each peptide/LPS mixture. The cells were washed and the binding of FITC-LPS to macrophages was analyzed by FACS Caliber flow cytometer (black line). (B) RAW264.7 (5×10^5 cells/mL) cells were pre-incubated with FITC-LPS for 1 h in absence of peptides. The cells were washed and treated with or without peptides for additional 1 h. The LPS-FITC that remained bound to the cells was analyzed by flow cytometry (black line). The control was determined by recording the fluorescence of the untreated macrophages. Values given with the peaks represent the mean fluorescence intensity of the cell bound to FITC-LPS.

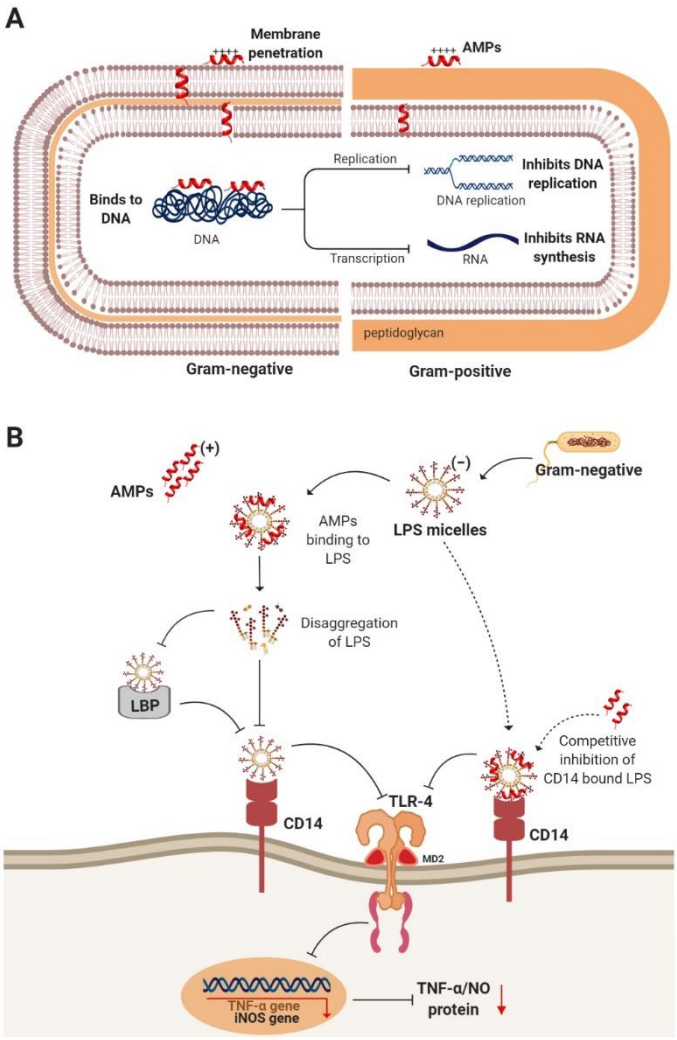

Fig. 16. Schematic diagram showing potential mechanism of bactericidal and endotoxin neutralization of dCATH 12-4 and dCATH 12-5. (A) Intracellular targeting mechanism of AMPs. (B). Suppression of LPS-induced inflammatory response in RAW 264.7 macrophages. Illustration was created with BioRender.com.

References

[1] W.H. Organization, Global priority list of antibiotic-resistant bacteria to guide research, discovery, and development of new antibiotics. Geneva: WHO; 2017, (2017).

[2] C.R. Raetz, C. Whitfield, Lipopolysaccharide endotoxins, Annu. Rev. Biochem. 71 (2002) 635-700.

[3] G. Maróti, A. Kereszt, E. Kondorosi, P. Mergaert, Natural roles of antimicrobial peptides in microbes, plants and animals, Res. Microbiol. 162 (2011) 363-374.

[4] C.D. Fjell, J.A. Hiss, R.E. Hancock, G. Schneider, Designing antimicrobial peptides: form follows function, Nat. Rev. Drug Discovery. 11 (2012) 37-51.

[5] C.-F. Le, C.-M. Fang, S.D. Sekaran, Intracellular targeting mechanisms by antimicrobial peptides, Antimicrob. Agents Chemother. 61 (2017) e02340-02316.

[6] R.E. Hancock, G. Diamond, The role of cationic antimicrobial peptides in innate host defences, Trends Microbiol. 8 (2000) 402-410.

[7] L.M. Yin, M.A. Edwards, J. Li, C.M. Yip, C.M. Deber, Roles of hydrophobicity and charge distribution of cationic antimicrobial peptides in peptide-membrane interactions, J. Biol. Chem. 287 (2012) 7738-7745.

[8] N. Wiradharma, M.Y. Sng, M. Khan, Z.Y. Ong, Y.Y. Yang, Rationally designed α-helical broad-spectrum antimicrobial peptides with idealized facial amphiphilicity, Macromol. Rapid. Commun. 34 (2013) 74-80.

[9] B. Jacob, I.S. Park, J.K. Bang, S.Y. Shin, Short KR-12 analogs designed from human cathelicidin LL-37 possessing both antimicrobial and antiendotoxic activities without mammalian cell toxicity, J. Pept. Sci. 19 (2013) 700-707.

[10] I. Zelezetsky, A. Tossi, Alpha-helical antimicrobial peptides—Using a sequence template to guide structure–activity relationship studies, Biochim. Biophys. Acta Biomembr. 1758 (2006) 1436-1449.

[11] Y. Xiao, H. Dai, Y.R. Bommineni, J.L. Soulages, Y.X. Gong, O. Prakash, G. Zhang, Structure–activity relationships of fowlicidin-1, a cathelicidin antimicrobial peptide in chicken, FEBS J. 273 (2006) 2581-2593.

[12] M. Golec, Cathelicidin LL-37: LPS-neutralizing, pleiotropic peptide, Ann. Agric. Environ Med. 14 (2007).

[13] G. Rajasekaran, E.Y. Kim, S.Y. Shin, LL-37-derived membrane-active FK-13 analogs possessing cell selectivity, anti-biofilm activity and synergy with chloramphenicol and anti-inflammatory activity, Biochim. Biophys. Acta Biomembr. 1859 (2017) 722-733.

[14] G. Rajasekaran, S.D. Kumar, S. Yang, S.Y. Shin, The design of a cell-selective fowlicidin-1-derived peptide with both antimicrobial and anti-inflammatory activities, Eur. J. Med. Chem. 182 (2019) 111623.

[15] W. Gao, L. Xing, P. Qu, T. Tan, N. Yang, D. Li, H. Chen, X. Feng, Identification of a novel cathelicidin antimicrobial peptide from ducks and determination of its functional activity and antibacterial mechanism, Sci. Rep. 5 (2015) 17260.

[16] A. Lamiable, P. Thévenet, J. Rey, M. Vavrusa, P. Derreumaux, P. Tufféry, PEP-FOLD3: faster de novo structure prediction for linear peptides in solution and in complex, Nucleic acids res. 44 (2016) W449-W454.

[17] E.F. Pettersen, T.D. Goddard, C.C. Huang, G.S. Couch, D.M. Greenblatt, E.C. Meng, T.E. Ferrin, UCSF Chimera—a visualization system for exploratory research and analysis, J. Comput Chem. 25 (2004) 1605-1612.

[18] A.R. Mol, M.S. Castro, W. Fontes, NetWheels: A web application to create high quality peptide helical wheel and net projections, BioRxiv, (2018) 416347.

[19] L. Whitmore, B.A. Wallace, Protein secondary structure analyses from circular dichroism spectroscopy: methods and reference databases, Biopolymers 89 (2008) 392-400.

[20] A.S.-T. Edition, CLSI document M07-A10 [2015], Clinical and Laboratory Standards Institute, 950.

[21] Clinical, L.S. Institute, Performance standards for antifungal susceptibility testing of yeasts, CLSI supplement M60, (2017).

[22] P. Jantaruk, S. Roytrakul, S. Sitthisak, D. Kunthalert, Potential role of an antimicrobial peptide, KLK in inhibiting lipopolysaccharide-induced macrophage inflammation, PLoS One. 12 (2017).

[23] J.S. Khara, Y. Wang, X.-Y. Ke, S. Liu, S.M. Newton, P.R. Langford, Y.Y. Yang, P.L.R. Ee, Anti-mycobacterial activities of synthetic cationic α-helical peptides and their synergism with rifampicin, Biomaterials 35 (2014) 2032-2038.

[24] NCCLS. Methods for determining bactericidal activity of antimicrobial agents; approved guidelines, M26-A, vol. 19. National Committee for Clinical Laboratory Standards, Wayne, PA (1999).

[25] F. Silva, O. Lourenço, J.A. Queiroz, F.C. Domingues, Bacteriostatic versus bactericidal activity of ciprofloxacin in Escherichia coli assessed by flow cytometry using a novel far-red dye, J. antibiotics. 64 (2011) 321-325.

[26] S.-C. Park, M.-H. Kim, M.A. Hossain, S.Y. Shin, Y. Kim, L. Stella, J.D. Wade, Y. Park, K.-S. Hahm, Amphipathic α-helical peptide, HP (2–20), and its analogues derived from Helicobacter pylori: pore formation mechanism in various lipid compositions, Biochim. Biophys. Acta Biomembr. 1778 (2008) 229-241.

[27] J.-Y. Kim, S.-C. Park, M.-Y. Yoon, K.-S. Hahm, Y. Park, C-terminal amidation of PMAP-23: translocation to the inner membrane of Gram-negative bacteria, Amino Acids. 40 (2011) 183-195.

[28] C.S. Alves, M.N. Melo, H.G. Franquelim, R. Ferre, M. Planas, L. Feliu, E. Bardají, W. Kowalczyk, D. Andreu, N.C. Santos, Escherichia coli cell surface perturbation and disruption induced by antimicrobial peptides BP100 and pepR, J. Biol. Chem. 285 (2010) 27536–27544.

[29] C.L. Nobles, S.I. Green, A.W. Maresso, A product of heme catabolism modulates bacterial function and survival, PLoS Pathog 9 (2013)

e1003507.

[30] J. E Pollard, J. Snarr, V. Chaudhary, J.D. Jennings, H. Shaw, B. Christiansen, J. Wright, W. Jia, R. Bishop, P.B. Savage. (2012) In vitro evaluation of the potential for resistance development to ceragenin CSA-13. *Journal of Antimicrobial Chemotherapy 67(11)*, 2665–2672.

[31] Y. Lyu, X. Yang, S. Goswami, B.K. Gorityala, T. Idowu, R. Domalaon, G.G. Zhanel, A. Shan, F. Schweizer. (2017) Amphiphilic tobramycin-lysine conjugates sensitize multidrug resistant gram-negative bacteria to rifampicin and minocycline. *Journal of Medicinal Chemistry 60,* 3684–3702.

[32] G. Sautrey, L. Zimmermann, M. Deleu, A. Delbar, L.S. Machado, K. Jeannot, F. Van Bambeke, J.M. Buyck, J.-L. Decout, M.-P. Mingeot-Leclercq, New amphiphilic neamine derivatives active against resistant Pseudomonas aeruginosa and their interactions with lipopolysaccharides, Antimicrob. Agents Chemother. 58 (2014) 4420-4430.

[33] A. Bhunia, H. Mohanram, S. Bhattacharjya, Lipopolysaccharide bound structures of the active fragments of fowlicidin-1, a cathelicidin family of antimicrobial and antiendotoxic peptide from chicken, determined by transferred nuclear overhauser effect spectroscopy, Biopolymers 92 (2009) 9-22.

[34] C.J. de Haas, H.J. van Leeuwen, J. Verhoef, K.P. van Kessel, J.A. van Strijp, Analysis of lipopolysaccharide (LPS)-binding characteristics of serum components using gel filtration of FITC-labeled LPS, J. Immunol. Methods. 242 (2000) 79-89.

[35] Y. Rosenfeld, N. Papo, Y. Shai, Endotoxin (lipopolysaccharide) neutralization by innate immunity host-defense peptides peptide properties and plausible modes of action, J. Biol. Chem. 281 (2006) 1636-1643.

[36] J. Kim, B. Jacob, M. Jang, C. Kwak, Y. Lee, K. Son, S. Lee, I.D. Jung, M.S. Jeong, S.-H. Kwon, Development of a novel short 12-meric papiliocin-derived peptide that is effective against Gram-negative sepsis,

Sci. Rep. 9 (2019) 1-13.

[37] K.T. O'Neil, W.F. DeGrado, A thermodynamic scale for the helix-forming tendencies of the commonly occurring amino acids, Science 250 (1990) 646-651.

[38] K. Matsuzaki, Control of cell selectivity of antimicrobial peptides, Biochim. Biophys. Acta Biomembr. 1788 (2009) 1687-1692.

[39] W. Hu, K. Lee, T. Cross, Tryptophans in membrane proteins: indole ring orientations and functional implications in the gramicidin channel, Biochemistry 32 (1993) 7035-7047.

[40] S.R. Dennison, D.A. Phoenix, Influence of C-terminal amidation on the efficacy of modelin-5, *Biochemistry* 50 (2011) 501514-501523.

[41] S.M. Travis, N.N. Anderson, W.R. Forsyth, C. Espiritu, B.D. Conway, E. Greenberg, P.B. McCray, R.I. Lehrer, M.J. Welsh, B.F. Tack, Bactericidal activity of mammalian cathelicidin-derived peptides, Infect. Immun. 68 (2000) 2748-2755.

[42] S.D. Wright, P.S. Tobias, R.J. Ulevitch, R.A. Ramos, Lipopolysaccharide (LPS) binding protein opsonizes LPS-bearing particles for recognition by a novel receptor on macrophages, J. Exp. Med. 170 (1989) 1231-1241.

[43] I. Nagaoka, S. Hirota, F. Niyonsaba, M. Hirata, Y. Adachi, H. Tamura, S. Tanaka, D. Heumann, Augmentation of the lipopolysaccharide-neutralizing activities of human cathelicidin CAP18/LL-37-derived antimicrobial peptides by replacement with hydrophobic and cationic amino acid residues, Clin. Diagn. Lab. Immunol. 9 (2002) 972-982.

[44] M.M. Domingues, R.G. Inácio, J.M. Raimundo, M. Martins, M.A. Castanho, N.C. Santos, Biophysical characterization of polymyxin B interaction with LPS aggregates and membrane model systems, Biopolymers 98 (2012) 338-344.

[45] D. Takahashi, S.K. Shukla, O. Prakash, G. Zhang, Structural determinants of host defense peptides for antimicrobial activity and target cell selectivity, Biochimie 92 (2010) 1236-1241.

[46] N. Dong, Q. Ma, A. Shan, Y. Lv, W. Hu, Y. Gu, Y. Li, Strand length-dependent antimicrobial activity and membrane-active mechanism of arginine-and valine-rich β-hairpin-like antimicrobial peptides, Antimicrob. Agents Chemother. 56 (2012) 2994-3003

[47] B. Deslouches, M.L. Hasek, J.K. Craigo, J.D. Steckbeck and R.C. Montelaro, Comparative functional properties of engineered cationic antimicrobial peptides consisting exclusively of tryptophan and either lysine or arginine, J. Med. Micro, 64 (2016) 554-565

[48] C.M. Santiveri, M.A. Jiménez, Tryptophan residues: Scarce in proteins but strong stabilizers of β-hairpin peptides, Biopolymers 94 (2010) 779-790.

[49] Y.H. Nan, S.H. Lee, H.J. Kim, S.Y. Shin, Mammalian cell toxicity and candidacidal mechanism of Arg-or Lys-containing Trp-rich model antimicrobial peptides and their D-enantiomeric peptides, Peptides 31 (2010) 1826-1831.

[50] Y. Chen, C.T. Mant, S.W. Farmer, R.E. Hancock, M.L. Vasil, R.S. Hodges, Rational design of α-helical antimicrobial peptides with enhanced activities and specificity/therapeutic index, J. Biol. Chem. 280 (2005) 12316-12329.

[51] A.J. Wolf, G.Y. Liu, D.M. Underhill, Inflammatory properties of antibiotic-treated bacteria, J. Leukoc. Biol. 101 (2017) 127-134.

[52] M.J. McDonnell, L. Rivas, C.M. Burgess, S. Fanning, G. Duffy, Inhibition of verocytotoxigenic *Escherichia coli* by antimicrobial peptides caseicin A and B and the factors affecting their antimicrobial activities, Int. J. Food Microbiol. 153 (2012) 260-268.

[53] H. Sugiarto, P.-L. Yu, Effects of cations on antimicrobial activity of ostricacins-1 and 2 on E. coli O157: H7 and S. aureus 1056MRSA, Curr. Microbiol. 55 (2007) 36-41.

[54] B. Deslouches, K. Islam, J.K. Craigo, S.M. Paranjape, R.C. Montelaro, T.A. Mietzner, Activity of the de novo engineered antimicrobial peptide WLBU2 against Pseudomonas aeruginosa in human serum and whole

blood: implications for systemic applications, Antimicrob. Agents Chemother. 49 (2005) 3208-3216.

[55] Z. Oren, Y. Shai, Mode of action of linear amphipathic α-helical antimicrobial peptides, Biopolymers 47 (1998) 451-463.

[56] K.A. Brogden, Antimicrobial peptides: pore formers or metabolic inhibitors in bacteria?, Nat. Rev. Microbiol. 3 (2005) 238-250.

[57] C. Subbalakshmi, N. Sitaram, Mechanism of antimicrobial action of indolicidin, FEMS Microbiol. Lett. 160 (1998) 91-96.

[58] C.B. Park, H.S. Kim, S.C. Kim, Mechanism of action of the antimicrobial peptide buforin II: buforin II kills microorganisms by penetrating the cell membrane and inhibiting cellular functions, Biochem. Biophys. Res. Commun. 244 (1998) 253-257.

[59] J. Lutkenhaus, Regulation of cell division in *E. coli,* Trends Genet. 6 (1990) 22-25.

[60] F. Silva, O. Lourenco, J.A. Queiroz and F. C. Domingues, Bacteriostatic versus bactericidal activity of ciprofloxacin in *Escherichia coli* assessed by flow cytometry using a novel far-red dye, J. Antibiotics. 64 (2011) 321-325.

[61] H. Hrebenda, H. Heleszko, K. Brzostek, J. Bielecki, Mutation affecting resistance of Escherichia coli K12 to nalidixic acid. J. Gen. Microbiol. 131(1985) 2285-2292.

[62] D. Derossi, G. Chassaing, A. Prochiantz, Trojan peptides: the penetratin system for intracellular delivery, Trends Cell Biol. 8 (1998) 84-87.

[63] M.H. Cardoso, B.T. Meneguetti, B.O. Costa, D.F. Buccini, K.G. Oshiro, S.L. Preza, C.M. Carvalho, L. Migliolo, O.L. Franco, Non-Lytic Antibacterial Peptides That Translocate Through Bacterial Membranes to Act on Intracellular Targets, Int. J. Mol Sci. 20 (2019) 4877.

[64] V.V. Andrushchenko, H.J. Vogel, E.J. Prenner, Interactions of tryptophan-rich cathelicidin antimicrobial peptides with model membranes studied by differential scanning calorimetry, Biochim. Biophys. Acta Biomembr.

1768 (2007) 2447-2458.

[65] Z.Y. Ong, S.J. Gao, Y.Y. Yang, Short synthetic β-sheet forming peptide amphiphiles as broad spectrum antimicrobials with antibiofilm and endotoxin neutralizing capabilities, Adv. Funct Mater. 23 (2013) 3682-3692.

[66] L. Ding, L. Yang, T.M. Weiss, A.J. Waring, R.I. Lehrer, H.W. Huang, Interaction of antimicrobial peptides with lipopolysaccharides, Biochemistry 42 (2003) 12251-12259.

[67] S. David, K. Balasubramanian, V. Mathan, P. Balaram, Analysis of the binding of polymyxin B to endotoxic lipid A and core glycolipid using a fluorescent displacement probe, Biochim. Biophys. Acta. 1165 (1992) 147-152.

[68] M. Mueller, B. Lindner, S. Kusumoto, K. Fukase, A.B. Schromm, U. Seydel, Aggregates are the biologically active units of endotoxin, J. Biol. Chem. 279 (2004) 26307–26313.

[69] M.G. Scott, A.C. Vreugdenhil, W.A. Buurman, R.E. Hancock, M.R. Gold, Cutting edge: cationic antimicrobial peptides block the binding of lipopolysaccharide (LPS) to LPS binding protein, J. Immunol. 164 (2000) 549-553.

[70] R.M. Srivastava, S. Srivastava, M. Singh, V.K. Bajpai, J.K. Ghosh, Consequences of alteration in leucine zipper sequence of melittin in its neutralization of lipopolysaccharide-induced proinflammatory response in macrophage cells and interaction with lipopolysaccharide, J. Biol. Chem. 287 (2012) 1980–1995.

PART II

The design of a cell-selective fowlicidin-1-derived peptide with both antimicrobial and anti-inflammatory activities

1. Introduction

Antimicrobial peptides (AMPs) are an important component of the innate immune system and have been identified in virtually all living species [1,2]. Unlike most conventional antibiotics that act mainly by blocking limited intracellular targets, their bactericidal activity most often stems from their ability to disrupt bacterial membrane integrity [1,2]. In addition to directing bactericidal activity, many AMPs can neutralize endotoxin-induced proinflammatory responses [2,3]. Because of these desirable features, several AMPs are currently being developed clinically as a new class of antimicrobial agents.

Cathelicidins comprise a major family of AMPs that have been identified in vertebrates [4–6]. They all have a highly conserved cathelin pro-sequence at the N-terminus, with extremely variable C-terminal sequences that have antimicrobial and immune regulatory activities, and have been shown to exert multifunctional activities, including antimicrobial and anti-inflammatory activities [7–9]. In a previous study, three novel cathelicidins were identified via the computational screening of the chicken genome, and, one of these, 26-meric fowlicidin-1 (Fowl-1), which had antimicrobial potency like SMAP-29, proved to be highly active against both gram-negative and -positive bacterial strains, including methicillin-resistant *Staphylococcus aureus* (MRSA), with minimum inhibitory concentrations (MIC) ranging between 1 and 2 μM [10]. Notably, its antimicrobial activity is largely unaffected by serum or salt, including high NaCl concentration. Additionally, it is also characterized by high LPS affinity or endotoxin neutralization activities [10,11]. In membrane-mimic environments, Fowl-1 is predominantly α-helical, with a slight kink induced by Gly^{16} close to its center, and a short flexible unstructured region comprising the first five amino acid residues [11].

Lipopolysaccharides (LPS), which are well known endotoxins, are a major component of the cell wall of gram-negative bacteria. During infection, their release from gram-negative bacteria into the bloodstream may cause serious and unwanted stimulation of the patient's immune system, leading to septic shock,

which frequently results in death [12–14]. Some AMPs, including human LL-37 [15,16] and β-defensins [17,18], are capable of binding to LPS and inhibiting LPS-induced cellular inflammatory cytokine and/or nitric oxide (NO) release. Likewise, Fowl-1 is known to exhibit potent LPS-neutralizing activity, eliminating nearly 95% of LPS-induced cytokine and chemokine gene expression in RAW264.7 mouse macrophages at 5–10 μM [10,19]. Thus, its antimicrobial and anti-inflammatory (anti-endotoxic) properties make it a promising therapeutic agent in the treatment of bacterial infections and LPS-induced inflammatory diseases. However, at a concentration range of 6 to 40 μM, Fowl-1 showed cytotoxicity, killing 50% of mammalian erythrocytes or epithelial cells [10]. Thus, its therapeutic application is hindered by its low cell selectivity, i.e., its inability to selectively differentiate between bacterial and human red blood cells.

In this study, the objective of which was to develop a short Fowl-1 analog possessing antimicrobial and anti-inflammatory activities without hemolytic activity, a series of N- and C-terminal-truncated 19-meric Fowl-1 fragments were synthesized and functionally evaluated. Their cell selectivity, determined using the therapeutic index (TI), which is defined as the ratio of the concentration of hemolytic activity (minimum hemolytic concentration, MHC) to antimicrobial activity (MIC), was investigated by examining their antimicrobial activity against gram-positive and gram-negative bacterial strains and their hemolytic activity against sheep red blood cells. With the exception of Fowl-1(5-23), all the other fragments showed higher cell selectivity compared with Fowl-1, with the highest value shown by Fowl-1(8-26), which, however, displayed relatively low inhibitory activity against NO and tumor necrosis factor-α (TNF-α) release from LPS-stimulated RAW 264.7 mouse cells.

In order to improve anti-inflammatory activity while retaining high cell selectivity, Fowl-1(8-26)-WRK (LVIRWVRAGYKLYRAIKKK-NH_2), which displayed increased peptide amphipathicity via $Thr^5 \rightarrow$Trp, $Ile^7 \rightarrow$Arg, and $Asn^{11} \rightarrow$Lys substitutions, was engineered using the α-helical wheel diagram of Fowl-1(8-26). The designed Fowl-1(8-26)-WRK, which was amidated at the C-

terminus to improve stability, retained relatively good cell selectivity. Furthermore, it significantly suppressed NO and TNF-α release from LPS-stimulated RAW 264.7 macrophage cells by reducing TNF-α mRNA and inducible nitric oxide synthase (iNOS) levels. The antimicrobial activity of Fowl-1(8-26)-WRK against MRSA, multidrug-resistant *Pseudomonas aeruginosa* (MDRPA), and vancomycin-resistant *Enterococcus faecium* (VREF) was evaluated, and its stability in human serum and in the presence of physiological salts was assessed. Additionally, its synergistic effects in combination with three conventional antibiotics (chloramphenicol, ciprofloxacin, and oxacillin), which have different mechanisms of action against MDRPA and MRSA, were investigated. In order to understand its bacterial killing mechanism, membrane depolarization, SYTOX Green uptake, and flow cytometry experiments were performed. Conclusively, we believe that the results of this study can contribute to the design of novel antibiotics that possess both antimicrobial and anti-inflammatory properties as well as the ability to act synergistically with conventional antibiotics without causing host cytotoxicity.

2. Materials and methods

2.1. Materials

9-fluorenyl-methoxycarbonyl (Fmoc) amino acids were purchased from Novabiochem (La Jolla, CA, USA). Lipopolysaccharide (LPS) purified from *Escherichia coli* O111:B4, 2,2,2-trifluoroethanol (TFE), sodium dodecyl sulfate (SDS), 3-(4,5-dimethylthiazol-2-yl)-2,5-diphenyl-2H-tetrazolium bromide (MTT), and diSC_3-5 were supplied from Sigma-Aldrich (St. Louis, MO, USA). HyClone Dulbecco's modified Eagle medium (DMEM) and fetal bovine serum (FBS) were obtained from SeouLin Bioscience (Seoul, Korea). The ELISA kits for TNF-α was procured from R&D Systems (Minneapolis, MN, USA). SYTOX green was purchased from Life Technologies (Eugene, OR, USA). Buffers were prepared using Milli-Q ultrapure water (Merck Millipore, Billerica, MA, USA). All other reagents were of analytical grade. We used total 12 microbial strains in this study. Three strains of Gram-positive bacteria (*Bacillus subtilis* [KCTC 3068], *Staphylococcus epidermidis* [KCTC 1917], and *Staphylococcus aureus* [KCTC 1621]) and three strains of Gram-negative bacteria (*Escherichia coli* [KCTC 1682], *Pseudomonas aeruginosa* [KCTC 1637], and *Salmonella typhimurium* [KCTC 1926]) were procured from the Korean Collection for Type Cultures (KCTC) of the Korea Research Institute of Bioscience and Biotechnology (KRIBB). Methicillin-resistant *Staphylococcus aureus* strains (MRSA; CCARM 3089, CCARM 3090, and CCARM 3095) and multidrug-resistant *Pseudomonas aeruginosa* strains *(MDRPA; CCARM 2095, and CCARM 2109)* were obtained from the Culture Collection of Antibiotic-Resistant Microbes (CCARM) of Seoul Women's University in Korea. Vancomycin-resistant *Enterococcus faecium* (VREF; ATCC 51559) was supplied from the American Type Culture Collection (Manassas, VA, USA). All bacterial strains were purchased from the Korean Collection for Type Cultures (KCTC), the American Type Culture Collection (ATCC), or the Culture Collection of antibiotic-resistant microbes (CCARM). These strains were stored at

-80 °C in 20 % (v/v) glycerol until sub-cultured onto Luria-Bertani (LB) agar plate for further studies.

2.2. Peptide synthesis

The peptides were synthesized manually by SPPS using Fmoc chemistry (0.06 mmole scale) starting from MBHA-Rink Amide resin (0.4–0.7 mmol/g loading). Fmoc from the resin was removed with 20% piperidine, wash resin with DMF and swell resin with DCM. Coupling reactions between the C-terminal residue and the resin, and between subsequent amino acid residues, were carried out for 120 min per coupling cycle under the activation of 1-hydroxybenzotriazole (HOBt) (10 equiv.) and dicyclohexylcarbodiimide (DCC) (10 equiv.) in DMF at 25 ºC. The Fmoc protecting group of amino acid was removed with 20% piperidine in DMF after each coupling cycle. The final cleavage of the peptide from the resin and deprotection of amino acid side chain were carried out with a cocktail solution of TFA/TIS/phenol/H_2O/EDT (with a volume ratio of 82.5:5:5:5:2.5) for 3 h at 25 ºC. The cleaved crude peptides were thoroughly washed with cold diethyl ether three times and were lyophilized. The linear peptides were purified using RP-HPLC (Shimadzu, Japan) on a preparative Vydac C_{18} column (length: 250 mm, internal diameter: 20 mm, pore size: 300 Å, particle size: 15 mm) monitored by UV absorbance at 224 nm. The mobile phase components were 0.05% TFA in water (solvent A) and 0.05% TFA in acetonitrile (ACN) (solvent B). The purity of the synthesized peptides was confirmed by analytical RP-HPLC. The purified products were confirmed by matrix-assisted laser desorption/ionization time-of-flight (MALDI-TOF) mass spectrometry (Shimadzu, Kyoto, Japan) analysis.

2.3. Antimicrobial activity assay

The antimicrobial activity of the peptides was determined by measuring the minimal inhibitory concentrations (MIC) using the microtiter broth dilution method [20,21]. Aliquots (100 μL) of bacterial cell suspension at 4×10^6 CFU/mL in 1% peptone were added to 100 μL of the sample solutions (serial 2-fold dilutions in 1%

peptone). The MICs were defined as the lowest concentration that inhibited visible turbidity by visual inspection after incubation at 37 °C for 18 h. The MIC was defined as the lowest concentration that inhibits bacterial growth as determined visually or spectrophotometrically by OD_{600} readings taken with a Microplate Autoreader (Bio-Tek; EL 800). Experiments were performed in triplicate and repeated three times.

2.4. Salt and serum sensitivity assay

Briefly, bacteria were incubated in the presence of different final concentrations of physiological salts (150mM NaCl, 4.5 mM KCl, 6 μM NH_4Cl, 1mM $MgCl_2$, 2.5 mM $CaCl_2$, and 4 μM $FeCl_3$) and 20% human serum. The MIC assay was the same as described above.

2.5. Circular dichroism (CD) spectroscopy

To detect the secondary structure of the peptides in different environments, circular dichroism (CD) was measured. CD spectra of peptides were detected in 10 mM sodium phosphate buffer (pH 7.4), 50% TFE, and 30 mM SDS micelles at 25 °C with a J-715 spectropolarimeter (Jasco, Tokyo, Japan) equipped with a rectangular quartz cell with a path length of 0.1cm. The spectra were recorded between 190 nm and 250 nm at a scanning speed of 10nm/min. The results from three scans were collected and calculated for each peptide. The final concentration of peptides in each buffer was 100 μg/mL. The mean residue ellipticity was calculated according to the following equation: $[\theta]_M = (\theta_{obs} \times 1000) / (c \times l \times n)$ where θ_M is the mean residue ellipticity (deg cm^2 $dmol^{-1}$), θ_{obs} the observed ellipticity corrected for the buffer at a given wavelength (mdeg), c the peptide concentration (mM), l the path length (mm), and n the number of amino acids.

2.6. Hemolytic activity assay

Fresh sheep red blood cells (sRBCs) was washed 3 times with phosphate-buffered saline (PBS), centrifuged for 5 minutes at 1000 rpm, and diluted to a

concentration of 2% in PBS. Both peptide solution (100 μL) and 2% sRBC (100 μL) were added simultaneously to each well of a 96-well plate and then further incubated at 37 ºC for 2 h. After the plate was centrifuged at 120×g for 5 minutes, the supernatant (100 μL) from each well was transferred to a new 96-well plate and measured by a microplate ELISA reader (Molecular Devices, Sunnyvale, CA, USA) at 414 nm [22,23]. Zero and 100% hemolysis were determined in PBS and 0.1 % Triton-X 100, respectively.

2.7. Cytotoxicity against RAW 264.7 cells

To determine the cytotoxicity of the peptides against RAW 264.7 cells, we used the MTT dye reduction assay. RAW 264.7 cells (1×10^4 cells/well) were placed into 96-well microplates, and then incubated for 24 h at 37 °C in 5% CO_2. The next day, peptides were added to cell cultures at final concentrations of 40 μM, and untreated cell cultures served as controls. The cell cultures were further incubated for 48 h, and then mixed with MTT (20 μL, 0.5 mg/mL). After the mixtures were incubated for 4 h at 37 °C, 150 μL of DMSO was added to dissolve the formazan crystals formed. Finally, the OD was measured using a microplate reader (Bio-Tek Instruments EL800, USA) at 550 nm. Cell viability was expressed as (A_{550nm} of treated sample) / (A_{550nm} of control) ×100%.

2.8. Measurement of NO production from LPS-stimulated RAW264.7 cells

RAW264.7 cells were plated at a density of 5×10^5 cells/ml in 96-well culture plates and stimulated with LPS (20 ng/mL) in the presence or absence of peptides for 24 h. Isolated supernatant fractions were mixed with an equal volume of Griess reagent (1% sulfanilamide, 0.1% naphthylethylenediamine dihydrochloride and 2% phosphoric acid) and incubated at room temperature for 10 min. Nitrite production was quantified by measuring absorbance at 540 nm, and concentrations were determined using a standard curve generated with $NaNO_2$.

2.9. Measurement of TNF-α release from LPS-stimulated RAW264.7 cells

RAW264.7 cells were seeded in 96-well plates (5×10^4 cells/well) and incubated overnight. Peptides were added and the cultures were incubated at 37 °C for one hour. Subsequently, 20 ng/mL LPS was added and the cells were incubated for another 6 h at 37 °C. The concentration of TNF-α in each sample was measured using a mouse TNF-α ELISA kit (R&D Systems, Minneapolis, MN, USA) according to the manufacturer's protocol.

2.10. Reverse-transcription polymerase chain reaction (RT-PCR)

RAW264.7 cells were plated at a concentration of 5×10^5 cells/well in six-well plates and incubated overnight. Each peptide was added to the wells. The final concentration of the small molecule compounds was 4 μM (for NO) or 8 μM (for TNF-α). Cells to be used for quantification of TNF-α and iNOS were treated for 3 h and 6 h, respectively, with or without (negative control) 20 ng/ml LPS, in the presence or absence of peptide, in DMEM supplemented with 10% bovine serum. The cells were detached from the wells and washed once with PBS. Total RNA was extracted by Trizol Reagent (Ambion, USA). Then, 1 μg of total RNA was converted to cDNA using a TakaRa Primescript™ Reverse Transcriptase (TakaRa, Seoul, Korea). The primers used were purchased from Bioneer (Seoul, Korea). The cDNA products were amplified by AccuPower® PCR PreMix (Bioneer, Daejeon, Korea). For iNOS (forward, 5′-CTGCAGCACTTGGATCAGGAACCTG-3′; reverse, 5′-GGGAGTAGCCTGTGTGCACCTGGAA-3′), TNF-α (forward, 5′-CCTGTAGCCCACGTCGTAGC-3′; reverse, 5′-TTGACCTCAGCGCTGAGTTG-3′), or GAPDH (forward, 5′-GACATCAAGAAGGTGGTGAA-3'; reverse, 5′-TGTCATACCAGGAAATGAGC-3'). The amplification protocol consisted of an initial denaturation step of 5 min at 94 °C, followed by 30 cycles of denaturation at

94 °C for 1min, annealing at 55 °C for 1.5 min, and extension at 72 °C for 1 min, and afterwards by a final extension step of 5 min at 72 °C.

2.11. LPS-neutralization assay

The LPS-neutralizing activity of the peptides was examined by a BODIPY-TR-cadaverine displacement assay [24]. Briefly, *E. coli* O111:B4 LPS (25 μg/mL), BODIPY-TRcadaverine (2.5 μg/mL) and 50 mM Tris buffer (pH 7.4) were mixed. A volume of 2 mL of this mixture was added to a quartz cuvette. The fluorescence was recorded at an excitation wavelength of 580 nm and an emission wavelength of 620 nm with a Shimadzu RF-5300PC fluorescence spectrophotometer (Shimadzu Scientific Instruments, Kyoto, Japan). The experiment was performed at least three times with replicates.

2.12. Checkerboard assay

Firstly, 2-fold serial dilutions of each antibiotic and each peptide were prepared and added in a 1:1 volume ratio to the wells of a 96-well plate. An equal volume of bacterial solution (100 μL) at ~10^6 CFU/mL was then seeded into each well. The plates were incubated in a shaking incubator at 37 °C and 200 rpm and read after 72 h. Bacterial growth was assessed visually or spectrophotometrically via OD_{600} readings taken by a microplate ELISA reader (Molecular Devices, Sunnyvale, CA, USA). The fractional inhibitory concentration index (FICI) for each drug combination was calculated using the following equation: $FICI = FIC_A + FIC_B = [A]/MIC_A + [B]/MIC_B$, where MIC_A and MIC_B are the MIC of antibiotic and peptide, respectively, while [A] and [B] are the MIC of antibiotic and peptide in combination, respectively. FICI of ≤ 0.5 was interpreted as synergy, 0.5 < FICI ≤ 1.0 as additive, 1.0 < FICI ≤ 4.0 as indifferent, and an FICI > 4.0 as antagonism.

2.13. SYTOX Green uptake assay

S. aureus cells were grown to mid-logarithmic phase at 37 °C, washed and suspended (2×10^6 CFU/mL) in buffer (20 mM glucose, 5 mM HEPES and 10 mM

KCl, pH7.4), after which SYTOX Green (Molecular probes) was added to a final concentration of 1 mM, and the cells were incubated at 37 °C for 15 min with agitation in dark. After the addition of peptides at the appropriate concentrations, the time-dependent increases in fluorescence caused by the binding of the cationic dye to intracellular DNA were monitored. Thereafter, without peptide and the peptides (2 × MIC) was added, and then the increase in fluorescence was monitored using a Shimadzu RF-5300PC fluorescence spectrophotometer (Shimadzu Scientific Instruments, Kyoto, Japan) with an excitation wavelength of 485 nm and an emission wavelength of 520 nm. This is possible because the cationic dye, which can only cross compromised membranes, binds to intracellular DNA and this interaction results in a significant increase of fluorescence intensity. Bacteria treated with melittin (a toxin from bee venom) and LL-37 were used as positive controls to provide maximal permeabilization values.

2.14. Cytoplasmic membrane depolarization assay

The interaction of peptides with the cytoplasmic membrane of bacteria cells was detected using the membrane potential-sensitive fluorescent dye diSC_3-5. Briefly, *S. aureus* cells were cultured to the mid-log phase at 37 °C and diluted to an OD_{600} of 0.08 in buffer (5 mM HEPES, 20 mM glucose, and 10 mM KCl, pH 7.4). The bacteria cells were incubated with 20 nM diSC_3-5 until a stable reduction of the fluorescence was achieved. The cell suspension (3 mL) was placed in a 1-cm-path-length cuvette, and the peptides (2 × MIC) were added. The fluorescence intensity changes were monitored using a Shimadzu RF-5300PC fluorescence spectrophotometer (Shimadzu Scientific Instruments, Kyoto, Japan) with an excitation wavelength of 622 nm and an emission wavelength of 670 nm. The membrane potential was fully abolished by adding 0.1% Triton X-100.

2.15. FACScan analysis

The membrane damage by the peptides was determined by flow cytometry. In brief, *E. coli* was grown to mid-log phase in LB, washed thrice with PBS and

diluted to with PBS to 2×10^7 CFU/mL. The peptides were incubated with the bacterial suspension at a fixed PI concentration of 10 μg/mL for 1 h or 2 h at 37 ºC, followed by the removal of the unbound dye through washing with an excess of PBS. The data were recorded using a FACScan instrument (FACSCalibur, Beckman Coulter Inc., USA) with a laser excitation wavelength of 488 nm.

2.16. Statistical analysis

All results are presented as averages of values derived from three independent experiments, with triplicates used in each experiment. Error bars represent the mean ± standard deviation of the mean. The statistical significance of differences between samples and respective controls (no added antimicrobial agent) were determined by one-way analysis of variance (ANOVA) with Bonferroni's post-test method using Sigma plot v12.0 (Systat Software Inc., San Jose, CA, USA). Differences with $P < 0.001$ were considered statistically significant.

3. Results

3.1. Synthesis of truncated peptides from Fowl-1

In order to identify Fowl-1 truncated peptides with high antimicrobial and non-hemolytic activities, a series of N- and C-terminal truncated peptides were synthesized, and their molecular weights verified using MALDI-TOF-MS. Fig. 1 shows the predicted α-helical wheel diagrams of each synthesized peptide, whereas Table 1 summarizes their theoretically calculated and measured molecular weights. The measured molecular weight of Fowl-1 closely matched the theoretical values, indicating that the peptides had been successfully synthesized. The different analytical C_{18}-column HPLC retention times of the peptides reflected their relative hydrophobicity, in the following order: Fowl-1(5-23) > Fowl-1 > Fowl-1(3-21) > Fowl-1(1-19) > Fowl-1(8-26). Their hydrophobic moment (μH) values, which determined the amphipathicity degree of these α-helical peptides, ranged from 0.284 to 0.363 (Table 1).

3.2. Antimicrobial and hemolytic activities of Fowl-1 and its truncated peptides

The antimicrobial activity of Fowl-1 and its truncated peptides against three gram-positive and three gram-negative bacterial strains was tested by determining the MIC, as summarized in Table 2. Generally, relative to the parent Fowl-1, all the truncated peptides showed lower antimicrobial activity, with Fowl-1(8-26) exhibiting the highest antimicrobial activity.

The toxicity of Fowl-1 and its truncated peptides against mammalian cells was determined by investigating their ability to lyse sheep erythrocytes, measured as a function of their concentrations (range, 0.5 to 256 μM). To measure their relative hemolytic activity, MHC, which is defined as the lowest peptide concentration that lysed 10% of sheep red blood cells (Table 3), was determined, and their relative

potencies were as follows: Fowl-1 > Fowl-1(5-23) > Fowl-1(3-21) > Fowl-1(8-26) > Fowl-1(1-19).

To assess their use as a new generation of antimicrobial agents, it was necessary to evaluate the side-effects induced by their interaction with normal mammalian cells. The therapeutic potential of antimicrobial agents depends on their ability to selectively kill bacteria over normal mammalian cells. The therapeutic index (TI) was used to evaluate the cell selectivity of the peptides towards negatively charged bacterial cell membranes over the zwitterionic mammalian cell membranes [25–27]. The TI values of the peptides, defined as ratio of the MHC to the GM (the geometric mean of the MICs) and indicative of peptide cell selectivity, are presented in Table 3. Thus, a high TI value is indicative of two antimicrobial agent characteristics: high MHC (low hemolysis) and low MIC (high antimicrobial activity). Of all the truncated peptides, Fowl-1(8-26) showed the highest TI value (35.8), which was 3.5-folds higher than that of Fowl-1.

3.3. Inhibitory effect of Fowl-1 and its truncated peptides on LPS-stimulated NO and TNF-α release

Before the determination of the anti-inflammatory activity of Fowl-1 and its truncated peptides in LPS-induced RAW 264.7 mouse cells, their cytotoxicity in these animal model cells was tested using the MTT assay. As shown in Fig. 2, the results revealed that at concentrations of up to 16 μM, none of the peptides were cytotoxic. Thus, all assays on peptide anti-inflammatory activity in LPS-induced RAW 264.7 mouse cells were performed at peptide concentrations <16 μM.

To investigate the potential of these peptides in suppressing NO and TNF-α release from LPS-stimulated macrophage RAW 264.7 cells, NO and TNF-α levels in the medium containing mouse RAW 264.7 cells incubated with LPS and LPS + peptide, were measured. RAW 264.7 mouse cells were stimulated with LPS (20 ng/mL) in the presence of the respective peptides (4 μM), and NO production was determined using the Griess method, which detects nitrite accumulation in a culture medium. At 4 μM, Fowl-1, Fowl-1(1-19), Fowl-1(3-21), Fowl-1(5-23), and Fowl-

1(8-26) inhibited NO production by 96.7, 2.3, 3.4, 91.9, and 16.2%, respectively (Fig. 3-a and Table 3). The TNF-α release inhibition effect of the peptides in LPS (20 ng/ml)-stimulated RAW 264.7 cells was investigated using commercially available ELISA kits. At 8 μM, Fowl-1, Fowl-1(1-19), Fowl-1(3-21), Fowl-1(5-23), and Fowl-1(8-26) inhibited TNF-α production by 73.5, 1.1, 10.7, 41.5, and 13.8%, respectively (Fig. 3-b and Table 3).

Additionally, LPS induces the expression of iNOS and TNF-α genes, which are correlated with NO and TNF-α production in RAW 264.7 cells. Thus, the effects of Fowl-1 and its analogs on LPS-induced iNOS and TNF-α expression were examined using RT-PCR. As observed with LL-37, Fowl-1 and Fowl-1(5-23) significantly suppressed iNOS and TNF-α expression at 4 μM and 8 μM, respectively, corresponding with the observed inhibition of NO and TNF-α release by these peptides (Fig. 3-c).

3.4. Antimicrobial and anti-inflammatory activities of Fowl-1(8-26)-WRK

An effective antimicrobial peptide should not only exert antimicrobial activity without mammalian cell toxicity, it should also have LPS-neutralizing ability, thus eliminating its toxicity. Therefore, antimicrobial and anti-inflammatory activities are two characteristics that are highly desirable in antimicrobial agents. Of all the truncated peptides, Fowl-1(8-26) showed the highest cell selectivity; however, it demonstrated little or no LPS-induced inflammation inhibition activity. Therefore, to increase its antimicrobial potency and inhibitory activity with respect to LPS-induced inflammation, without significantly changing its hemolytic activity, Fowl-1(8-26)-WRK was designed using the α-helical wheel diagram of Fowl-1(8-26) via $Thr^{5}\rightarrow$Trp, $Ile^{7}\rightarrow$Arg, and $Asn^{11}\rightarrow$Lys substitutions. As shown in Table 3, Fowl-1(8-26)-WRK displayed antimicrobial activity like Fowl-1, but showed low hemolytic activity (MHC = 105 μM). Relative to Fowl-1, its TI increased approximately 2.8-folds, and at 4 μM and 8 μM, it was found to suppress LPS-mediated production of NO and TNF-α in macrophages by 94.2 and 75.2%,

respectively (Figs. 3-a and –b and Table 3). Additionally, at 4 μM and 8 μM, it significantly reduced iNOS and TNF-α expression in LPS-stimulated macrophages, respectively (Fig. 3-c). Hence, to thoroughly evaluate its therapeutic potential as an antimicrobial/anti-inflammatory agent, as well as the mechanism of its antimicrobial action, Fowl-1(8-26)-WRK was developed as the lead peptide.

3.5. CD spectroscopy

CD spectroscopy was used to determine the structural conformations of the peptides in different environments. The hydrophobic and helix stabilizing agent TFE, was employed to assess the inherent helical propensity of Fowl-1 and its analogs, and an SDS micelle with a negatively charged surface was used to mimic an anionic membrane environment [28]. The spectra of Fowl-1, Fowl-1(8-26), and Fowl-1(8-26)-WRK in 10 mM sodium phosphate buffer (pH 7.4) were characteristic of unordered conformations, with a minimum close to 198 nm (Fig. 4). In the presence of 50% TFE and 30 mM anionic SDS, the presence of two negative dichroic bands at ~208 and 222 nm were observed in these peptides, consistent with the predominant induction of α-helical conformations (Fig. 4).

3.6. Binding studies of Fowl-1(8-26)-WRK to LPS

To investigate whether the inhibitory activity of Fowl-1(8-26)-WRK against LPS-induced macrophage inflammation was due to LPS and Fowl-1(8-26)-WRK binding, RAW 264.7 cells were pre-treated with Fowl-1(8-26)-WRK for 1 h and thoroughly washed to remove unbound/exogenous peptide. Subsequently, the cells were stimulated with LPS, and NO was measured in the cell-free supernatant after 24 h. As observed with polymyxin B (PMB) (a well-known LPS-neutralizing cyclic lipopeptide), the removal of exogenous Fowl-1(8-26)-WRK prior to LPS stimulation eliminated the ability to inhibit LPS-induced NO production (Fig. 5). In addition, the LPS-neutralizing activity of Fowl-1(8-26)-WRK was investigated using the BODIPY-TR-cadaverine (BC) displacement assay, and as shown in Fig.

6, like PMB, Fowl-1(8-26)-WRK at 16 μM showed a concentration-dependent increase in fluorescence intensity with almost complete LPS-neutralizing activity.

3.7. Fowl-1(8-26)-WRK shows strong antimicrobial activity against antibiotic-resistant bacteria

To investigate the efficacy of Fowl-1(8-26)-WRK against antibiotic-resistant bacteria, its antimicrobial activity was tested against three *MRSA* strains, two *MDRPA* strains, and one *VREF* strain (Table 4). The results revealed that Fowl-1(8-26)-WRK showed 2- to 8-fold higher antimicrobial activity against all tested antibiotic-resistant bacterial strains, compared with human AMP, LL-37, and honey bee AMP, melittin (Table 4), indicating that Fowl-1(8-26)-WRK may represent a new class of antimicrobial agents effective against antibiotic-resistant bacteria.

3.8. Fowl-1(8-26)-WRK has salt and human serum stability

To investigate the effects of cationic salts on Fowl-1(8-26)-WRK antimicrobial activity, its MIC values against *E. coli* and *S. aureus* cells were measured after the addition of several physiological salts. As shown in Table 5, the addition of monovalent (Na^+, K^+, and NH_4^+), divalent (Mg^{2+} and Ca^{2+}), and trivalent (Fe^{3+}) cations had little effect on Fowl-1(8-26)-WRK antimicrobial activity. In addition to salt stability, the effect of serum proteases on its antimicrobial potency was assessed by measuring the MIC values of the peptide pre-incubated in 20% human serum. Fowl-1(8-26)-WRK only showed a 2-fold reduction in antimicrobial activity against *E. coli* and S. *aureus*, clearly indicating that it is resistant to cationic salts and human serum proteases.

3.9. Fowl-1(8-26)-WRK acts as a promising adjuvant in combination with conventional antibiotics against MDRPA and MRSA

The fractional inhibitory concentration index (FICI) data on the combination of three conventional antibiotics and Fowl-1(8-26)-WRK or human cathelicidin AMP LL-37 against MDRPA and MRSA, are summarized in Tables 6 and 7, respectively. The interactions between Fowl-1(8-26)-WRK and conventional antibiotics were assessed using the FICI, whereby values ≤ 0.5, $0.5 < x \leq 1.0$, $1.0 < x \leq 4.0$, and >4 were interpreted as synergistic, additive, indifferent, and antagonistic, respectively. With the three conventional antibiotics, Fowl-1(8-26)-WRK demonstrated synergistic or additive interactions against MDRPA, with an FICI range between 0.281 and 0.625, compared with LL-37 (FICI range between 0.75 and 2.0) (Table 6). With the same three conventional antibiotics, it also showed synergistic interaction against MRSA (FICI range between 0.25 and 0.5). Contrarily, LL-37 demonstrated additive or indifferent interactions with an FICI range between 0.75 and 1.25 (Table 7).

Additionally, the MICs of chloramphenicol, ciprofloxacin, and oxacillin against MDRPA and MRSA reduced by 4- to 16-folds and 4- to 32-folds, respectively, in the presence of $1/16^{th}$ Fowl-1(8-26)-WRK MIC (Fig. 7).

3.10. Mechanism of antimicrobial action of Fowl-1(8-26)-WRK

To investigate the mechanism of the antimicrobial action of Fowl-1(8-26)-WRK, its membrane potential was first monitored using the fluorescent dye 3,3'-dipropylthiadicarbocyanine iodide ($diSC_3$-5) (Fig. 8-a) [29,30], which is taken up by bacterial cell membranes in proportion with the electrical potential gradient across the bacterial cytoplasmic membrane. This cationic dye concentrates in the cytoplasmic membrane under the influence of membrane potential, which is internally oriented as negative, thus resulting in the self-quenching of its own fluorescence. Once the bacterial cytoplasmic membrane is disturbed and damaged by the peptides, its electrical potential dissipates and $diSC_3$-5 is released into the medium, resulting in a subsequent enhancement in fluorescence-intensity [30–32]. The depolarization ability of Fowl-1(8-26)-WRK at 2 × MIC against *S. aureus* was monitored over a period of 600 s. Like the membrane-active AMPs, melittin and

LL-37, it caused a large and immediate increase in fluorescence, indicating a loss of membrane potential. Contrarily, without the peptides, membrane-inactive (intracellular targeting) buforin-2 did not induce any increase in fluorescence.

Thereafter, a SYTOX Green assay was performed. SYTOX Green is a high-affinity nucleic acid-binding dye that only penetrates bacteria with damaged membranes, thus enhancing its fluorescence intensity [33–35]. Fig. 8-b displays the effect of Fowl-1(8-26)-WRK, LL-37, melittin, and buforin-2 at 2 × MIC against SYTOX Green-incubated *E. coli*. Like melittin and LL-37, Fowl-1(8-26)-WRK induced rapid permeabilization and achieved maximum SYTOX Green accumulation within 4 min. Contrarily, due to the lack of interaction between buforin-2 and the bacterial membrane, buforin-2 induced a very low increase in fluorescence intensity. Overall, the membrane depolarization and SYTOX Green uptake assays indicated that Fowl-1(8-26)-WRK most likely killed bacterial cells via membrane disruption/permeabilization. However, the involvement of other mechanisms cannot be ruled out.

Finally, to study the effects of Fowl-1(8-26)-WRK treatment on membrane integrity, *E. coli* cells were propidium iodide (PI)-stained. PI, which exhibits the fluorescent staining of nucleic acids in cells, can be used to reveal compromised cell membranes and cell death. In the absence of the peptides, the percentage of PI-positive cells was 2.97%, indicating that the membranes were intact (Fig. 9). However, following treatment with Fowl-1(8-26)-WRK, LL-37, and melittin at 2 × MIC, the percentage of PI-positive cells increased to 68.98, 75.38, and 55.50%, respectively. Conversely, the percentage of PI-positive cells after buforin-2 treatment was 3.57%, suggesting that Fowl-1(8-26)-WRK may have the potential to disrupt bacterial membrane integrity.

3. Discussion

Fowl-1 displays powerful antimicrobial activity against a range of bacteria, including antibiotic-resistant strains [10]. Additionally, based on previous studies, it binds to LPS and inhibits LPS-induced proinflammatory cytokine production in RAW264.7 cells [10,19]. However, in mammalian erythrocytes and epithelial cells, its toxicity is high [10]. In this study, Fowl-1(8-26), a 19-amino acid Fowl-1 truncated peptide, retained much of the parent antimicrobial activity with substantially reduced hemolytic activity (MHC = 240 μM) (Table 3). Consistent with our results, Xiao *et al*. demonstrated that it shows powerful antimicrobial activity, with less hemolytic activity and mammalian cell toxicity [11]. In addition, the N-terminal segment, consisting of three amino acids (residues 5-7), and the carboxyl-terminal α-helix, consisting of a stretch of eight amino acids (residues 16-23) after the kink, play a very important role in the antimicrobial, LPS-neutralizing, and cytotoxic activities of the peptide [11]. Fowl-1(6-26)-NH_2, which is a carboxyl-terminal amidated form of fowl-1(6-26), retained the antimicrobial LPS-neutralizing activities, with a >4-fold reduction in cytotoxicity [19]. Importantly, Fowl-1(6-26)-NH_2 was shown to protect mice from MRSA-induced lethal infections [19]. In our previous study, α-helicity and hydrophobicity reduction by the Tyr→Pro substitution in position 20 in Fowl-1, induced human erythrocytes and macrophage toxicity, while retaining antimicrobial activity [36]. This suggests that the continuous α-helix of residues 16–23 in Fowl-1 are responsible for antimicrobial and hemolytic activities [36].

Despite its high cell selectivity, Fowl-1 (8-26) showed less or no LPS-induced inflammation inhibitory activity in macrophage cells. Consequently, its analog Fowl-1(8-26)-WRK, was synthesized to enhance therapeutic potential (cell selectivity) and LPS-induced inflammation inhibitory activity in macrophage cells. Fowl-1(8-26)-WRK was designed via Thr^5→Trp, Ile^7→Arg, and Asn^{11}→Lys substitutions in the active Fowl-1(8-26) fragment to exhibit more amphipathicity.

LPS, also known as an endotoxin, is a highly conserved major component of the outer membrane of gram-negative bacteria that is released spontaneously and rapidly during bacterial growth and after antibiotic exposure [37,38]. It is the primary trigger of sepsis, and it stimulates host cells to produce large amounts of proinflammatory cytokines such as TNF-α, IL-1β, and IL-6, which play a pivotal role in the pathogenesis of multiple organ failure [39–41]. It is becoming increasingly clear that apart from their direct antimicrobial activity, some AMPs of the cathelicidin family, such as LL-37 and indolicidin, play an important role in modulating host immune and inflammatory responses [42–48]. Additionally, Fowl-1(8-26)-WRK significantly inhibited NO and TNF-α release and expression in LPS-stimulated macrophages at concentrations of 4 μM and 8 μM, respectively (Fig. 3). Thus, the most important finding of this study is the identification of Fowl-1(8-26)-WRK, which maintains its antimicrobial and anti-inflammatory activity with less or no hemolytic activity, compared with Fowl-1, the full-length peptide.

Many AMPs exert their anti-inflammatory effects via LPS neutralization [47-49]. Hence, it was investigated whether the inhibitory activity of Fowl-1(8-26)-WRK on LPS-induced macrophage inflammation was due to LPS binding with the peptide. Like PMB, the removal of unbound/exogenous Fowl-1(8-26)-WRK prior to LPS stimulation significantly reduced inhibitory activity, leading to NO production from LPS-stimulated macrophage cells (Fig. 5). Additionally, Fowl-1(8-26)-WRK exhibited almost the same LPS-neutralizing activity as PMB in the BODIPY-TR-cadaverine displacement assay (Fig. 6). This observation suggests that the inhibitory activity of Fowl-1 (8-26)-WRK on LPS-induced inflammation is mainly due to the binding of the peptide and LPS.

In recent years, the emergence of bacteria resistance to conventional antibiotics is increasing at an alarming rate, especially in hospital settings, seriously hampering the effective treatment of infections [50]. In 2005, it was estimated that MRSA has caused 94,000 infections that led to 19,000 deaths [51], and together with other multidrug resistant (MDR) strains of *Pseudomonas aeruginosa*, presents an increasing public health threat [52]. Interestingly, Fowl-(8-26)-WRK was more

active against various antibiotic-resistant bacteria strains, including MRSA, MDRPA, and VREF, than LL-37 and melittin, indicating that it may a have strong therapeutic potential in drug-resistant infections.

The development of AMPs has been hindered by several problems, one of which is salt sensitivity [53]. The efficacy of human β-defensin-1 is greatly reduced by high salt concentrations in bronchopulmonary fluids, which are usually found in cystic fibrosis patients [54]. Generally, it is believed that most cationic AMPs are salt-sensitive, with reduced/lost antimicrobial activity at higher salt concentrations [55–57]. Interestingly, Fowl-1(8-26)-WRK maintained its antimicrobial activity in the presence of physiological concentrations of monovalent (Na^+, K^+, and NH_4^+) and divalent (Mg^{2+} and Ca^{2+}) salts (Table 4). Next, its serum sensitivity against *E. coli* and *S. aureus* was also investigated in the presence of 20 % human serum, and the results showed only 2-fold reduction in its antimicrobial activity against *E. coli* and *S. aureus* (Table 4), suggesting that it is stable to degradation by serum proteases.

The increase in antibiotic-resistant and multi-drug resistant (MDR) bacterial infections has serious implications on the future of healthcare [58–60]. Therefore, there is an urgent need for the development of new antimicrobial agents or alternative therapies for combating MDR infections. Combining antimicrobial agents to expand the antimicrobial spectrum, improve therapeutic outcome, and reduce antibiotic-resistance emergence, is a well-established strategy in antimicrobial chemotherapy [61–65]. As most AMPs act on bacterial membranes, synergy with antibiotics was likely due to membrane permeabilization and disorganization, which led to increased intracellular antibiotic concentration (increased membrane permeability of antibiotic) [66,67]. Hence, to evaluate Fowl-1(8-26)-WRK as an adjuvant in combination with conventional antibiotics, its synergistic effects in combination with conventional antibiotics against MDRPA and MRSA were investigated using a checkerboard assay, in which three conventional antibiotics (chloramphenicol, ciprofloxacin, and oxacillin) with different mechanisms of action, were used. Chloramphenicol is a bacteriostatic

broad-spectrum antibiotic that inhibits bacterial protein synthesis through binding with the bacterial 50S ribosomal subunit. Ciprofloxacin is a broad-spectrum fluoroquinolone that acts by inhibiting DNA gyrase and topoisomerase types II and IV, and oxacillin is a narrow-spectrum β-lactam antibiotic that inhibits bacterial cell wall synthesis. The site of action of ciprofloxacin and chloramphenicol is the cytoplasm, whereas oxacillin acts outside of the cytoplasmic membrane.

Compared with LL-37, Fowl-1(8-26)-WRK showed a greater synergistic effect with ciprofloxacin and chloramphenicol against MDRPA and MRSA. The combination of LL-37, ciprofloxacin, and chloramphenicol did not reach the cutoff for consideration as being synergistic. This is possibly because it causes weak membrane depolarization against MRSA, compared with Fowl-1 (8-26)-WRK (Fig. 10). Therefore, the decreased or lack of synergy of LL-37 with ciprofloxacin and chloramphenicol against antibiotic-resistant bacteria is due to the fact that LL-37 has a weaker effect on tethered lipid bilayers compared with Fowl-1 (8-26)-WRK, which contains the membrane-interacting amino acid tryptophan [68,69], absent in LL-37. Summarily, Fowl-1(8-26)-WRK in combination with conventional antibiotics, is a promising adjuvant against antibiotic-resistant bacteria, thereby improving the effectiveness of these antibiotics and reducing the development of resistance to antibiotics.

The predominant mechanism of the antimicrobial action of α-helical AMPs is the rapid perturbation and destruction of microbial membranes, leading to the leakage of cytoplasmic contents and eventual cell death [2,3]. The mechanism of the antimicrobial action of Fowl-1(8-26)-WRK was investigated using membrane depolarization, SYTOX Green uptake, and flow cytometry. At 2 × MIC, like melittin and LL-37, it induced nearly complete depolarization of *S. aureus* membrane and rapid permeabilization, with a maximum SYTOX Green accumulation within 4 min. additionally, like melittin and LL-37, its incubation with PI dye significantly exhibited an increase in fluorescence intensity. Summarily, these observations indicate that Fowl-1(8-26)-WRK kills bacteria by membrane disruption/permeabilization.

Conclusively, we successfully engineered a short Fowl-1 analog; Fowl-1(8-26)-WRK, with both antimicrobial and ant-inflammatory activities but low hemolytic activity. Fowl-1(8-26)-WRK possesses high salt and serum tolerance and shows synergistic interactions with conventional antibiotics. It also showed dramatic LPS-neutralizing activity and a potent membrane-disruptive mechanism against microbial cells. Summarily, the results of this study suggest that Fowl-1(8-26)-WRK can be further developed as a novel antimicrobial/anti-inflammatory agent for the treatment of drug-resistant bacterial infections.

Table 1. Amino acid sequences and physicochemical properties of Fowl-1 and its analogs.

Peptides	Amino acid sequence	Molecular weight (Da)		Charge	R_t[b]
		calculated	observed[a]		
Fowl-1	RVKRVWPLVIRTVIAGYNLYRAIKKK	3141.8	3141.2	8	27.8
Fowl-1(1-19)	RVKRVWPLVIRTVIAGYNL	2253.7	2253	4	25
Fowl-1(3-21)	KRVWPLVIRTVIAGYNLYR	2317.8	2317.5	4	25.5
Fowl-1(5-23)	VWPLVIRTVIAGYNLYRAI	2217.6	2217.6	2	30.6
Fowl-1(8-26)	LVIRTVIAGYNLYRAIKKK	2219.7	2219.2	5	22.2
Fowl-1(8-26)-WRK	LVIR**W**V**R**AGY**K**LYRAIKKK-NH_2	2360.9	2360.3	7	21.7

The substituted amino acids are shown in bold and underlined.

[a] Molecular mass were determined using matrix-assisted laser desorption/ionization (MALDI)-time-of-flight (TOF)-mass spectrometry (MS).

[b] Retention time (Rt) was measured using a C-18 reversed-phase analytical HPLC column (5 mm; 4.6 mm ´ 250 mm; Vydac).

Peptides were eluted for 60 min, by using a linear gradient of 0-90% (v/v) acetonitrile in water containing 0.05% (v/v) TFA.

c Hydrophobicity moment (mH) were calculated online at: http://heliquest.ipmc.cnrs.fr/cgi-bin/ComputParams.py.

Table 2 Minimum inhibitory concentration (MIC[a], in μM) of Fowl-1 and its analogs

Peptides	Gram-negative bacteria			Gram-positive bacteria		
	E. coli [KCTC 1682]	*P. aeruginosa [KCTC 1637]*	*S. typhimurium [KCTC 1926]*	*B. subtilis [KCTC 3068]*	*S. epidermidis [KCTC 1917]*	*S. aureus [KCTC1621]*
Fowl-1	4	8	2	2	4	2
Fowl-1(1-19)	16	32	16	8	8	16
Fowl-1(3-21)	4	32	16	8	4	8
Fowl-1(5-23)	16	32	32	2	16	2
Fowl-1(8-26)	8	16	8	2	4	2
Fowl-1(8-26)-WRK	4	8	2	2	4	2
melittin	4	2	2	1	4	2

[a] MIC was determined as the lowest concentration of peptide that caused 100 % inhibition of microbial growth.

Table 3 GM, MHC, TI, and anti-inflammatory activity of Fowl-1 and its analogs

Peptides	GM (μM)[a]	MHC (μM)[b]	TI[c] (MHC/GM)	Fold	% NO inhibition[d]	% TNF-α inhibition[e]
Fowl-1	3.7	38	10.3	1.0	96.7	73.5
Fowl-1(1-19)	16.0	> 256	32.0	3.1	2.3	1.1
Fowl-1(3-21)	12.0	230	19.2	1.9	3.4	10.7
Fowl-1(5-23)	16.7	63	3.8	0.4	91.9	41.5
Fowl-1(8-26)	6.7	240	35.8	3.5	16.2	13.8
Fowl-1(8-26)-WRK	3.7	105	28.4	2.8	94.2	75.2

[a] GM denotes the geometric mean of MIC values from all bacterial strains.
[b] MHC is the hemolytic concentration that caused 10% hemolysis.
[c] The therapeutic index (TI) is the ratio of the MHC value (μM) to GM (μM).
When no detectable hemolytic activity was observed at 256 μM, a value of 514 μM was used to calculate the TI.
[d] Percent inhibition of NO production at 4 μM.
[e] Percent inhibition of TNF-α production at 8 μM.

Table 4 Antimicrobial activities of Fowl-1(8-26)-WRK against antibiotic-resistant bacterial strains

Microorganisms	MIC (μM)		
	Fowl-1(8-26)-WRK	LL-37	melittin
MRSA[a]			
CCARM 3089	4	8	4
CCARM 3090	2	16	4
CCARM 3095	2	16	4
MDRPA			
CCARM 2095	2	4	8
CCARM 2109	4	8	8
VREF[c]			
ATCC 51559	4	8	8

[a] MRSA: methicillin-resistant *Staphylococcus aureus*
[b] MDRPA: multidrug-resistant *Pseudomonas aeruginosa*
[c] VREF: vancomycin-resistant *Enterococcus faecium*

Table 5 MIC values of Fowl-1(8-26)-WRK in the presence of physiological salts and human serum (20%) against *E. coli* and *S. aureus*.

Control[a]	150 mM NaCl	4.5 mM KCl	6 µM NH_4Cl	1 mM $MgCl_2$	2.5 mM $CaCl_2$	4µM $FeCl_3$	20% HS[b]
E. coli (KCTC 1682)							
4	4	4	4	4	4	4	8
S. aureus (KCTC1621)							
2	2	2	2	4	2	4	4

[a]Control represents bacteria treated with peptide only. [b]HS: human serum

Table 6 Synergy between Fowl-1(8-26)-WRK or LL-37 and conventional antibiotics against MDRPA (CCARM 2095)

MIC_A	[A]	FIC_A	MIC_B	[B]	FIC_B	FICI	Interaction
Chloramphenicol			Fowl-1(8-26)-WRK				
1024	32	0.031	4	1	0.25	0.281	synergy
Chloramphenicol			LL-37				
1024	256	0.25	4	2	0.5	0.75	additive
Ciprofloxacin			Fowl-1(8-26)-WRK				
512	64	0.125	2	1	0.5	0.625	additive
Ciprofloxacin			LL-37				
512	128	0.25	4	2	0.5	0.75	additive
Oxacillin			Fowl-1(8-26)-WRK				
512	128	0.25	2	0.5	0.25	0.5	synergy
Oxacillin			LL-37				
512	512	1.0	4	4	1.0	2.0	indifferent

FICI of ≤ 0.5 was interpreted as synergy, $0.5 < FICI \leq 1.0$ as additive, $1.0 < FICI \leq 4.0$ as indifferent, and an $FICI > 4.0$ as antagonism.

Table 7 Synergy between Fowl-1(8-26)-WRK or LL-37 and conventional antibiotics against MRSA(CCARM 3089)

MIC_A	[A]	FIC_A	MIC_B	[B]	FIC_B	FICI	Interaction
Chloramphenicol			Fowl-1(8-26)-WRK				
128	16	0.125	4	0.5	0.125	0.25	synergy
Chloramphenicol			LL-37				
128	64	0.5	8	4	0.5	1.0	additive
Ciprofloxacin			Fowl-1(8-26)-WRK				
1024	256	0.25	4	0.5	0.125	0.375	synergy
Ciprofloxacin			LL-37				
1024	256	0.25	8	8	1.0	1.25	additive
Oxacillin			Fowl-1(8-26)-WRK				
512	128	0.25	4	1	0.25	0.5	synergy
Oxacillin			LL-37				
512	256	0.5	8	2	0.25	0.75	additive

FICI of ≤ 0.5 was interpreted as synergy, $0.5 < FICI \leq 1.0$ as additive, $1.0 < FICI \leq 4.0$ as indifferent, and an $FICI > 4.0$ as antagonism.

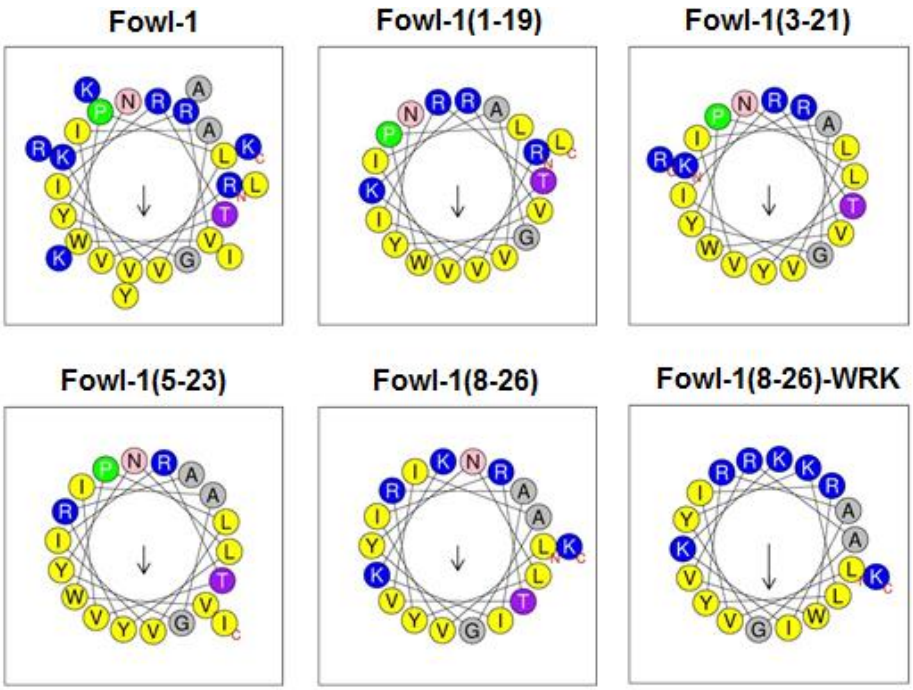

Fig. 1. Predicted peptide amphiphilicity based on amino acid sequence and hydrophobic moment. The helical wheel plots are drawn using the HeliQuest tool (http://heliquest.ipmc.cnrs.fr/). Here, the positively charged polar (blue), uncharged polar (pink/purple), and non-polar (yellow, green, and gray) residues are shown, where Pro (green) induces helical bends and Gly (gray) is neutral and flexible. The overall hydrophobic moment (μH, arrow) of the peptides is also depicted.

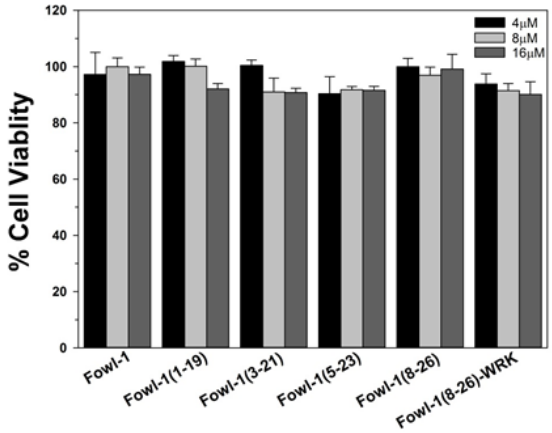

Fig. 2. Cytotoxicity of the peptides against mouse macrophage RAW264.7 cells.

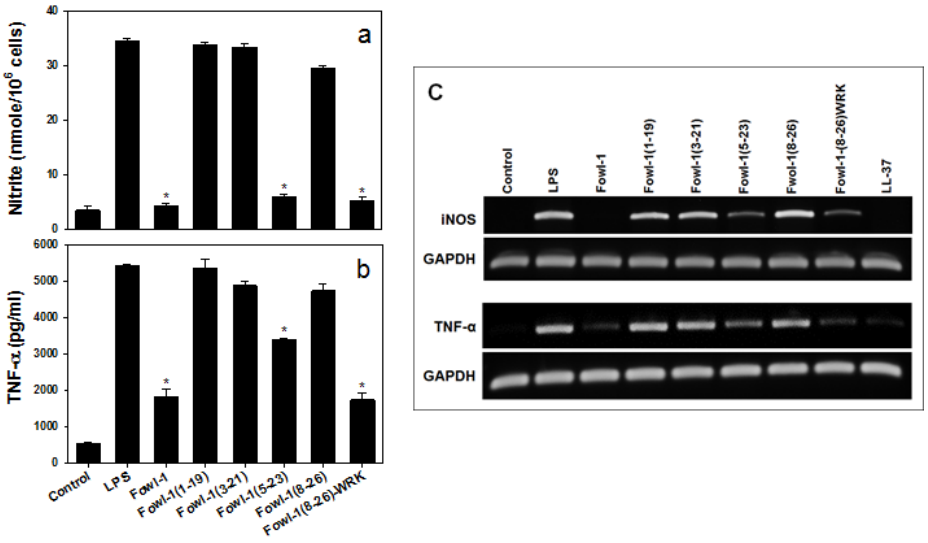

Fig. 3. (a) Effects of the peptides on NO release from LPS-stimulated RAW 264.7 cells. RAW 264.7 cells were stimulated with LPS (20 ng/mL) in the presence and absence (control) of peptides (4 μM). **(b)** Effects of the peptides on TNF-α release from LPS-stimulated RAW 264.7 cells. RAW 264.7 cells were stimulated with LPS (20 ng/mL) in the presence and absence (control) of peptides (8 μM). Secreted NO and TNF-α in the supernatants were measured after 24 h of LPS-stimulation using ELISA. Asterisks (*) indicate significant effects of the peptides when compared to LPS-treated cells. Data was analyzed using one-way analysis of variance (ANOVA) with Bonferroni's post-test (*, $P < 0.001$ for each agonist). The data represents mean ± SEM of technical triplicates. The findings were similar when the experiments were repeated using different cells. **(c)** Effects of the peptides on iNOS and TNF-α mRNA expression in LPS-stimulated RAW 264.7 cells. RAW 264.7 cells (5×10^5 cells/well) were incubated with peptides (4 μM and 8 μM for iNOS and TNF-α, respectively) in the presence of LPS (20 ng/mL) for 3 h (TNF-α) or 6 h (iNOS). Total RNA was isolated and analyzed with RT-PCR to determine iNOS and TNF-α mRNA levels.

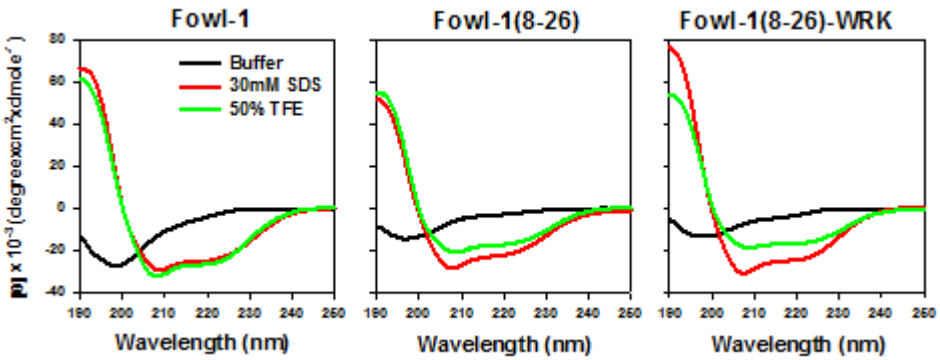

Fig. 4. The CD spectra of the peptides. The peptides were dissolved in 10 mM sodium phosphate buffer (pH 7.4), 50% TFE, and 30 mM SDS micelles. The mean residue ellipticity was plotted against wavelength.

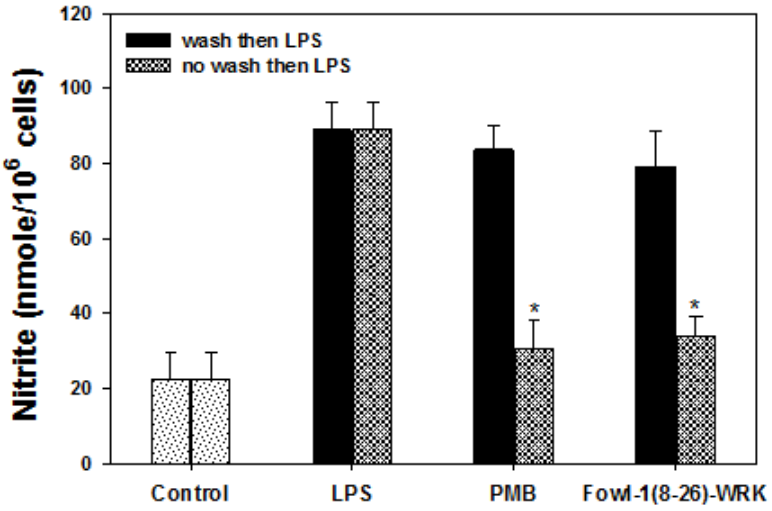

Fig. 5. Binding of Fowl-1(8-26)-WRK to LPS. RAW 264.7 cells were pre-treated in medium containing 10 μM of Fowl-1(8-26)-WRK and polymyxin B (PMB) for 1 h, washed three times and then stimulated with LPS (1 μg/mL). After 48 hr incubation, nitrite from culture supernatant was measured by Griess assay.

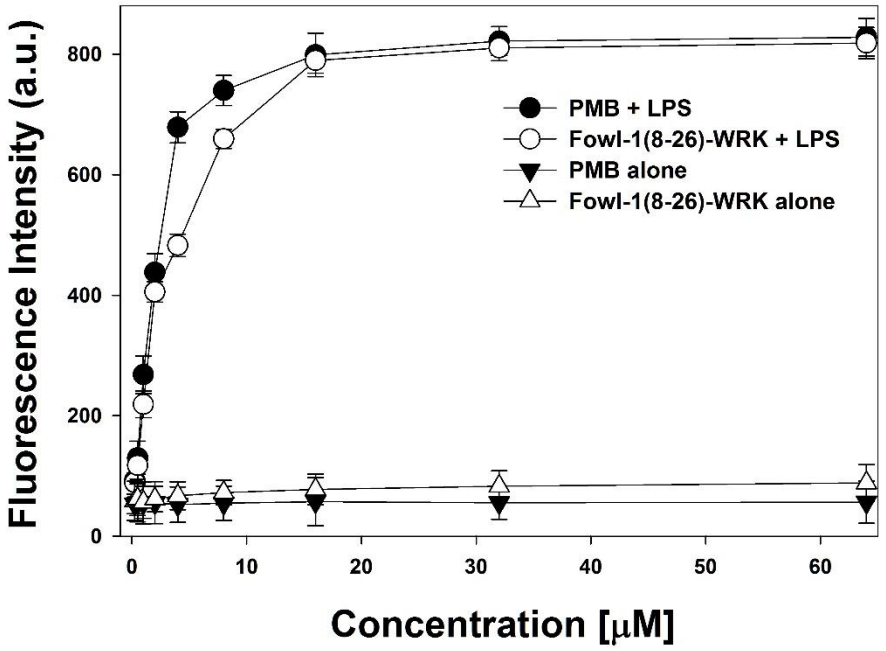

Fig. 6. Binding affinity of the peptides to LPS from *E. coli* O55:B5. *E. coli* O55:B5 LPS at 25 μg/mL, BODIPYTR-cadaverine at 2.5 μg/mL, and 50 mM of Tris buffer (pH 7.4) were mixed. A volume of 3 ml of this mixture was then added to a quartz cuvette. Aliquots of the peptides were added to the cuvette and fluorescence was recorded.

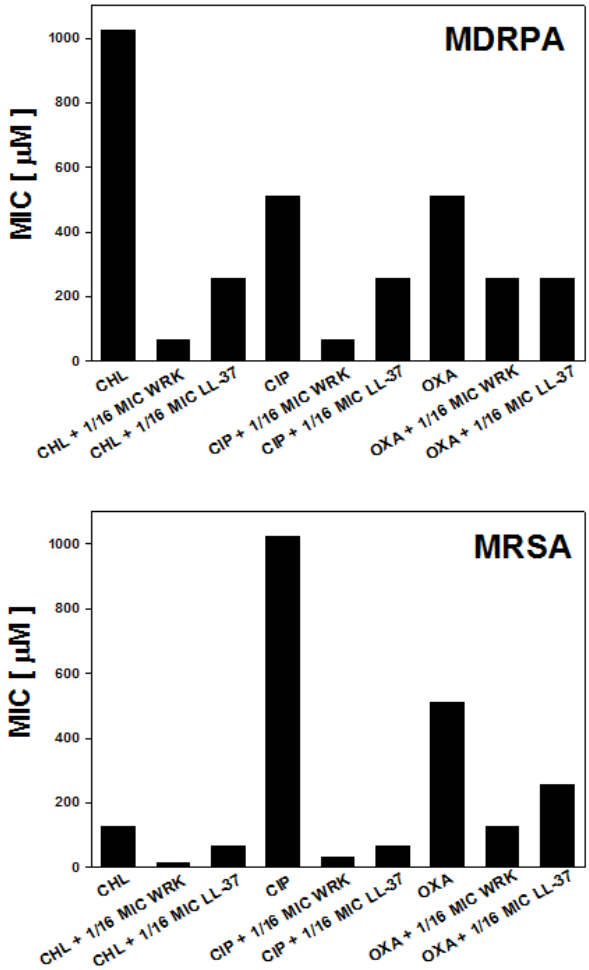

Fig. 7. MIC values of chloramphenicol (CHL), ciprofloxacin (CIP), and oxacillin (OXA) in combination with the peptides against MDRPA (CCARM 2095) or MRSA (CCARM 3089). WRK: Fowl-1(8-26)-WRK.

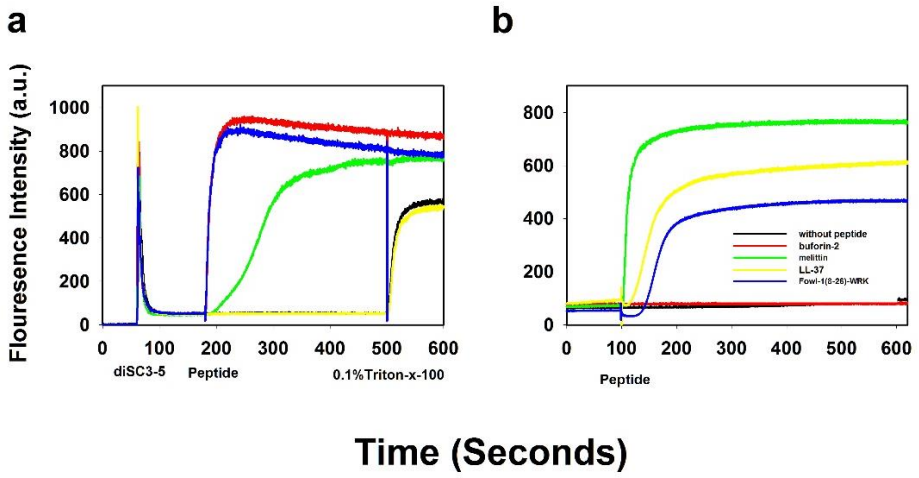

Fig. 8. (a) Depolarization of the *S. aureus* cytoplasmic membrane induced by peptides at 2 × MIC and determined using the membrane potential-sensitive fluorescent dye $DiSC_3$-5. Dye release was monitored by measuring fluorescence at an excitation wavelength of 622 nm and an emission wavelength of 670 nm, and plotting the emission against time. Curves corresponding to the positive control peptides (LL-37 and melittin) and negative control peptide (buforin-2) are also shown. 2 × MIC: melittin, 4 μM; LL-37, 16 μM; buforin-2, 32 μM; Fowl-1(8-26)-WRK, 8 μM. **(b)** Kinetics of the *S. aureus* membrane permeabilization caused by peptides at 2 × MIC. The positive control peptides (LL-37 and melittin) and negative control peptide (buforin-2) are also shown. Alterations in the cytoplasmic membrane allow the SYTOX Green probe to enter the cell and bind to DNA, resulting in an increase in fluorescence. 2 × MIC: melittin, 4 μM; LL-37, 16 μM; buforin-2, 32 μM; Fowl-1(8-26)-WRK, 8 μM.

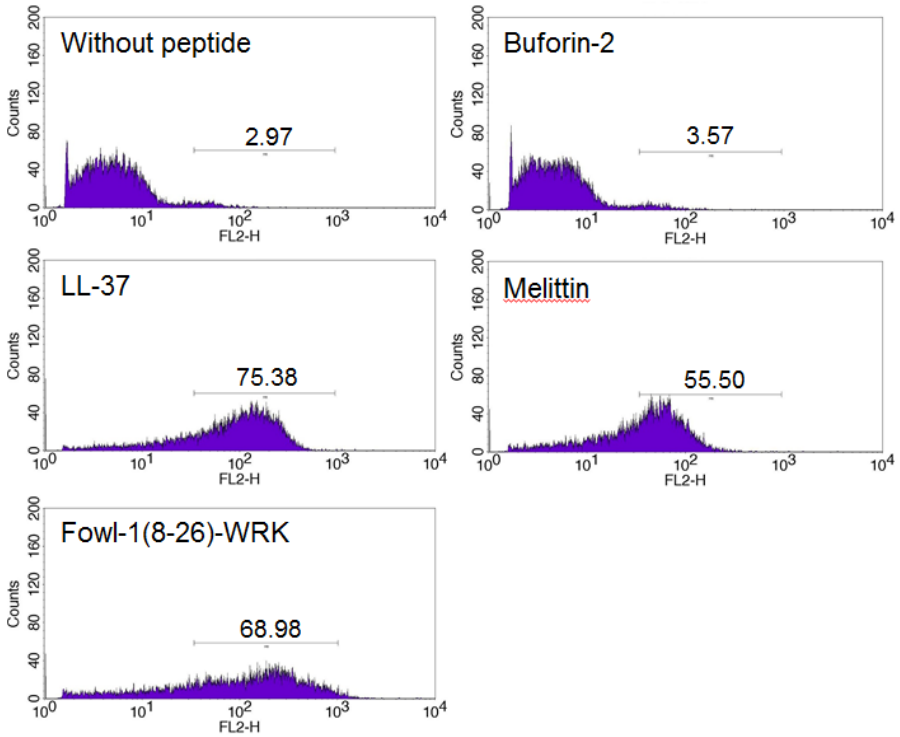

Fig. 9. Membrane damage in *E. coli* cells treated with the peptides (2 × MIC). Membrane damage was measured by an increase in PI (10 μg/mL) fluorescence intensity at 4 °C for 30 min. 2× MIC: melittin, (4 μM), LL-37 (16 μM), buforin-2 (32 μM), Fowl-1(8-26)-WRK (8 μM).

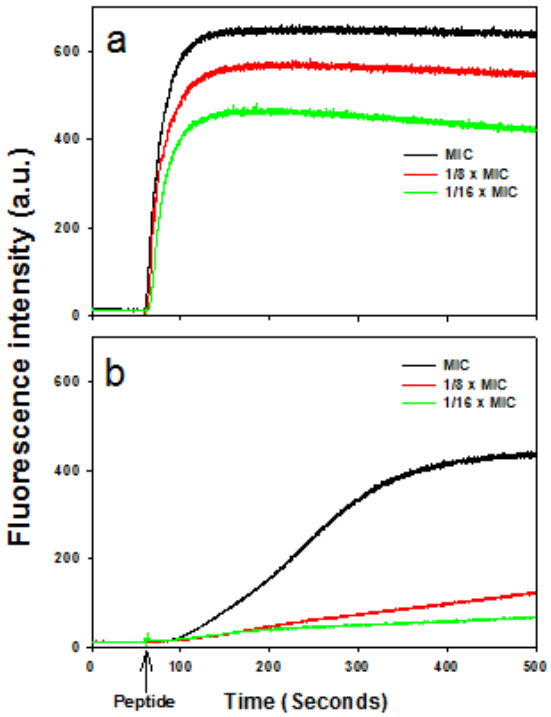

Fig. 10. Depolarization of MRSA (CCARM 3089) cytoplasmic membrane induced by Fowl-1(8-26)-WRK (a) and LL-37 (b) at MIC and sub-MICs (1/8 × MIC and 1/16 × MIC) and determined using the membrane potential-sensitive fluorescent dye $DiSC_3$-5.

References

[1] K.A. Brogden, Antimicrobial peptides: pore formers or metabolic inhibitors in bacteria? Nat. Rev. Microbiol. 3 (2005) 238–250.

[2] R.E. Hancock, H.G. Sahl, Antimicrobial and host-defense peptides as new antiinfective therapeutic strategies. Nat. Biotechnol. 24 (2006) 1551–1557.

[3] K. Brandenburg, L. Heinbockel, W. Correa, K. Lohner K, Peptides with dual mode of action: Killing bacteria and preventing endotoxin-induced sepsis. Biochim. Biophys. Acta Biomembr.1858 (2016) 971–979.

[4] R.I. Lehrer, T. Ganz, Cathelicidins: a family of endogenous antimicrobial peptides, Curr. Opin. Hematol. 9 (2002) 18–22.

[5] M. Zaiou, R.L. Gallo, Cathelicidins, essential gene-encoded mammalian antibiotics, J. Mol. Med. 80 (2002) 549–561.

[6] M. Zanetti, Cathelicidins, multifunctional peptides of the innate immunity, J. Leukoc. Biol. 75 (2004) 39–48.

[7] U.H. Durr, U.S. Sudheendra, A. Ramamoorthy, LL-37, the only human member of the cathelicidin family of antimicrobial peptides, Biochim. Biophys. Acta Biomembr.1758 (2006) 1408–1425.

[8] R. Gennaro, M. Zanetti, Structural features and biological activities of the cathelicidin-derived antimicrobial peptides, Biopolymers 55 (2000) 31–49.

[9] A. Bardan, V. Nizet, R.L. Gallo, Antimicrobial peptides and the skin, Expert Opin. Biol. Ther. 4 (2004) 543–549.

[10] Y. Xiao, Y. Cai, Y.R. Bommineni, S.C. Fernando, O. Prakash, S.E. Gilliland, G. Zhang, Identification and functional characterization of three chicken cathelicidins with potent antimicrobial activity, J. Biol. Chem. 281 (2006) 2858–2867.

[11] Y. Xiao, H. Dai, Y.R. Bommineni, J.L. Soulages, Y.X. Gong, O. Prakash, G. Zhang, Structure-activity relationships of fowlicidin-1, a cathelicidin antimicrobial peptide in chicken, FEBS J. 273 (2006) 2581–2593.

[12] J.L. Fox, Antimicrobial peptides stage a comeback, Nat. Biotechnol. 31 (2013) 379–382.

[13] D.C. Angus, W.T. Linde-Zwirble, J. Lidicker, G. Clermont, J. Carcillo, M.R. Pinsky, Epidemiology of severe sepsis in the United States: analysis of incidence, outcome, and associated costs of care, Crit. Care Med. 29 (2001) 1303–1310.

[14] E.T. Rietschel, H. Brade, O. Holst, L. Brade, S. Muller-Loennies, U. Mamat, U. Zahringer, F. Beckmann, U. Seydel, K. Brandenburg, A.J. Ulmer, T. Mattern, H. Heine, J. Schletter, H. Loppnow, U. Schonbeck, H.D. Flad, S. Hauschildt, U.F. Schade, F. Di Padova, S. Kusumoto, R.R. Schumann, Bacterial endotoxin: chemical constitution, biological recognition, host response, and immunological detoxification, Curr. Top. Microbiol. Immunol. 216 (1996) 39–81.

[15] I. Nagaoka, S. Hirota, F. Niyonsaba, M. Hirata, Y. Adachi, H. Tamura, A. Tanaka, D. Heumann, Augmentation of lipopolysaccharide-neutralizing activities of human cathelicidin CAP18/LL37-derived from antimicrobial peptides by replacement with hydrophobic and cationic amino acid residues, Clin. Diagn. Lab. Immunol. 9 (2002) 972–982.

[16] Y.H. Nan, J.K. Bang, B. Jacob, I.S. Park, S.Y. Shin, Prokaryotic selectivity and LPS-neutralizing activity of short antimicrobial peptides designed from the human antimicrobial peptide LL-37, Peptides 35 (2012) 239–247.

[17] D. Motzkus, S. Schulz-Maronde, A. Heitland, A. Svhulz, W.G. Forssmann, M. Jübner, E. Maronde, The novel β-defensin DEFB123 prevents lipopolysaccharide-mediated effects in vitro and in vivo, FASEB J. 20 (2006) 1701–1702.

[18] F. Semple, J. Dorin, β-Defensins: multifunctional modulators of infection, inflammation and more? J. Innate Immun. 4 (2012) 337–348.

[19] Y.R. Bommineni, M. Achanta, J. Alexander, L.T. Sunkara, J.W. Ritchey, G. Zhang G, A fowlicidin-1 analog protects mice from lethal infections induced

by methicillin-resistant *Staphylococcus aureus*. Peptides 31 (2010) 1225-1230.

[20] J. Nam, H. Yun, G. Rajasekaran, S.D. Kumar, J.I. Kim, H.J. Min, S.Y. Shin, C.W. Lee, Structural and Functional Assessment of mBjAMP1, an Antimicrobial Peptide from Branchiostoma japonicum, Revealed a Novel α-Hairpinin-like Scaffold with Membrane Permeable and DNA Binding Activity. J. Med. Chem. 61 (2018) 11101−11113.

[21] J. Kim, B. Jacob, M. Jang, C. Kwak, Y. Lee, K. Son, S. Lee, I.D. Jung, M.S. Jeong S.H. Kwon, Y. Kim, Development of a novel short 12-meric papiliocin-derived peptide that is effective against Gram-negative sepsis. Sci. Rep. 9 (2019) 3817

[22] G.J. Gabriel, A.E. Madkour, J.M. Dabkowski, C.F. Nelson, K. Nüsslein, G.N. Tew, Synthetic mimic of antimicrobial peptide with nonmembrane-disrupting antibacterial properties, Biomacromolecules 9 (2008) 2980–2983

[23] S. Joshi, S. Mumtaz, J. Singh, S. Pasha, K. Mukhopadhyay, Novel Miniature Membrane Active Lipopeptidomimetics against Planktonic and Biofilm Embedded Methicillin-Resistant *Staphylococcus aureus*, Sci. Rep. 8 (2018) 1021

[24] S.J. Wood, K.A. Miller, S.A. David, Anti-endotoxin agents. 1. Development of a fluorescent probe displacement method optimized for the rapid identification of lipopolysaccharide-binding agents, Comb. Chem. High Throughput Screening 7 (2004) 239–249.

[25] N. Dong, X. Zhu, S. Chou, A. Shan, W. Li, J. Jiang, Antimicrobial potency and selectivity of simplified symmetric-end peptides, Biomaterials 35 (2014) 8028–8039.

[26] X. Dou, X. Zhu, J. Wang, N. Dong, A. Shan, Novel design of heptad amphiphiles to enhance cell selectivity, salt resistance, antibiofilm properties and their membrane-disruptive mechanism, J. Med. Chem. 60 (2017) 2257–2270.

[27] R.M. Dawson, M.A. Fox, H.S. Atkins, C.Q. Liu, Potent antimicrobial peptides with selectivity for *Bacillus anthracis* over human erythrocytes, Int. J. Antimicrob. Agents 38 (2011) 237–242.

[28] Q.Q. Ma, Y.F. Lv, Y. Gu, N. Dong, D.S. Li, A.S. Shan, Rational design of cationic antimicrobial peptides by the tandem of leucine-rich repeat, Amino Acids 44 (2013) 1215−1224.

[29] L. Zhang, P. Dhillon, H. Yan, S. Farmer, R.E. Hancock, Interactions of bacterial cationic peptide antibiotics with outer and cytoplasmic membranes of *Pseudomonas aeruginosa*, Antimicrob. Agents Chemother. 44 (2000) 3317–3321.

[30] M. Ahn, P. Gunasekaran, G. Rajasekaran, E.Y. Kim, S.J. Lee, G. Bang, K. Cho, J.K. Hyun, H.J. Lee, Y.H. Jeon, N.H. Kim, E.K. Ryu, S.Y. Shin, J.K. Bang, Pyrazole derived ultra-short antimicrobial peptidomimetics with potent anti-biofilm activity, Eur. J. Med. Chem. 125 (2017) 551–564.

[31] C. Nagant , B. Pitts, K. Nazmi, M. Vandenbranden, J.G. Bolscher, P.S. Stewart, J.P. Dehaye, Identification of peptides derived from the human antimicrobial peptide LL-37 active against biofilms formed by *Pseudomonas aeruginosa* using a library of truncated fragments, Antimicrob. Agents Chemother. 56 (2012) 5698–5708.

[32] N. Dong, X. Zhu, S. Chou, A. Shan, W. Li, J. Jiang, Antimicrobial potency and selectivity of simplified symmetric-end peptides, Biomaterials 35 (2014) 8028–8039.

[33] G. Rajasekaran, S. Dinesh Kumar, J. Nam, D. Jeon, Y. Kim, C.W. Lee, I.S. Park, S.Y. Shin, Antimicrobial and anti-inflammatory activities of chemokine CXCL14-derived antimicrobial peptide and its analogs, Biochim. Biophys. Acta Biomembr. 861 (2019) 256−267.

[34] J.J. Koh, H. Zou, S. Lin, H. Lin, R.T. Soh, F.H. Lim, W.L. Koh, J. Li, R. Lakshminarayanan, C. Verma, D.T. Tan, D. Cao, R.W. Beuerman, S. Liu, Nonpeptidic amphiphilic xanthone derivatives: structure-activity relationship and membrane-targeting properties, J. Med. Chem. 59 (2016) 171−193.

[35] L. Jin, X. Bai, N. Luan, H. Yao, Z. Zhang, W. Liu, Y. Chen, X. Yan, M. Rong, R. Lai, Q. Lu, A designed tryptophan- and lysine/arginine-rich antimicrobial peptide with therapeutic potential for clinical antibiotic-resistant *candida albicans* vaginitis, J. Med. Chem. 59 (2016) 1791−1799.

[36] G. Rajasekaran, S.D. Kumar, S. Yang, S.Y. Shin, Bull. Kor. Chem. Soc. 40 (2019) 429–434.

[37] P. Langevelde, K.M. Kwappenberg, P.H. Groeneveld, H. Mattie, J.T. Dissel, Antibiotic-induced lipopolysaccharide (LPS) release from *Salmonella typhi*: delay between killing by ceftazidime and imipenem and release of LPS, Antimicrob. Agents Chemother. 42 (1998) 739–743.

[38] J.J. Jackson, H. Kropp, β-Lactam antibiotic-induced release of free endotoxin: in vitro comparison of penicillin-binding protein (PBP) 2-specific imipenem and PBP 3-specific ceftazidime, J. Infect. Dis. 165 (1992) 1033–1041.

[39] R.C. Bone, The pathogenesis of sepsis, Ann. Intern. Med. 115 (1991) 457–469.

[40] H.R. Michie, Detection of circulating tumor necrosis factor after endotoxin administration, N. Engl. J. Med. 318 (1988) 1481–1486.

[41] M. Kalle, P. Papareddy, G. Kasetty, M. Mörgelin, M.J. van der Plas, V. Rydengård, M. Malmsten, B. Albiger, A. Schmidtchen, Host defense peptides of thrombin modulate inflammation and coagulation in endotoxin-mediated shock and *Pseudomonas aeruginosa* sepsis, PLoS One **7** (2012) e51313.

[42] D.M. Bowdish, D.J. Davidson, M.G. Scott, R.E. Hancock, Immunomodulatory activities of small host defense peptides, Antimicrob. Agents Chemother. 49 (2005) 1727–1732.

[43] C.D. Ciornei, T. Sigurdardóttir, A. Schmidtchen, M. Bodelsson, Antimicrobial and chemoattractant activity, lipopolysaccharide neutralization, cytotoxicity, and inhibition by serum of analogs of human cathelicidin LL-37, Antimicrob Agents Chemother. 49 (2005) 2845–2850.

[44] K.L. Brown, G.F. Poon, D. Birkenhead, O.M. Pena, R. Falsafi, C. Dahlgren, A. Karlsson, J. Bylund, R.E. Hancock, P. Johnson, Host defense peptide LL-

37 selectively reduces proinflammatory macrophage responses, J. Immunol. 186 (2011) 5497–5505.

[45] E.Y. Kim, G. Rajasekaran, S.Y. Shin, LL-37-derived short antimicrobial peptide KR-12-a5 and its d-amino acid substituted analogs with cell selectivity, anti-biofilm activity, synergistic effect with conventional antibiotics, and anti-inflammatory activity, Eur. J. Med. Chem. 136 (2017) 428–441.

[46] Y.H. Nan, K.H. Park, Y. Park, Y.J. Jeon, Y. Kim, I.S. Park, K.S. Hahm, S.Y. Shin, Investigating the effects of positive charge and hydrophobicity on the cell selectivity, mechanism of action and anti-inflammatory activity of a Trp-rich antimicrobial peptide indolicidin, FEMS Microbiol. Lett. 292 (2009) 134–140.

[47] G. Rajasekaran, E.Y. Kim, S.Y. Shin, LL-37-derived membrane-active FK-13 analogs possessing cell selectivity, anti-biofilm activity and synergy with chloramphenicol and anti-inflammatory activity. Biochim. Biophys. Acta Biomembr. 1859 (2017) 722−733.

[48] Scott, S. Weldon, P.J. Buchanan, B. Schock, R.K. Ernst, D.F. McAuley, M.M. Tunney, C.R. Irwin, J.S. Elborn, C.C. Taggart, Evaluation of the ability of LL-37 to neutralise LPS *in vitro* and *ex vivo*. PLoS One 6 (2011) e26525.

[49] J.K. Kim, E. Lee, S. Shin, K.W. Jeong, J.Y. Lee, S.Y. Bae, S.H. Kim, J. Lee, S.R. Kim, D.G. Lee, J.S. Hwang, Y. Kim, Structure and function of papiliocin with antimicrobial and anti-inflammatory activities isolated from the swallowtail butterfly, *Papilio xuthus*. J. Biol. Chem. 286 (2011) 41296–41311.

[50] F. von Nussbaum, M. Brands, B. Hinzen, S. Weigand, D. Habich, Antibacterial natural products in medicinal chemistry-exodus or revival? Angew. Chem. Int. Ed. Engl. 45 (2006) 5072−5129.

[51] R.M. Klevens, M.A. Morrison, J. Nadle, S. Petit, K. Gershman, S. Ray, L.H. Harrison, R. Lynfield, G. Dumyati, J.M. Townes, A.S. Craig, E.R. Zell, G.E. Fosheim, L.K. McDougal, R.B. Carey, S.K. Fridkin, Invasive methicillin-

resistant *Staphylococcus aureus* infections in the United States, JAMA 298 (2007) 1763−1771.

[52] M.A. Fischbach, C.T. Walsh, Antibiotics for emerging pathogens, Science 325 (2009) 1089−1093.

[53] I.Y. Park, J.H. Cho, K.S. Kim, Y.B. Kim, M.S. Kim, S.C. Kim, Helix stability confers salt resistance upon helical antimicrobial peptides, J. Biol. Chem. 279 (2004) 13896–13901.

[54] M.J. Goldman, G.M. Anderson, E.D. Stolzenberg, U.P. Kari, M. J.M. Zasloff,Human β-defensin-1 is a salt-sensitive antibiotic in lung that is inactivated in cystic fibrosis, Cell 88 (1997) 553–560.

[55] J. Huang, D. Hao, Y. Chen, Y. Xu, J. Tan, Y. Huang, F. Li, Y. Chen, Inhibitory effects and mechanisms of physiological conditions on the activity of enantiomeric forms of an α-helical antibacterial peptide against bacteria, Peptides 32 (2011) 1488–1495.

[56] Scudiero, S. Galdiero, M. Cantisani, R. Di Noto, M. Vitiello, M. Galdiero, G. Naclerio, J.J. Cassiman, C. Pedone, G. Castaldo, F. Salvatore, Novel synthetic, salt-resistant analogs of human beta-defensins 1 and 3 endowed with enhanced antimicrobial activity, Antimicrob. Agents Chemother. 54 (2010) 2312–2322.

[57] T. Tomita, S. Hitomi, T. Nagase, H. Matsui, T. Matsuse, S. Kimura, Y. Ouchi, Effect of ions on antibacterial activity of human beta defensin 2, Microbiol. Immunol. 44 (2000) 749–754.

[58] A.M. George, Multidrug resistance in enteric and other gram-negative bacteria, FEMS Microbiol. Lett. 139 (1996) 1–10.

[59] R.E.W. Hancock, Resistance mechanisms in *Pseudomonas aeruginosa* and other nonfermentative gram-negative bacteria, Clin. Infect. Dis. 27 (1998) S93–S99.

[60] J.P. Quinn, Clinical problems posed by multiresistant nonfermenting gram-negative pathogens, Clin. Infect. Dis. 27 (1998) S117–S124.

[61] L. Kalan, G.D. Wright, Antibiotic adjuvants: multicomponent antiinfective strategies, Expert. Rev. Mol. Med. 13 (2011) e5.

[62] Y. Hu, A. Liu, J. Vaudrey, B. Vaiciunaite, C. Moigboi, S.M. McTavish, A. Kearns, A. Coates, Combinations of β-lactam or aminoglycoside antibiotics with plectasin are synergistic against methicillin-sensitive and methicillin-resistant *Staphylococcus aureus*, PLoS One 10 (2015) e0117664

[63] G. Soothill, Y. Hu, A. Coates, Can we prevent antimicrobial resistance by using antimicrobials better? Pathogens 2 (2013) 422–435.

[64] J.N. Steenbergen, J.F. Mohr, G.M. Thorne Effects of daptomycin in combination with other antimicrobial agents: a review of in vitro and animal model studies, J. Antimicrob. Chemother. 64 (2009) 1130–1138.

[65] P. Jorge, M. Pérez-Pérez , G. Pérez Rodríguez, M.O. Pereira, A. Lourenco, A network perspective on antimicrobial peptide combination therapies: the potential of colistin, polymyxin B and nisin, Int. J. Antimicrob. Agents 49 (2017) 668–676.

[66] Giacometti, O. Cirioni, M.S. Del Prete, F. Barchiesi, M. Fortuna, D. Drenaggi, G. Scalise, In vitro activities of membrane-active peptides alone and in combination with clinically used antimicrobial agents against *Stenotrophomonas maltophilia*, Antimicrob. Agents Chemother. 44 (2000) 1716–1719.

[67] L. Fassi Fehri, H. Wr_oblewski, A. Blanchard, Activities of antimicrobial peptides and synergy with enrofloxacin against Mycoplasma pulmonis, Antimicrob. Agents Chemother. 51 (2007) 468–474.

[68] A.K. Mishra, J. Choi, E. Moon, K.H. Baek, Tryptophan-rich and proline-rich antimicrobial peptides. Molecules 23 (2018)

[69] X. Zhu, Z. Ma, J. Wang, S. Chou, A. Shan, Importance of tryptophan in transforming an amphipathic peptide into a *Pseudomonas aeruginosa*-targeted antimicrobial peptide. PLoS One 9 (2014) e114605.

Acknowledgements

This study was performed at the Peptide biochemistry laboratory, School of biomedical sciences, Chosun University. I would first like to thank my thesis advisor, **Prof. Song Yub Shin** for mentoring and supporting me throughout the duration of this study. I am most grateful to him for all his help and invaluable comments concerning my thesis. His wealth of knowledge, encouragement and genuine interest in my project were essential for the finishing of this work.

I want to express my gratitude also to my collaborators, **Prof. Chul Won Lee, Prof. Jeong-Kyu Bang, Prof, Jiwon Seo and Dr. Sung Tae Yang** with whom I share publicartions. I sincerely thank my senior **Dr. Rajasekaran** who has guding me both personally and professionally. I really admire his patience in guiding me from basics to advance techniques. I am lucky to have him in my Ph.D. life.

My warmest thanks go to my labmates **Dr. Eun Young Kim** and **Mr. Ajish** for helping me in various experiments and for making work life stress free. I would also like to express my appreciation to other lab members and collaborators, **Dr. Jiyong Nam, Dr. Hyosuk Yun, Dr. Pethaiah Gunasekaran** and **Mr. Ho Yeon Nam**.

Many thanks to **Dr. Pavithra,** a sister from another mother who motivated me, guided me and helped me in all possible way, making my life in Korea memorable. I also want to thank my friends **Dr. Swapnil, Dr. Seketoulie Keretsu, Dr. Tamiliniyan, Dr. Immanuel, Dr. Kamalakannan, and Mr. Devaneyan Joseph** who were there for me in anytime. They are important reasons for enriching my work life balance with fun elements like hiking, long drive, movies and cooking.

Last but not least, I am thankful to my parents **Mr. Sukumar (late)** and **Mrs. Gayathri** for their love and encouragement throughout my life. I am thankful to them for trusting me more than I trust myself. Without their love I would have never made this far.

List of publications

1. Nam, Jiyoung, Hyosuk Yun, Ganesan Rajasekaran, **S. Dinesh Kumar**, Jae Il Kim, Hye Jung Min, Song Yub Shin, and Chul Won Lee. "Structural and functional assessment of mBjAMP1, an antimicrobial peptide from Branchiostoma japonicum, revealed a novel α-hairpinin-like scaffold with membrane permeable and DNA binding activity." ***Journal of medicinal chemistry*** 61, no. 24 (2018): 11101-11113.

2. Rajasekaran, Ganesan, **S. Dinesh Kumar**, Jiyoung Nam, Dasom Jeon, Yangmee Kim, Chul Won Lee, Il-Seon Park, and Song Yub Shin. "Antimicrobial and anti-inflammatory activities of chemokine CXCL14-derived antimicrobial peptide and its analogs." ***Biochimica Et Biophysica Acta (Bba)-Biomembranes*** 1861, no. 1 (2019): 256-267.

3. Rajasekaran, Ganesan, **S. Dinesh Kumar**, Sungtae Yang, and Song Yub Shin. "Improving Cell Selectivity of Fowlicidin-1 by Swapping Residues between Pro-7 and Tyr-20." ***Bulletin of the Korean Chemical Society*** 40, no. 5 (2019): 429-434.

4. Rajasekaran, Ganesan, **S. Dinesh Kumar**, Sungtae Yang, and Song Yub Shin. "The design of a cell-selective fowlicidin-1-derived peptide with both antimicrobial and anti-inflammatory activities." ***European journal of medicinal chemistry*** 182 (2019): 111623.

5. Ajish, Chelladurai, Sungtae Yang, **S. Dinesh Kumar**, and Song Yub Shin. "Proadrenomedullin N-terminal 20 peptide (PAMP) and its C-terminal 12-residue peptide, PAMP (9–20): Cell selectivity and antimicrobial mechanism." ***Biochemical and Biophysical Research Communications*** (2020).

6. Nam, Ho Yeon, Jieun Choi, **S. Dinesh Kumar**, Josefine Eilsø Nielsen, Minkyu Kyeong, Sungrok Wang, Dahyun Kang et al. "Helicity modulation improves the selectivity of antimicrobial peptoids." ***ACS Infectious Diseases*** 6, no. 10 (2020): 2732-2744.

7. **Kumar, S. Dinesh**, and Song Yub Shin. "Antimicrobial and anti-inflammatory activities of short dodecapeptides derived from duck cathelicidin: Plausible mechanism of bactericidal action and endotoxin neutralization." ***European Journal of Medicinal Chemistry*** 204 (2020): 112580.

8. Kim, Eun Young, **S. Dinesh Kumar**, Jeong Kyu Bang, and Song Yub Shin. "Mechanisms of antimicrobial and antiendotoxin activities of a triazine-based amphipathic polymer." ***Biotechnology and Bioengineering*** 117, no. 11 (2020): 3508-3521.